

**A STUDY OF HYDRAULIC JUMP IN ABRUPTLY EXPANDED
SLOPING CHANNEL**

by

MOHAMMAD ASHRAFUL ISLAM
(Roll No. - 040016025P)



A thesis submitted in partial fulfillment of the requirements for the degree of
Master of Science in Water Resources Engineering

**DEPARTMENT OF WATER RESOURCES ENGINEERING
BANGLADESH UNIVERSITY OF ENGINEERING AND TECHNOLOGY**

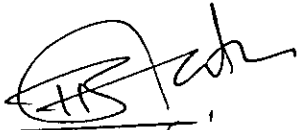
September 2002



CERTIFICATE

The thesis titled "A study of hydraulic jump in abruptly expanded sloping channel", submitted by Mohammad Ashraf Islam, Roll No: 040016025P, has been accepted as satisfactory in partial fulfillment of the requirements for the degree of Master of Science in Water Resources Engineering.

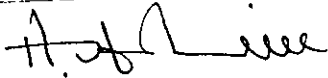
BOARD OF EXAMINERS



Dr. M. A. Matin

Professor and Head, Department of Water Resources Engineering
BUET, Dhaka - 1000

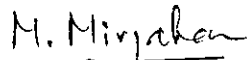
Chairman



Dr. Md. Abdul Halim

Professor, Department of Water Resources Engineering
BUET, Dhaka - 1000

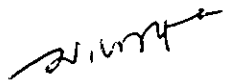
Member



Dr. M. Mirjahan

Professor, Department of Water Resources Engineering
BUET, Dhaka - 1000

Member



Mr. H.S. Mozaddad Faruque

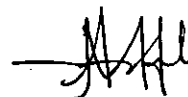
Director

WARPO

Member
(External)

DECLARATION

This is declared that this work entitled “ A study of hydraulic jump in abruptly expanded sloping channel” has been done by the Author under the supervision of Dr. M. Abdul Matin, Professor and Head, Department of Water Resources Engineering, Bangladesh University of Engineering and Technology (BUET), Dhaka. This is also declared that this or any part of it has not been submitted elsewhere for the award of any degree or diploma.



Mohammad Ashraf Islam

Signature of the Candidate

TABLE OF CONTENTS

	Page
LIST OF TABLES	viii
LIST OF FIGURES	ix
LIST OF NOTATIONS	xiii
ACKNOWLEDGEMENT	xv
ABSTRACT	xvi
<i>Chapter One:</i> INTRODUCTION	
1.1 GENERAL	1
1.2 SCOPE AND IMPORTANCE OF THE STUDY	2
1.3 OBJECTIVES OF THE STUDY	3
1.4 ORGANIZATION OF THE REPORT	3
<i>Chapter Two:</i> LITERATURE REVIEW	
2.1 INTRODUCTION	5
2.2 APPLICATIONS OF HYDRAULIC JUMP	5
2.3 FORMATION OF HYDRAULIC JUMP	6
2.4 CLASSICAL HYDRAULIC JUMP	6
2.4.1 Introduction	6
2.4.2 Main characteristics	6
2.5 HYDRAULIC JUMP IN SLOPING CHANNEL	9
2.5.1 Introduction	9
2.5.2 Types of hydraulic jump in sloping channel	10
2.5.3 Historical review	12

2.5.4 Characteristics of jump on sloping floor	15
2.6 HYDRAULIC JUMP IN EXPANDING CHANNEL	18
2.6.1 Introduction	18
2.6.2 Classification of hydraulic jump in expansions	18
2.6.3 Classical jump versus T-jump	20
2.6.4 Previous investigations	21

Chapter Three: THEORETICAL FORMULATION

3.1 INTRODUCTION	27
3.2 ASSUMPTIONS	27
3.3 GOVERNING EQUATIONS	28
3.4 THEORETICAL FORMULATION	29
3.5 CALIBRATION OF THE DEVELOPED THEORETICAL EQUATION	33

Chapter Four: EXPERIMENTAL SETUP

4.1 INTRODUCTION	34
4.2 DESIGN OF EXPANDING STILLING BASIN	34
4.2.1 Introduction	34
4.2.2 Design	34
4.2.3 Constriction elements in the stilling basin	35
4.2.4 Transitions in the stilling basin	35
4.3 EXPERIMENTAL FACILITIES	37
4.3.1 Laboratory flume	37
4.3.2 Pump	39
4.3.3 Motor	39
4.4 MEASURING DEVICES	39
4.4.1 Water meter	39
4.4.2 Miniature propeller current meter	39

4.4.3 Velocity meter	40
4.4.4 Point gauge	41
4.5 MEASUREMENTS	42
4.5.1 Discharge	42
4.5.2 Water surface elevation	42
4.5.3 Velocity	42

Chapter Five: EXPERIMENTAL PROCEDURE

5.1 INTRODUCTION	43
5.2 STEPWISE PRE-EXPERIMENTAL MEASURES	43
5.3 STEPWISE EXPERIMENTAL PROCEDURE	44
5.4 EXPERIMENT NUMBERING	44
5.5 DATA COLLECTION	45

Chapter Six: RESULTS AND DISCUSSIONS

6.1 INTRODUCTION	56
6.2 ANALYSIS OF INFLOW FROUDE NUMBER WITH DISCHARGE FOR DIFFERENT HYDRAULIC CONDITIONS	56
6.3 VARIATION OF SEQUENT DEPTH RATIO WITH INFLOW FROUDE NUMBER	57
6.4 ANALYSIS OF THE PARAMETERS k_1 AND k_2 AT DIFFERENT HYDRAULIC CONDITIONS	64
6.4.1 Variation of factor k_1 with F_1	64
6.4.2 Modification of the prediction equation of k_1	64
6.4.3 Comparison between the observed and predicted values of k_1	65
6.4.4 Prediction equation for parameter k_2	65
6.4.5 Comparison between the observed and predicted values of k_2	66
6.5 CALIBRATION OF THE PREDICTION MODEL	73

6.6 APPLICABILITY OF THE PROPOSED EQUATION	85
6.6.1 Introduction	85
6.6.2 Horizontal channel with sudden expansion	85
6.6.3 Sloping rectangular channel	85
 <i>Chapter Seven: CONCLUSIONS AND RECOMMENDATIONS</i>	
7.1 INTRODUCTION	89
7.2 CONCLUSIONS	89
7.3 RECOMMENDATIONS	90
 REFERENCES	 92

LIST OF TABLES

Name	Title	Page
Table 5.1	Experimental data for $B = 0.8$, Slope = 0.0042	49
Table 5.2	Experimental data for $B = 0.8$, Slope = 0.0089	49
Table 5.3	Experimental data for $B = 0.8$, Slope = 0.0131	50
Table 5.4	Experimental data for $B = 0.7$, Slope = 0.0131	50
Table 5.5	Experimental data for $B = 0.7$, Slope = 0.0089	51
Table 5.6	Experimental data for $B = 0.7$, Slope = 0.0042	51
Table 5.7	Experimental data for $B = 0.7$, Slope = 0.0000	52
Table 5.8	Experimental data for $B = 0.6$, Slope = 0.0042	52
Table 5.9	Experimental data for $B = 0.6$, Slope = 0.0131	53
Table 5.10	Experimental data for $B = 0.6$, Slope = 0.0089	53
Table 5.11	Experimental data for $B = 0.5$, Slope = 0.0042	54
Table 5.12	Experimental data for $B = 0.5$, Slope = 0.0089	54
Table 5.13	Experimental data for $B = 0.5$, Slope = 0.0131	55
Table 5.14	Experimental data for $B = 0.5$, Slope = 0.0000	55
Table 6.1	Statistical result of the performance of the prediction equation	82

LIST OF FIGURES

No.	Title	Page
Figure 1.1	Definition sketch of a hydraulic jump	2
Figure 2.1	Length characteristics of a classical jump	7
Figure 2.2	Length of hydraulic jump on horizontal floor	8
Figure 2.3	Relation between $D (=h_2/h_1)$ and F_1 for classical jump	9
Figure 2.4	Jumps in sloping channel, case 1	11
Figure 2.5	Jumps in sloping channel, case 2	12
Figure 2.6	Experimental relation between F_1 and y_2/y_1 or d_2/d_1 for jumps in sloping channel	14
Figure 2.7a	Variation of y_1/y_2	16
Figure 2.7b	Length of jump on sloping floor	17
Figure 2.8	Types of jumps in abruptly expanding channel, (R) jump, (b) S jump, (c) T jump, (d) Classical jump	19
Figure 2.9	Jump at an abrupt expansion, (<i>Unny</i> , 1961)	22
Figure 3.1a	Definition sketch of hydraulic jump in a sloping channel	30
Figure 3.1b	Expansion geometry	30
Figure 4.1	Photograph of experimental setup, downstream of sluice gate	35
Figure 4.2	Photograph of transition elements at upstream of sluice gate	36
Figure 4.3	Photograph of the 70 ft long laboratory tilting flume	37
Figure 4.4	Photograph of point gauge	41
Figure 5.1	Side view of a T-jump ($B = 0.5$, Slope = 0.0131, gate opening = 13cm)	46
Figure 5.2	Hydraulic jump in a horizontal rectangular channel	46
Figure 5.3	Close view of turbulence created in jump at the abrupt expansion of a sloping channel	47
Figure 5.4	Jump is approaching towards the expansion section due to raising the tail water gate	47
Figure 5.5	Asymmetric jump formed at the section of sudden expansion	48

Figure 5.6	Initial stage of jump formation in an expanding channel	48
Figure 6.1	Inflow Froude number Vs Discharge for various slope and gate openings with expansion ratio $B = 0.80$; (a) Slope = 0.0042, (b) Slope = 0.0089, (c) Slope = 0.0131	58
Figure 6.2	Inflow Froude number Vs Discharge for various slope and gate openings with expansion ratio $B = 0.70$; (a) Slope = 0.0042, (b) Slope = 0.0089, (c) Slope = 0.0131	59
Figure 6.3	Inflow Froude number Vs Discharge for various slope and gate openings with expansion ratio $B = 0.60$; (a) Slope = 0.0042, (b) Slope = 0.0089, (c) Slope = 0.0131	60
Figure 6.4	Inflow Froude number Vs Discharge for various slope and gate openings with expansion ratio $B = 0.50$; (a) Slope = 0.0042, (b) Slope = 0.0089, (c) Slope = 0.0131	61
Figure 6.5	D Vs F_1 for different channel slopes with expansion ratio, $B = 0.80$	62
Figure 6.6	D Vs F_1 for different channel slopes with expansion ratio, $B = 0.70$	62
Figure 6.7	D Vs F_1 for different channel slopes with expansion ratio, $B = 0.60$	63
Figure 6.8	D Vs F_1 for different channel slopes with expansion ratio, $B = 0.50$	63
Figure 6.9	Variation of parameter k_1 with F_1 for different expansion ratios; (a) Slope = 0.0042, (b) Slope = 0.0089, (c) Slope = 0.0131	67
Figure 6.10	k_1 Vs Inflow Froude number, F_1 with expansion ratio, $B = 0.8$; (a) Slope = 0.0042, (b) Slope = 0.0089, (c) Slope = 0.0131	67
Figure 6.11	k_1 Vs Inflow Froude number, F_1 with expansion ratio, $B = 0.7$; (a) Slope = 0.0042, (b) Slope = 0.0089, (c) Slope = 0.0131	69
Figure 6.12	k_1 Vs Inflow Froude number, F_1 with expansion ratio, $B = 0.6$; (a) Slope = 0.0042, (b) Slope = 0.0089, (c) Slope = 0.0131	70
Figure 6.13	k_1 Vs Inflow Froude number, F_1 with expansion ratio, $B = 0.5$; (a) Slope = 0.0042, (b) Slope = 0.0089, (c) Slope = 0.0131	71
Figure 6.14	k_2 Vs Inflow Froude number, F_1 with expansion ratio, $B = 0.5$;	72

	(a) Slope = 0.0042, (b) Slope = 0.0089, (c) Slope = 0.0131	
Figure 6.15	D Vs F_1 with expansion ratio, $B = 0.8$; (a) Slope = 0.0042, (b) Slope = 0.0089, (c) Slope = 0.0131	74
Figure 6.16	D Vs F_1 with expansion ratio, $B = 0.7$; (a) Slope = 0.0042, (b) Slope = 0.0089, (c) Slope = 0.0131	75
Figure 6.17	D Vs F_1 with expansion ratio, $B = 0.6$; (a) Slope = 0.0042, (b) Slope = 0.0089, (c) Slope = 0.0131	76
Figure 6.18	D Vs F_1 with expansion ratio, $B = 0.5$; (a) Slope = 0.0042, (b) Slope = 0.0089, (c) Slope = 0.0131	77
Figure 6.19	Comparison between predicted D and observed D with expansion ratio, $B = 0.8$; (a) Slope = 0.0042, (b) Slope = 0.0089, (c) Slope = 0.0131	78
Figure 6.20	Comparison between predicted D and observed D with expansion ratio, $B = 0.7$; (a) Slope = 0.0042, (b) Slope = 0.0089, (c) Slope = 0.0131	79
Figure 6.21	Comparison between predicted D and observed D with expansion ratio, $B = 0.6$; (a) Slope = 0.0042, (b) Slope = 0.0089, (c) Slope = 0.0131	80
Figure 6.22	Comparison between predicted D and observed D with expansion ratio, $B = 0.5$; (a) Slope = 0.0042, (b) Slope = 0.0089, (c) Slope = 0.0131	81
Figure 6.23	Sequent depth ratio Vs inflow Froude number for different expansion ratios	87
Figure 6.24	Sequent depth ratio Vs inflow Froude number for different channel slopes	87
Figure 6.25	Sequent depth ratio Vs inflow Froude number with observed and predicted data for a horizontal abruptly expanding channel	88
Figure 6.26	Sequent depth ratio Vs inflow Froude number with observed and predicted data for a rectangular sloping channel	88

LIST OF NOTATIONS

Symbols	Description
A	Cross sectional area normal to the direction of flow
b	Channel width
B	Expansion ratio
D	Sequent depth ratio
e	The ratio of the flow depth at the expansion section to the upstream flow depth
E	Specific energy
E_1	Modified inflow Froude number
E_L	Loss of Specific energy
F_1	Inflow Froude number
F_f	External frictional force
P	Pressure force
g	Acceleration due to gravity
h	Flow depth
k_1	The modification factor to account for the effect of expansion ratio
k_2	The modification factor to account for the effect of channel slope
L_j	Length of the jump
L_r	Roller length of the jump
Q	Discharge
U	Velocity
W	Wight of water within the control volume
X	Ratio of the toe position from the expansion section towards the upstream to the roller length of the classical jump
z	Elevation head
α	Kinetic energy coefficient
β	Momentum coefficient
γ	Specific weight of water

ρ	Density of water
θ	Channel slope
η	Hydraulic jump efficiency
G	Modified Froude number
K	Modification factor due to assumption of linear jump profile
C_s	Coefficient to account the effect of slope
C_r	Coefficient to account the effect of roughness
I	Roughness density
λ	Depth ratio = y_1/b
D^*	Sequent depth ratio of classical jump
L_r^*	Roller length of the classical jump
X	Relative toe position
ψ	Parameter to account the effect jump position and expansion ratio

ACKNOWLEDGEMENT

The author owes his deepest gratitude and thanks to Dr. M.A. Matin, Professor and Head of the Department of Water Resources Engineering, BUET who introduced the author to the interesting field of hydraulic jumps. The author is grateful to his supervisor for his affectionate encouragement, invaluable suggestions, unfailing enthusiasm and wise guidance throughout the experimental investigation and during the preparation of this thesis.

The author expresses his gratitude to Dr. M.A. Halim, Professor of the Department of Water Resources Engineering and Dean of the faculty of Civil Engineering, BUET for being a member of the examination board and his valuable support.

The author is greatly indebted to Dr. M. Mirjahan, Professor of the Department of Water Resources Engineering for his encouragement and affectionate guidance during the course of the study.

The author is grateful to Mr. H.S. Mozaddad Faruque, Director, WARPO for his keen interest in the subject of research. The author wishes to convey his thanks to him for his kind consent to be a member of the examination board.

The author gratefully acknowledges his parents for their continued encouragement and moral supports without which the work could not have been completed. The author also wishes to give thanks to his friends and colleagues for their encouragement.

Finally, the author profoundly acknowledges the efforts made by laboratory staffs during the course of experimental study.

Mohammad Ashraful Islam

September 2002

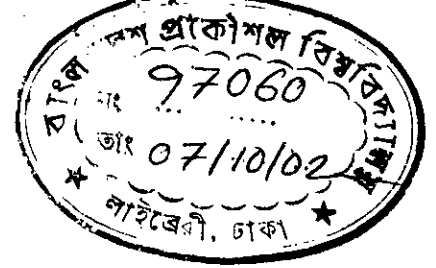
ABSTRACT

Hydraulic jump primarily serves as an energy dissipator to dissipate excess energy of flowing water downstream of hydraulic structures, such as spillways and sluice gates. Considering its immense practical utility in hydraulic engineering and allied fields, this phenomenon has given a considerable attention by the researchers for the last 180 years. During the last four decades, the hydraulic jump in a channel with a lateral expansion was found to be interesting. This type of jump is of practical importance in dissipating excess energy downstream of spillways, weirs etc., when tail water depth is inadequate to give a good jump. If this type of jump occurs in a sloping condition the analysis of the phenomenon becomes very complex due to the inclusion of so many parameters related to sudden expansion and channel slope. The sequent depth ratio of a hydraulic jump in an abrupt expansion of a sloping channel is considered in this present study.

The basic equation is based on the application of the one-dimensional momentum equation and continuity equation. The results of the present experimental study were used to evaluate a developed prediction equation for computing sequent depth ratio in an expanding channel whose format is similar to the well-known Belanger equation for classical jump with modification of Froude number. The modified Froude number term contains two additional parameters, one of them incorporates the effect of sudden expansion and the second one represents for describing the effect of channel slope. This theoretically-based equation is easy and simple to apply in design of enlarged stilling basin compared to other approaches.

Experiments were conducted in the Hydraulics and River Engineering Laboratory of BUET. A 70 ft long tilting flume has been used to carry out the investigations. Several contraction geometries were inserted in the channel to reduce the width of the supercritical flow upstream of the expansion section. Downstream width was kept constant and four expansion ratios of 0.5, 0.6, 0.7 and 0.8 were maintained together with three different channel slopes (0.0042, 0.0089 and 0.0131). The initial depth, sequent depth, velocity etc. were measured with different combinations of expansion ratio and channel slope. From the entire test runs two desired parameters

k_1 and k_2 were calculated and then these two were calibrated with the experimental data to relate these factors with some known variables like expansion ratio, channel slope and inflow Froude number. With the aid of these factors, modified inflow Froude number will be calculated to get the desired form of Belanger's format prediction model.



Chapter One

INTRODUCTION

1.1 GENERAL

In open channel flow, the abrupt transition from a supercritical flow to a subcritical flow is called a hydraulic jump. The hydraulic jump has attracted wide attention for many years not only because of its importance in the design of stilling basins and other hydraulic engineering works, but also because of its fascinating complexity. After many years of sustained research, many of its hydraulic features are now well understood.

In the classical jump the water surface starts rising abruptly at the beginning, or toe of the jump, which oscillates about a mean position, and it continues to rise up to a section beyond which it is essentially level. This section denotes the end of the jump. The hydraulic jump is accompanied by considerable turbulence and energy dissipation. At the beginning of the jump, turbulent eddies of large sizes are formed which extract energy from the mean flow. The large-sized eddies are broken up into the smaller ones and the energy is transferred from the larger eddies into the smaller ones. The smaller eddies are responsible for the dissipation of turbulence energy to the heat energy.

For a horizontal rectangular channel of constant width, and neglecting the bed and wall friction, the sequent depth ratio of the hydraulic jump is calculated by the well-known Belanger equation

$$\frac{h_2}{h_1} = \frac{1}{2} \left(\sqrt{1 + 8F_1^2} - 1 \right) \quad \dots(1.1)$$

where the subscripts 1 and 2 stand for upstream and downstream flow conditions of the hydraulic jump (Fig.1.1), respectively; and F_1 is the inflow Froude number. In this derivation, velocity distribution is assumed to be uniform over the section and the pressure distribution is hydrostatic both at the beginning and the end of the jump.

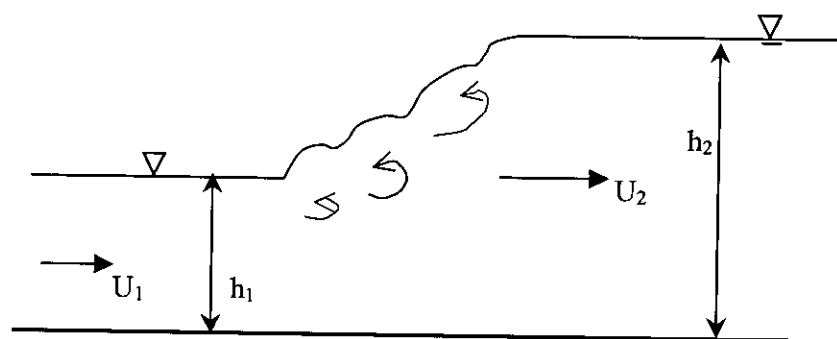


Figure 1.1: Definition sketch of a hydraulic jump

The hydraulic jump may appear in two different ways; either with a varying location in a channel, depending on the boundary conditions, or as a means to dissipate excess energy in a stilling basin with a fixed location.

Hydraulic jumps in expanding channels have received considerable attention, although only limited information on successful energy dissipation are available (Nettleton and McCorquodale, 1989). Abrupt expansion form is one type of open channel transitions, e.g. a transition structure of a spillway, a flood relief canal or a bottom outlet gallery as a part of a hydraulic scheme. The flow pattern in such expansions is complex, and knowledge of the hydraulic performance and design procedures is poor.

Hydraulic jumps in expansion may be described by the approaching conditions, that is the inflow depth h_1 , the inflow Froude number F_1 and the position of toe x relative to the expansion section. In this study, a hydraulic jump in the section of abrupt expansion of a sloping channel is considered.

1.2 SCOPE AND IMPORTANCE OF THE STUDY

When the tail water depth is inadequate to give a classical jump in a channel of constant width even with the aid of appurtenances and if it is not possible to depress the basin floor because of difficulties in excavation in the stilling basin area or operational conditions, then a lateral expansion remains the only possibility for guaranteeing the necessary energy dissipation (Herbrand, 1973). Again, if this situation may occur in a sloping channel like weirs with sloping faces or spillways.

In such basins, there are mainly two problems faced by the field engineers who monitor the performance of the design. One is the determination of sequent depth and the other is the estimation of energy loss (Agarwal, 2001).

A Belanger's format prediction model to determine the sequent depth for expanding sloping channel is developed using one-dimensional momentum and continuity equation. This model contains two unknown parameters and experimentation is required to evaluate these parameters. From experimental data it will be possible to develop a mathematical relationship in terms of some known variables such as expansion ratio, channel slope, upstream Froude number etc. Therefore, the present study is directed towards the evaluation of related parameters using the experimental data in the laboratory flume.

1.3 OBJECTIVES OF THE STUDY

The objectives for the present study are:

- (1) To develop a theoretical model to determine the sequent depth in sloping channel with abrupt expansion.
- (2) To develop an experimental setup and conduct the study for analysis of hydraulic jump.
- (3) To evaluate the necessary parameters of the developed model for sequent depth with experimental data.

1.4 ORGANIZATION OF THE THESIS

The subject matter of this thesis report has been arranged in seven chapters. The first chapter provides an introduction with objectives, scope, importance and organization of this report. Second chapter reviews previous theoretical and experimental studies available in connection with the present study. Chapter three deals with the theoretical formulation of the solution to the problem. The detailed description of the "experimental setup" has been included in the fourth chapter. This is followed by the "methodology of the experiment" in chapter five. The "Results and Discussions"

have been outlined in chapter six and finally "conclusions and recommendations" have been presented in chapter seven.

Chapter Two

LITERATURE REVIEW

2.1 INTRODUCTION

Hydraulic jump has extensively been studied in the field of hydraulic engineering. It is an intriguing and interesting phenomenon that has caught the imagination of many researchers since its first description by Leonardo da Vinci. The Italian engineer Bidone in 1818 is credited with the first experimental investigation of hydraulic jump (after Chow, 1959). Since then considerable research effort has gone into the study of this subject. The results of the analytical treatment by Belanger in 1828 (Equation 1.1) are still valid. The literature on this topic is vast and ever-expanding. The main reason for such continued interest in this topic is its immense practical utility in hydraulic engineering and allied fields.

2.2 APPLICATIONS OF HYDRAULIC JUMP

The most important application of the hydraulic jump is in the dissipation of energy below sluiceways, weirs, gates, etc. so that objectionable scour in the downstream channel is prevented. The high energy loss that occurs in hydraulic jump has led to its adoption as a part of the energy dissipator system below a hydraulic structure. Downstream portion of a hydraulic structure where the energy dissipation is deliberately allowed to occur so that the outgoing stream can safely be conducted to the channel below is known as a stilling basin. It is a fully paved channel and may have additional appurtenances, such as baffle blocks and sills to aid in the efficient performance over a wide range of operating conditions. It has also been used to raise the water level downstream to provide the requisite head for diversion into canals and also to increase the water load on aprons, thereby counteracting the uplift pressure and thus lessening the thickness of the concrete apron required in structures on permeable foundations. Some of the other important uses of hydraulic jump are: a) efficient operation of flow measurement flumes, b) mixing of chemicals, c) to aid intense mixing and gas transfer in chemical processes, d) in the desalination of sea

water and e) in the aeration of streams which are polluted by bio-degradable wastes (Ranga Raju, 1993).

2.3 FORMATION OF HYDRAULIC JUMP

Hydraulic jump is a flow phenomenon associated with the abrupt transition of a supercritical (inertia-dominated) flow to a subcritical (gravity-dominated) flow. Subcritical flow is produced by downstream control and supercritical flow is produced by upstream control. A control fixes a certain depth-discharge relationship in its own vicinity; it also fixes the nature of the flow for some distance upstream or downstream. So, it will produce subcritical flow upstream and supercritical flow downstream. If the upstream control causes supercritical flow while the downstream control dictates subcritical flow, there is a conflict which can be resolved only if there is some means for the flow to pass from one flow condition to the other — thus *hydraulic jump* forms (Henderson, 1966).

2.4 CLASSICAL HYDRAULIC JUMP

2.4.1 Introduction

The classical hydraulic jump is the basic type of physical phenomenon that is commonly used in stilling basins. The hydraulic jump consists of an abrupt change from supercritical to subcritical flow. The jump formed in smooth, wide, and horizontal rectangular channel (prismatic channel) is known as the classical jump.

2.4.2 Main Characteristics

In the classical jump the water surface starts rising abruptly at the beginning, or toe, of the jump, which oscillates about a mean position, and it continues to rise up to a section beyond which it is essentially level. This section denotes the end of the jump. The supercritical depth at the beginning is called represented as y_1 which is termed as initial depth and the subcritical depth at the end is represented as y_2 which is termed as sequent depth.

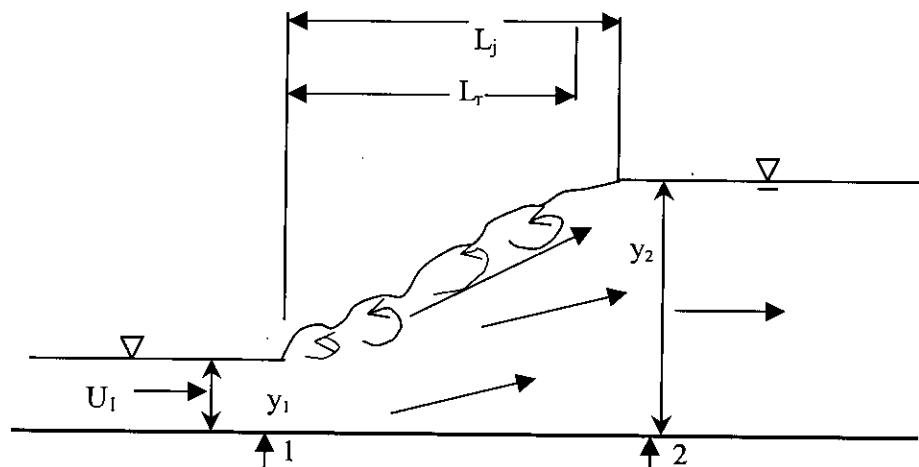


Figure 2.1: Length characteristics of a classical jump

At the toe of jump (section 1 in the figure 2.1) the flow depth is y_1 , and the average velocity, $U_1 = Q/(by_1)$ with Q = discharge and b = channel width. At the end of the jump (section 2 in the figure 2.1) the depth is y_2 and the velocity, $U_2 = Q/(by_2)$. The supercritical Froude number is given by:

$$F_1 = \frac{U_1}{\sqrt{gh_1}} \quad \dots (2.1)$$

The upstream condition of the hydraulic jump is called supercritical with a Froude number larger than one and the depth, which is lower than the critical depth. The downstream condition is called subcritical with a Froude number smaller than one and the depth higher than the critical depth. Specific energy at the upstream of jump is higher than that at the downstream, the difference is known as the energy loss in hydraulic jump.

If the velocity distribution is assumed to be uniform and the pressure distribution is hydrostatic both at the beginning and at the end of the jump, and if the boundary shear stress on the bed and the turbulent velocity fluctuations at the beginning and at the end are neglected, it can be shown that the ratio of the sequent depth to initial depth is given by the well-known Belanger equation:

$$\frac{y_2}{y_1} = \frac{1}{2} \left(\sqrt{1 + 8F_1^2} - 1 \right) \quad \dots(1.1)$$

On the surface of the jump there is a violent roller, which starts at the toe and ends after the jump. The length of the jump has been a controversial issue in the past. It is generally agreed that the end of the jump is the section at which the water surface becomes essentially level and the mean surface elevation is maximal. The horizontal distance from the toe to this section is taken as the length of the jump and is denoted by L_j . It is found that, if L_r is the length of the surface roller, in general it is less than L_j . Due to the surface breaking, a considerable amount of air is entrained in the jump. Large personal errors are introduced in the determination of the length L_j . Experimentally it is found that $L_j/y_2 = f(F_1)$. The variation of L_j/y_2 with F_1 obtained by Bradely and Peterika (1957) is shown in Figure 2.2. This curve is usually recommended for general use. It is evident from Figure 2.2 that while L_j/y_2 depends on F_1 for small values of inflow Froude number, at higher values (i.e., $F_1 > 5.0$) the relative jump length L_j/y_2 is practically constant at a value of 6.1. The graph of the Figure 2.3 can be mathematically expressed as:

$$L_j = 6.9(y_2 - y_1) \quad \dots (2.2)$$

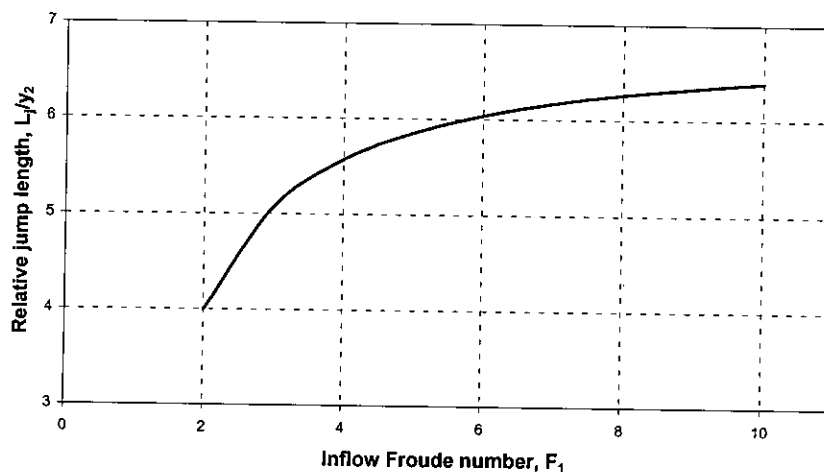


Figure 2.2: Length of hydraulic jump on horizontal floor

It is known that there is a large amount of energy dissipation in the jump. If E_1 and E_2 are the specific energies at the beginning and at the end of the jump respectively, and if E_L is the loss of specific energy in the jump, it can be shown that

$$\frac{E_L}{E_1} = \frac{8F_1^4 + 20F_1^2 - (8F_1^2 + 1)^{3/2} - 1}{8F_1^2(2 + F_1^2)} \quad \dots(2.3)$$

From this equation it can be found that for an inflow Froude number F_1 equal to 20 the energy loss is equal to $0.86 E_1$; that is, 86% of the initial specific energy is dissipated (Rajaratnam, 1967).

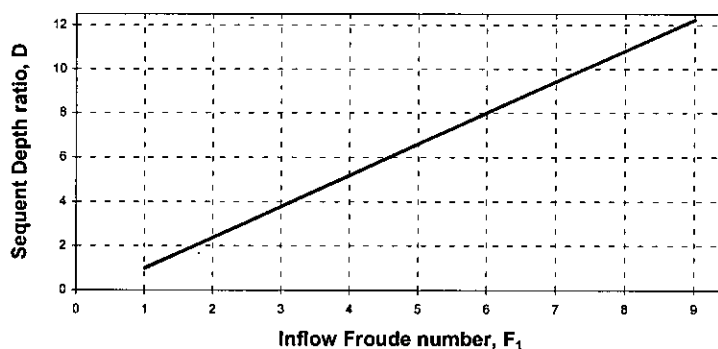


Figure 2.3: Relation between $D (= y_2/y_1)$ and F_1 for the classical jump

Equation (1.1) is shown in graphical form in Fig. 2.3. This curve has been verified satisfactorily with many experimental data and is found to be very useful in the analysis and design for hydraulic jump.

2.5 HYDRAULIC JUMP IN SLOPING CHANNEL

2.5.1 Introduction

In spite of the fact that considerably more is known about the jump formation in horizontal channels than in sloping channels the latter is often preferred for energy dissipation purposes, because it has many distinct advantages. Whereas the classical jump is has been precisely solved, it has not been possible to develop a comparatively satisfactory solution of the jump in sloping channels. The main difficulty is that, if the momentum equation is written for a direction parallel to the

bed of the channel, weight component of the body of the jump enters the relation. If, on the other hand, it is written for the horizontal direction, horizontal component of the pressure on the floor enters into the equation. That is why the solution to the problem of jump formation in sloping channels is found semi empirically with a heavy leaning on experimental information.

2.5.2 Types of hydraulic jump in sloping channel

For the development of simple methods of solution, it has been found useful to divide the general case of jump formation in sloping channels into a number of lesser cases according to their salient features.

In case 1 the jump is formed in a sloping channel ending with a level floor. In this case there are four possible types, as shown in Figure 2.5. In the figure, y_1 is the depth of the supercritical stream before the jump, measured normal to the bed, and y_2 is the vertical subcritical depth at the end of the jump.

It is generally accepted that the end of the jump, in horizontal channels is the section where the expanding stream attains maximal steady elevation. The definition cannot be applied to the case of sloping channels, however, because even after the jump action is over the water surface might be rising, owing to the flow expansion caused by the sloping bed. The end of the surface roller, instead, has been suggested by Kindsvater (1944) as the end of the jump. Hickox in 1944 found that for slopes steeper than 1 on 6 the end of the roller is practically the same as the section of maximal surface elevation (after Rajaratnam, 1967).

In Figure 2.5, y_t is the tail water depth and L_j is the length of the jump measured horizontally. For the sake of simplicity the depth of the supercritical stream is here assumed to be constant on the slope. If the jump occurs just after the end of the slope, the tail water depth y_t is equal to the subcritical sequent depth y_2 given by the Belanger equation (Equation 2.2); this is termed as A jump, which is almost the same as the classical jump. If y_t is greater than y_2 the jump is pushed up on the slope. If the end of the jump occurs at the junction of the slope and the level floor (the junction

section), the jump is a C jump. If the tail water depth is less than that required for a C jump but greater than y_2 the toe of the jump is on the slope but the end is on the level floor; this is a B jump. If the tail water depth is greater than that required for a C

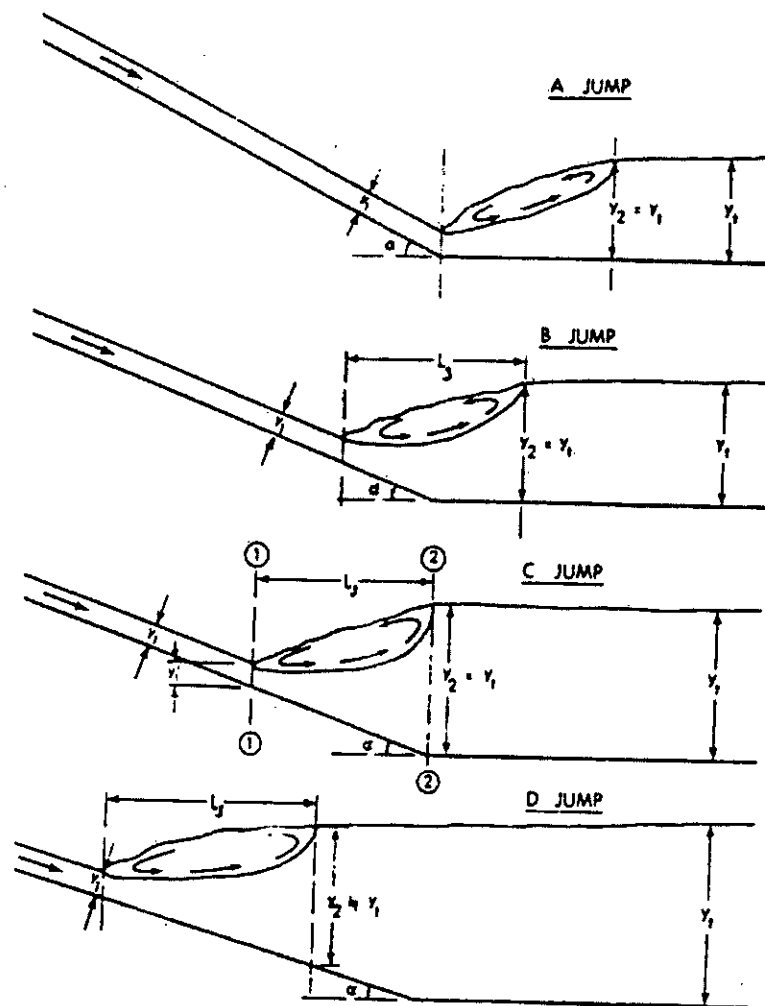


Figure 2.4: Jumps in sloping channel, case 1 (Kindsvater, 1944)

jump, the end of the jump also travels up the slope; this is a D jump. Case 1, comprising these four jumps is the most important case for the design of energy dissipators.

In case 2 the jump occurs in along channel of rather flat slope; (Figure 2.5). The water surface is parallel to the bed after the jump and therefore both depth y_1 and y_2

are measured normal to the bed. Case 2 is known as the E jump. Case 3 is the jump on an adverse slope and is called the F jump, also shown in Figure 2.5. This is a rare type of jump and occurs at the exit of certain types of stilling basins below drops. In the present study, E jump is taken for the analysis.

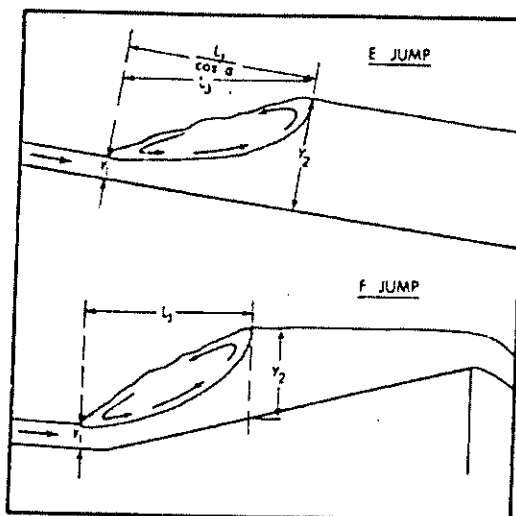


Figure 2.5: Jumps in sloping channels, case 2 (Kindsvater, 1944)

2.5.3 Historical review

The earliest experiments on the hydraulic jump, made by Bidone, were actually done in a sloping channel (after Rajaratnam, 1967). Bazin in 1865 and Beebe and Reigel in 1917 also experimented on sloping channel jumps (after Rajaratnam, 1967), and in 1927 Ellms attempted a theoretical and experimental study of this problem (after Rajaratnam, 1967). In 1934, Yarnell started an extensive research program with slopes of 1 in 6, 1 in 3 and 1 in 1, which was unfortunately interrupted by his death in 1937 (after Rajaratnam, 1967). In 1935 Rindlaub conducted an experimental study of slopes of 8.2° , 12.5° , 24.2° and 30° (with the horizontal), most of his experiments being made on the second of these (after Rajaratnam, 1967). Bakhmeteff and Matzke (1946) published a careful analysis of the problem with experimental data on very flat slopes.

The first rational and successful attack of this problem was made by Kindsvater (1944). Some experimental results from a slope of 1 in 3 were added by Hickox

(1944) to Kindsvater's results from the slope of 1 on 6, and Dutta in constructed from Kindsvater's equation some design charts for a few slopes (after Rajaratnam 1967). An extensive study of this problem was made by Bradley and Peterka (1957)

In 1954 Flores attempted to develop a general theory of jumps in sloping exponential channels (after Rajaratnam 1967). In 1958 Wigham extended the work of Bradley and Peterka (1957) to steeper slopes: 1 on 1, 1 on 2 and 1 on 3 (after Rajaratnam 1967).

In the analysis of hydraulic jumps in sloping channels or channels having appreciable slope, it is essential to consider the weight of water in the jump; in horizontal channel the effect of this weight is negligible. The conventional solution of the jump in sloping channel to find the sequent depth ratio involves the modified Froude number G which is a function of F_1 and θ . G is defined as:

$$G = \frac{F_1}{\sqrt{\cos \theta - \frac{KL_j \sin \theta}{d_2 - d_1}}} \quad \dots (2.4)$$

There is a general belief that K and $L_j/(d_2-d_1)$ vary primarily with F_1 and hence, G is a function of F_1 and θ , or $G = f(F_1, \theta)$. The sequent depth ratio is computed as:

$$\frac{d_2}{d_1} = \frac{1}{2} \left(\sqrt{1 + 8G^2} - 1 \right) \quad \dots (2.5)$$

The solution of this equation, based on the experimental data of Hickox (1944), Kindsvater (1944) and U.S.B.R. is presented in the graphical form (Figure 2.7)

The following empirical equation proposed by Rajaratnam (1967) can also be used instead of figure 2.7 to find G in equation 2.5 and hence the sequent depth ratio:

$$G^2 = K_1^2 F_1^2 \quad \dots (2.6)$$

and

$$K_1 = 10^{0.027\theta} \quad \dots (2.7)$$

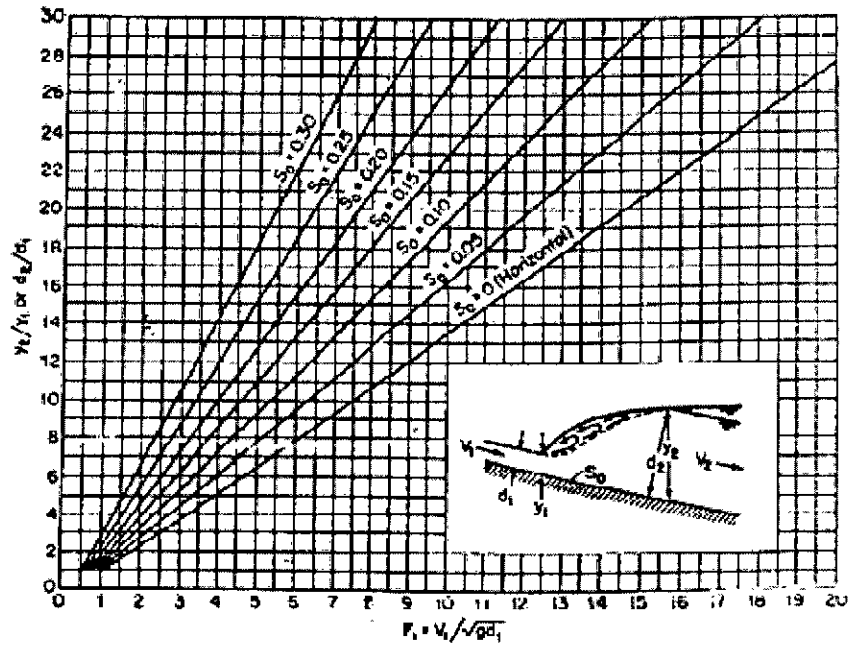


Figure 2.6: Experimental relations between F_1 and y_2/y_1 or d_2/d_1 for jumps in sloping channels (after Ranga Raju, 1993)

Alhamid, A.A. and Negm, A.M. (1966) studied the effect of channel slope and channel roughness on the value of the sequent depth ratio. They developed a theoretical prediction model using one-dimensional momentum and continuity equation. The equation is as follows:

$$\frac{d_2}{d_1} = \frac{1}{2} \left(\sqrt{1 + \frac{8}{(1 - C_s) \cos \theta} (1 - \frac{C_r}{2}) F_1^2} - 1 \right) \quad \dots (2.8)$$

In equation 2.6, effect of the slope is accounted for by the coefficient C_s while the coefficient C_r is introduced for the presence of the roughness elements. If the effects of both slope and roughness are excluded, i.e., $C_s = C_r = 0$, Equation corresponds to the Belanger's form.

The value of C_s and C_r were determined from experimental calibration. A linear regression analysis was used to compute a generalized equation for C_s in terms of the bed slope, S_0 to yield:

$$C_s = 1.8524 S_0^{0.595} \quad \dots (2.9)$$

The same procedure was used to evaluate the coefficient of roughness. This coefficient is a function of many parameters, such as the Froude number, F_1 , the roughness density, I , height of the roughness element, h_b and the length of the roughened bed, L_R . The roughness density, I , is defined as the ratio of the plan area of roughness elements to the surface area, i.e., $I = 100aN/L_Rb$, in which a = plan area of roughness element, N = number of roughness elements, L_R = length of the roughened bed, b = width of the channel. From an analysis of data an increasing trend for C_r to the flow and roughness parameters represented by the reciprocal factor $(F_1/I \times L_R/h_b)$ as ($R^2 = 0.954$):

$$\frac{C_r}{I} = 0.0007 \left[\frac{1}{\frac{F_1 L_R}{I h_b}} \right]^{-0.8963} \quad \dots (2.10)$$

Many experimental investigations were carried out to compute the sequent depth ratio and other related parameters of hydraulic jump in a sloping channel. Some prominent works in this topic of recent times were carried out by Hager (1992), Ohtsu and Yasuda (1991), Husain et al. (1995).

2.5.4 Characteristics of jump on sloping floor

Extensive experiments have been conducted by U.S.B.R. resulting in useful information on jumps on sloping floor. Based on U.S.B.R. study, the following significant characteristics of sloping floor jumps can be noted:

(a) *Sequent depth, y_t*

Defining y_2 = Equivalent sequent depth corresponding to y_t in a horizontal floor

jump = $\frac{y_t}{2} (-1 + \sqrt{1 + 8F_1^2})$, the sequent depth y_t is found to be related to y_2 as

$$\frac{y_t}{y_2} = f(\theta)$$

The variation of y_t/y_2 with $\tan\theta$ is shown in Figure 2.8a. By definition, $y_t/y_2 = 1.0$ when $\tan\theta = 0$ and it is seen from the figure that y_t/y_2 increases with the slope of the channel having typical values of 1.4 and 2.8 at $\tan\theta = 0.10$ and 0.30 respectively.

Thus the sloping floor jumps require more tail water depths than the corresponding horizontal floor jumps.

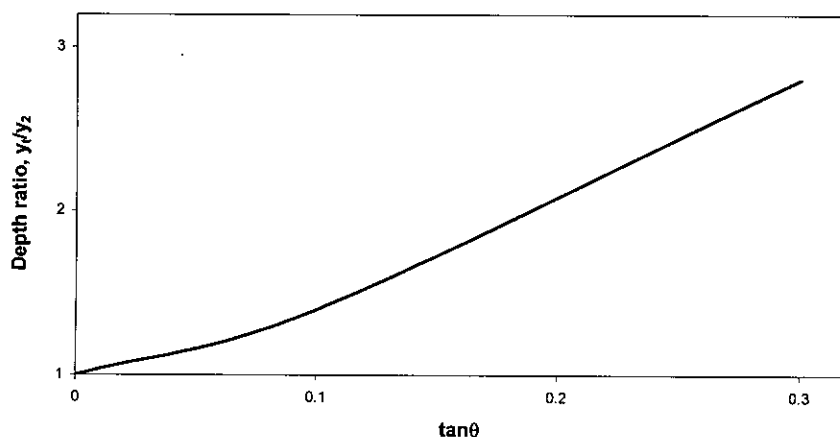


Figure 2.8a: Variation of y_1/y_2

(b) Length of the jump

Length of the jump L_j was defined in the USBR study as the horizontal distance between the commencement of the jump and a point on the subcritical flow region where the streamlines separate from the floor or to a point on the level water surface immediately downstream of the roller, whichever is longer.

The length of the jump on a sloping floor is longer than the corresponding L_j of a jump on a horizontal floor. The variation of L_j/y_2 with F_1 for any θ is similar to the variation for $\theta = 0$ case shown in Figure 2.3. In the range of $4.0 < F_1 < 13$, L_j/y_2 is essentially independent of F_1 and is a function of θ only. The variation can be approximately expressed as:

$$L_j/y_2 = 6.1 + 4.0 \tan \theta \quad \dots (2.11)$$

in the range of $4.0 < F_1 < 13$.

Elevatorski's analysis of the USBR data indicates the jump length can be expressed as:

$$L_j = m_s (y_t - y_1) \quad \dots (2.12)$$

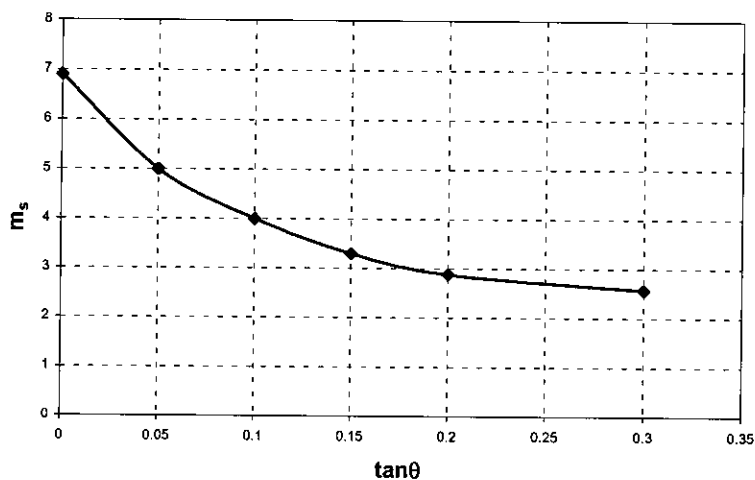


Figure 2.7b: Length of jump on sloping floor

In which $m_s = f(\theta)$. The variation of m_s with $\tan\theta$ is shown in Figure 2.7b. It may be seen that $m_s = 6.9$ for $\tan\theta = 0$ and decreases with an increase in the value of channel slope.

(c) Energy loss

Main use of the hydraulic jump is as an energy dissipator. So the energy loss occurred in the process of hydraulic jump is an important factor to be considered in the analysis.. Knowing the flow depths y_2 and y_1 and the length of the jump, the energy loss can be calculated as the difference between the upstream and downstream specific energy:

$$\begin{aligned}
 E_L &= (E_1 + L_j \tan\theta) - E_2 \\
 &= y_1 \cos\theta + \frac{V_1^2}{2g} + L_j \tan\theta - y_2 \cos\theta - \frac{V_2^2}{2g} \quad \dots (2.13)
 \end{aligned}$$

Where y_1 = sequent depth in a sloping channel at section 2. It is found that the relative energy loss E_L/H_1 decreases with an increase in the value of θ , being highest at $\tan\theta = 0$. The absolute value of E_L is a function of θ , being least when $\theta = 0$.

2.6 HYDRAULIC JUMP IN EXPANDING CHANNEL

2.6.1 Introduction

A channel whose cross-sectional shape varies along its length is a non-prismatic channel. The two distinctive non-prismatic channel stilling basins are the radially diverging stilling basin and the radially converging stilling basin (Whittington and Ali, 1969). Also classified as a non-prismatic stilling basin is the abruptly expanding basin (McCorquodale, 1986). Jumps in non-prismatic channels occur relatively often for low head dams with various parallel gates. If all of the gates are not opened, the supercritical flow may laterally expand in the stilling basin. Also the approaching channel to a stilling basin is always less wide than the tail water channel, given that a significant reduction of velocity occurs across the stilling basin. As a result the channel width must increase somewhere between the inflow to the stilling basin and the tail water channel. An economic solution involves a combination of width increase with the stilling of the high velocity flow.

In the present study, free expanding hydraulic jumps in a sloping smooth rectangular channel will be considered, whose sidewalls expand abruptly at the expansion section.

2.6.2 Classification of hydraulic jump in expansions

Hydraulic jumps in expanding channels may be described by the approaching conditions, such as the upstream depth h_1 , the inflow Froude number F_1 and the position of toe x relative to the expansion section. The geometry of expansion is given by expansion ratio $B = b_1/b_2$ where b_1 = channel width at the expansion section and b_2 = regular channel width.

A basic variable for hydraulic jumps is the tail water depth h_2 . Depending on the ratio of tail water depth to inflow depth ($D = h_2/h_1$) for any given combination of F_1 and B the toe position will be located either upstream or downstream from the expansion section. The expanding hydraulic jumps may be classified as follows (Rajaratnam and Subramanya, 1968; Bremen and Hager, 1993):

1. Repelled jump (R-jump),
2. Spatial jump (S-jump),
3. Transitional jump (T-jump).

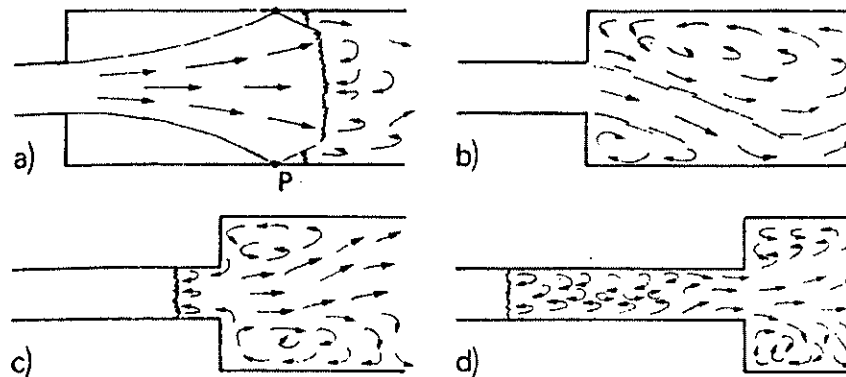


Figure 2.8: Types of jumps in abruptly expanding channel, (a) R-jump, (b) S-jump, (c) T-jump, (d) Classical jump

1. Repelled jump

The toe of the jump is located shortly downstream from the point where the two cross-waves hit the walls of the downstream channel (point P in Fig.2.9a). The toe within the cross-waves is located downstream from the jump fronts near the sidewalls. The R-jump has otherwise much analogy to the classical jump (Rajaratnam, 1967; Rajaratnam & Subramanya, 1968). The jump is symmetric but sensitive to tailwater variations.

2. Spatial jump

The toe of the jump is located between the expansion section and the point P. S-jumps are phenomena closer to a jet than to a jump. There is no marked toe of jump, but long fronts between forward and backward flow regions (Fig. 2.9b). S-jumps are asymmetric, either oscillatory or stably asymmetric, much in analogy to pressurized diffuser flow. Cyclic flow may even occur, with the intermediate formation of an R-jump, then breakdown and reformation of the S-jump.

3. Transitional jump

The toe of this jump is located upstream from the expansion section, may be considered as a transition between the spatial and the classical jump with a tail water expansion. A surface roller occurs in the upstream channel, and the toe is almost straight and perpendicular to the channel axis (Fig. 2.9c). T-jumps are extended partly in the upstream and partly in the downstream channel. In the latter, they may be either symmetric or asymmetric, depending on the jump position relative to the expansion section. The **classical jump** may be regarded as the asymptotic T-jump located in the upstream channel (Fig. 2.9d). Bremen and Hager (1993) discussed the main characteristics of the classical jump in comparison to the T-jump which are given in the following article.

2.6.3 Classical jump versus T-jump

The classical jump may be considered as the fundamental jump phenomena, as it retains the basic dissipation mechanisms and is not influenced by other effects such as the boundary geometry, wall roughness and inflow or outflow characteristics. The overall flow features of the classical jump are well understood today and may be summarized in terms of inflow Froude number F_1 exclusively. These include (Rajaratnam, 1967):

1. The sequent depth ratio D^* is defined by

$$D^* = \frac{1}{2} \left[(1 + 8F_1^2)^{1/2} - 1 \right]$$

or, if $F_1 > 2.5$ is considered

$$D^* = \sqrt{2}F_1 - \frac{1}{2}$$

2. The efficiency of jump $\eta^* = \Delta H / H_1$ as the relative head loss across the jump

$$\eta^* = 1 - (H_2/H_1) \cong \left[1 - \frac{\sqrt{2}}{F_1} \right]^2$$

The latter approximation holds for $F_1 > 2.5$.

3. The length of surface roller L_r^* is given as

$$\lambda_r^* = L_r^*/h_1 = -12 + 160 \tanh(F_1/20)$$

provided the inflow aspect ratio $h_1/b < 0.10$, and $F_1 > 2.5$.

- 3 The relative length of jump may be approximated as

$$\lambda_j^* = L_j^*/h_1 = 220 \tanh[(F_1 - 1)/22]$$

Two additional parameters must be considered for T-jumps, namely the relative toe position $X = x/L_r^*$ and the expansion ratio $B = b_1/b_2$. However, the combined parameter

$$\psi = (1 - \sqrt{B})[1 - \tanh(1.9X)]$$

suffices in conjunction with the characteristics of the classical jump for a thorough description of T-jumps. For $0.1 < X < 0.6$, and $4 < F_1 < 10$ as the significant domain of applications the following approximations apply:

1. Sequent depths ratio can be defined as

$$\gamma = D/D^* = 1 - 0.87\psi$$

2. Energy dissipation is given by

$$\delta = \eta/\eta^* \cong 2\sqrt{2}\psi F_1^{-1}$$

The linearisation on the right hand side indicates direct proportionality between δ and ψ .

3. Length of T-jump can be defined as

$$\beta = L_j/L_r^* = 1 + \psi$$

2.6.4 Previous Investigations

Over the past decades, many investigators had been studied the characteristics of hydraulic jumps in expanding channels as well as sloping channels. Early studies were presented by Jager in 1936 and by Frank in 1943 (after Rajaratnam, 1967). These studies did not have an exploratory character since neither the flow pattern of the jump, nor the disadvantages of jumps in expanding channel were observed (Hager, 1992).

Extensive experiments on abruptly expanding channels were conducted by Kusnetzow in 1958 (after Rajaratnam, 1967). He proposed a generalized equation for the sequent depth ratio D in terms of inflow Froude number F_1 and expansion ratio B . His equation is in disagreement with the well-known Belanger relation for the particular case of classical jump, however. After extensive experiments with b_1/b_2 varying from 0.01 to 1.0 and F_1 from 1 to 7.25 Kusnetzow presented the experimental equation:

$$\frac{y_2}{y_1} = 0.5 \frac{b_1}{b_2} \left[0.8 - 0.15 \left(0.9 - \frac{b_1}{b_2} \right) \right] \left(\sqrt{1 + \frac{8F_1^2}{b_1/b_2}} - 1 \right) \quad \dots (2.14)$$

Unny (1961) developed a more rational expression for y_2/y_1 by using the momentum equation and certain basic assumptions. According to his analysis the supercritical stream entrains water from the sides, and considerable turbulence is produced in the zones of maximal velocity gradients on the sides of this expanding stream. In addition there is vertical expansion in the jump. Because of the mixing and turbulence on the sides the energy dissipation in this jump is greater than in the corresponding classical jump, and so with comparable upstream conditions the h_2 required in this case will be smaller. Unny applied the momentum equation to the volume of fluid confined by the boundary ACDE (Figure 2.9) on the plan.

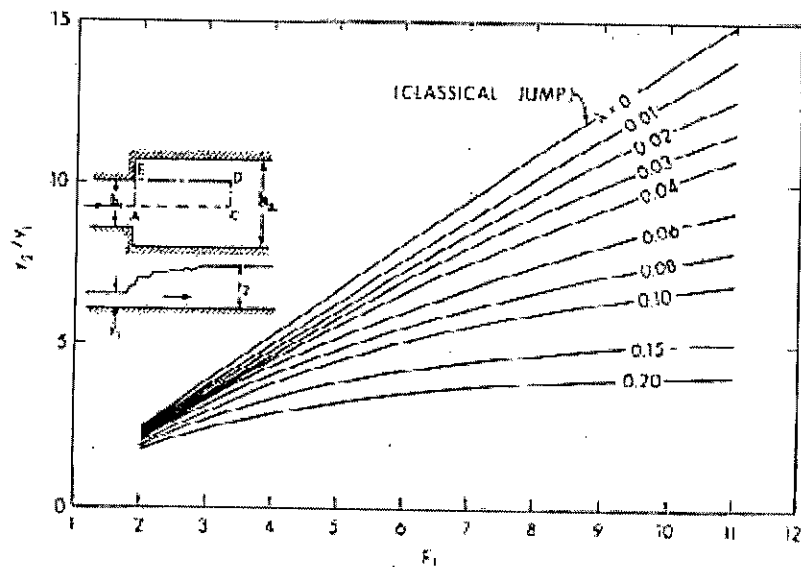


Figure 2.9: Jump at an abrupt expansion, Unny(1961)

He assumed the velocity distribution to be uniform at the two end sections and neglected the turbulent momentum and the integrated bed shear stress. This developed model was restricted to toe positions because of very closeness to the expansion section. On the basis of these premises the sequent depth ratio is:

$$\frac{y_2}{y_1} = \frac{1}{2} (1 + K_1 \lambda F_1^2) \left(\sqrt{1 + \frac{8F_1^2}{(1 + K_1 \lambda F_1^2)^2}} - 1 \right) \quad \dots (2.15)$$

Where $\lambda = y_1/b$ and K_1 is a coefficient. In experiments with $b/B = 0.5$ the coefficient K_1 was found equal to 2.2. Unny evaluated Equation 2.15 and plotted y_2/y_1 against F_1 for various values of λ and for $b/B = 0.5$; his plot is reproduced in Figure 2.11. It is seen that for any F_1 the sequent depth ratio is much less than that in the corresponding classical jump.

Herbrand (1973) investigated the spatial jumps in expanding channels and suggested a simple empirical relation for calculating the sequent depths ratio as

$$D/D^* = B^{3/8} \quad \dots (2.16)$$

where D is the sequent depth ratio of jumps in expanding channels, D^* is the sequent depth ratio of classical jumps in prismatic channels, and B is the expansion ratio. The experiments of Herbrand were confined to jumps of which the toe was located "slightly upstream from the expansion section". Froude number varied between 3.1 and 9.6 and expansion ratio B varied from 1 up to 0.288.

Magalhaes and Minton's (1975) configuration was particular as the test reach was in a channel of constant width. The upstream channel portion was subdivided by a wall. The discharge in both approaching channels was different and a number of phenomena were discussed. Additional results on the diffusion of jet were summarized by Magalhaes (1981).

Compared to the previous studies, the relative toe positions was accounted for as $X = x/L_r^*$, in which L_r^* is the roller length of the classical jump. Based on logical concepts and a larger number of experiments, where symmetric and asymmetric

expansions were considered, the equation for the sequent depths is (Bremen and Hager, 1993)

$$D = D^* - (D^* - 1) \left(1 - \sqrt{B}\right) \left[1 - \tanh(1.9X)\right] = \psi(B, X). \quad \dots (2.17)$$

They defined such types of jumps as Transitional jumps (T-jumps). They found that T-jumps are more effective energy dissipator than other types of jumps, such as Repelled jumps (R-jumps) and Stable jumps (S-jumps) in expanding channels. For $X=0$, Eqn (2.16) yields a similar features as Herbrand's relation (Equation 2.15) for free S-jumps which is formed at the expansion section. Eqn (2.6) for $X=0$ can be expressed as

$$D = 1 + \sqrt{B}(D^* - 1) \quad \dots(2.18)$$

A parameter ψ is the function of both B and X on the right hand side of Equation 2.16. For $X > 1.3$, that is if the end of jump is at the point of expansion, or for $B=1$, no effect of expansion occurs and $D = D^*$. For any given toe position $0 < X < 1.3$, the reduction of D increases as the toe position decreases and the expansion ratio increases.

Bremen and Hager (1993) were also able to relate the degree of asymmetry (either stable asymmetric, oscillating or symmetric) to the position parameter X and the expansion parameter B . For a parameter $\psi < (1 - 0.67X)/8$, nearly symmetrical T-jumps occur, whereas stable asymmetric flow was observed for $\psi > 0.28$. For intermediate ψ -values, the T-jump oscillates, much as it does for diffuser flow. The length of T-jump, L_j , based on the detrainment of air bubbles was related to the value relative to the value $\psi = \psi(B, X)$ and empirically found as

$$\frac{L_j}{L_j^*} = 1 + \psi. \quad \dots(2.19)$$

Predictive performance of Eqn. (2.16) against the experimental observations was not given in full details by Bremen and Hager.

Matin et al (1998) developed an simple prediction model for computing sequent depth ratio of hydraulic jumps in abruptly expanding rectangular channel. Format of

the prediction equation is similar to well known Belanger's equation for classical jump with modification in Froude number. Modified Froude number term of the derived equation contains two additional parameters, one of them incorporates the effect of abrupt expansion and the second one represents for describing the position of jump upstream the expansion. The relationship between the modified Froude number and Inflow Froude number is expressed as:

$$E_1^2 = k_1 + \frac{2F_1^2}{k_2} \quad \dots (2.20)$$

In which k_1 and k_2 are the assumed parameters to account for the jump position and effect of expansion ratio. These parameters are defined as:

$$k_1 = \frac{(e^2 - 1)(1 - B)}{2(1 - D^{-1})} \quad \dots (2.21)$$

$$k_2 = \frac{1 - D^{-1}}{B(1 - BD^{-1})} \quad \dots (2.22)$$

Here, $D = h_2/h_1$, $B = b_1/b_2$ and $e = h_e/h_1$

From the above equations, it is clear that for classical jump with $B = 1$, the parameters $k_1 = 0$ and $k_2 = 1$, then the equation reduces to well known Belenger's equation for classical jump in prismatic channel. If the toe position of the jump is located at the expansion, i.e., $e = 1$, then the parameter $k_1 = 0$, the jump is characterized only by parameter k_2 and termed as free jumps at the expansion.

From the experimental data two parameters were evaluated. They expressed these parameters as a function of independent known variables B , F_1 and X . Following expressions are found to fit the data well for the jump toe located at various positions upstream of the expansion section.

$$k_1 = -\frac{1}{2} X (\ln B) F_1^{1.5(B+1)} \quad \dots (2.23)$$

$$k_2 = 1 - 0.4 [\ln B] [1 + \ln F_1] \quad \dots (2.24)$$

Hasan (2001) conducted a study to determine the validity of the range of parameters used in the equation developed by Matin et al. (1997, 1998) Based on some experimental data he proposed two modified equation to compute the parameters k_1 and k_2 :

$$k_1 = -\frac{1}{2} X(\ln B) F_1^{2.25(B+0.8)} \quad \dots (2.25)$$

$$k_2 = 1 - 0.35[\ln B][1 + \ln F_1] \quad \dots (2.26)$$

This is revealed from the above discussion that many researches have been carried out to analyze the hydraulic jump in prismatic channels, channels with sudden expansion or sloping channel. No works have been carried out to compute the sequent depth ratio for hydraulic jump in an abrupt expansion of a sloping channel. This study has been directed to serve this purpose.

Chapter Three

THEORETICAL FORMULATION

3.1 INTRODUCTION

In spite of the fact that considerably more is known about the jump formation in horizontal channels than in irregular ones like sloping channel or channel with abrupt expansion, the latter ones are often preferred for energy dissipation or other purposes. The nature of the hydraulic jump in an abrupt expansion of a sloping channel is a complex and poorly understood problem. In the present study, particular attention is focused on free jump in the abruptly expanded sloping channel. Considering the complexity and scope of the problem, several assumptions and restrictions were made in order to make the problem simple. These are discussed in the following section.

3.2 ASSUMPTIONS

The following assumptions have been made in formulating the theoretical equation describing the relationship between the sequent depth ratio with upstream Froude number and other associated variables (expansion ratio, slope of the channel etc.).

The assumptions are:

- One-dimensional steady flow is taken into account.
- The channel is sloping, rectangular and straight.
- The fluid is incompressible.
- Velocity distribution over the upstream and downstream section is uniform.
- Channel banks are fixed.
- At the beginning and at the end of the jump, the pressure distribution is hydrostatic.
- Turbulence effects and air entrainment are not included in the analysis.
- The frictional resistance from the sidewalls and bed of the flume is neglected.
- The sequent depth is the temporal mean value of its fluctuations

3.3 GOVERNING EQUATIONS

Water motion is the essential process in open channel hydraulics. Three basic equations of fluid mechanics to describe water motion are the continuity equation, the energy equation and the momentum equation, which are based on the principles of conservation of mass, energy and momentum, respectively.

1. Continuity Equation

The continuity equation is the statement of the law of conservation of mass. In a steady, incompressible flow in an open channel or pipe, volumetric flow rate past various sections must be the same. Mathematically this is described as:

$$Q = AU \quad \dots(3.1)$$

where Q is the discharge flowing through the cross-sectional area A with a velocity U

2. Energy Equation

In the one-dimensional analysis of steady open channel flow, energy equation in the form of Bernoulli's equation is used. Energy equation, which is based on the principle of conservation of energy, can be described as follows, for prismatic channels:

$$z_{b1} + h_1 + \alpha_1 \frac{U_1^2}{2g} = z_{b2} + h_2 + \alpha_2 \frac{U_2^2}{2g} + h_f \quad \dots(3.2)$$

In the above equation each term represents the energy per unit weight of water. Here, z_b is the bed elevation, h is flow depth and the third term of both sides of the above equation represents the velocity head. Subscripts 1 and 2 denote the upstream and downstream flow conditions, respectively. h_f is the loss of energy between the sections.

3. Momentum Equation

In addition to continuity and energy equation, momentum equation is another important tool in the field of open channel hydraulics. The momentum equation commonly used in most of the open-channel flow problems is the linear-momentum equation. This equation states that the algebraic sum of all external forces acting in a

given direction on a fluid mass equals the time rate of change of linear momentum of the fluid mass in that direction. Mathematically:

$$\rho Q(\beta_2 U_2 - \beta_1 U_1) = F_{p1} - F_{p2} + W \sin \theta - F_f \quad \dots(3.3)$$

The left-hand side of the above equation represents the change of momentum and the right hand side represents the resultant force between the upstream and downstream sections of the flowing water. Terms of the R.H.S are:

F_{p1} = Hydrostatic force on section 1

F_{p2} = Hydrostatic force on section 2

$W \sin \theta$ = body force, i.e., the component of the weight of the fluid in the longitudinal direction.

F_f = Frictional force on the bed between two sections

Generally, it is necessary to compute two unknowns by using the basic equations. For example, it may be required to compute the depth of flow h and the flow velocity U at a downstream section in a channel when the flow conditions of an upstream section are known. Obviously, we need two equations to compute the two unknown quantities.

For the hydraulic jump downstream of the sluice gate, the energy equation cannot be used because of the significant internal energy loss h_f involved in the jump. However, the momentum equation can be used without difficulty since the jump takes place in a short distance and the external friction force F_f is negligible. Therefore, the continuity and momentum equations are used to compute the depth h_2 and the flow velocity U_2 . Once the depth h_2 is known, the energy equation may be used to compute the unknown energy loss h_f .

3.4 THEORETICAL FORMULATION

The definition sketch for a hydraulic jump in an abrupt expansion in a sloping channel is shown in Fig. 3.1. The toe of the hydraulic jump is located at the expansion section.

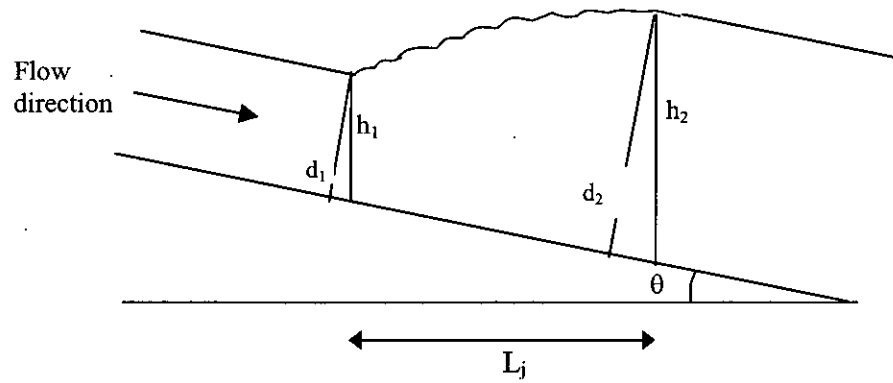


Figure 3.1a: Definition sketch of hydraulic jump in a sloping channel

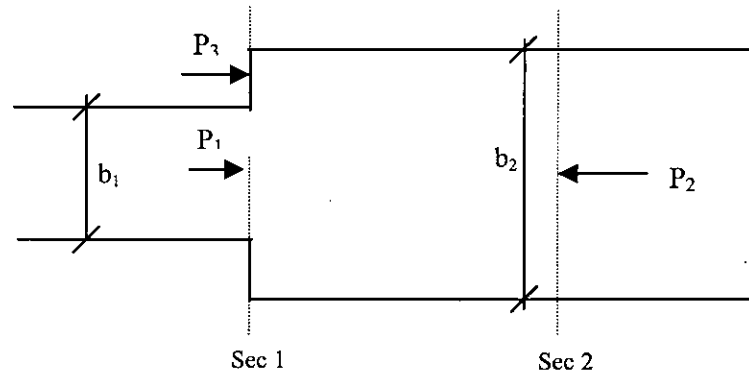


Figure 3.1b: Expansion geometry

Considering the assumptions in article 3.2, the momentum equation for the control volume between section 1 and section 2 of Fig 3.1b can be written as

$$P_1 + P_3 - P_2 + W \sin \theta = \frac{\gamma}{g} Q(U_2 - U_1) \quad \dots(3.4)$$

Here, P_1 , P_2 and P_3 are the hydrostatic pressure forces that can be defined as:

$$P_1 = \frac{1}{2} \gamma b_1 h_1^2 \cos^3 \theta = \frac{1}{2} \gamma b_1 d_1^2 \cos \theta,$$

$$P_2 = \frac{1}{2} \gamma b_2 h_2^2 \cos^3 \theta = \frac{1}{2} \gamma b_2 d_2^2 \cos \theta$$

$$P_3 = \frac{1}{2} \gamma (b_2 - b_1) h_1^2 \cos^3 \theta = \frac{1}{2} \gamma (b_2 - b_1) d_1^2 \cos \theta$$

and, $W \sin \theta$ = component of the weight of water in the control volume (bounded by section 1 and section 2) along the length of the channel.

Defining $W \sin \theta = \frac{1}{2} \gamma K L_j (d_1 + d_2) b_2 \sin \theta$, where

γ = Unit wt of water

θ = Channel bottom slope

L_j = Length of the hydraulic jump

d_2 = Downstream depth

d_1 = Upstream depth

K = Modification factor due to assumption of linear jump profile.

Using the continuity equation, $Q = U_1 b_1 h_1 = U_2 b_2 h_2$, where U_1 = upstream velocity and U_2 = downstream velocity, equation 3.4 takes the form:

$$\left(\frac{\gamma d_1^2}{2} - \frac{\gamma d_2^2}{2} \right) \cos \theta b_2 + \frac{1}{2} \gamma K L_j (d_1 + d_2) b_2 \sin \theta = \rho Q (U_2 - U_1) \quad \dots (3.5)$$

Rearranging, this can be written as:

$$(d_1^2 - d_2^2) \cos \theta + \gamma K L_j (d_1 + d_2) \sin \theta = \frac{2}{g} \left(\frac{Q^2}{b_2 d_2 b_2} - \frac{Q^2}{b_1 d_1 b_2} \right) \quad \dots (3.6)$$

Introducing the dimensionless terms:

B = expansion ratio = b_1/b_2

D = sequent depth ratio = d_2/d_1

F_1 = inflow Froude number = $\frac{U_1}{\sqrt{g d_1}}$

Equation 3.6 can be written as:

$$(D + D^2) \left[\cos \theta - \frac{\gamma K L_j \sin \theta}{d_2 - d_1} \right] = \frac{2 F_1^2 B (B - D)}{1 - D} \quad \dots (3.7)$$

To get a solution for D in the Belanger's format, equation 3.7 is modified as:

$$D^2 + D - 2 E_1^2 = 0 \quad \dots (3.8)$$

Where, E_1 = modified Froude number

$$\text{Mathematically, } E_1 = F_1 \sqrt{\frac{B(B-D)}{(1-D) \left[\cos\theta - \frac{\gamma K L_j \sin\theta}{d_2 - d_1} \right]}} \quad \dots (3.9)$$

The relationship between E_1 and F_1 can be rearranged as

$$E_1^2 = \frac{F_1^2}{k_1(1-k_2)\cos\theta} \quad \dots(3.10)$$

Where parameter k_1 is the modifying factor that incorporates the effect of sudden expansion and parameter k_2 is the modifying factor that incorporates the effect of channel slope.

k_1 and k_2 can be defined as:

$$k_1 = \frac{1-D}{B(B-D)} \quad \dots (3.11)$$

$$k_2 = K\gamma \frac{L_j}{d_2 - d_1} \tan\theta \quad \dots (3.12)$$

It is obvious that establishing the relation of sequent depth ratio requires determination of two parameters k_1 and k_2 . k_1 is a function of expansion ratio and Froude number. k_2 is a function of dimensionless jump length, $L_j/(d_2-d_1)$ and modifying factor K . These two quantities are again a function of θ and F_1 . So it is possible to find the factors k_1 and k_2 from the experimental data and then the sequent depth ratio can be found from the equation

The sequent depth ratio D is obtained by solving Equation (3.8) as

$$D = \frac{1}{2} \left(\sqrt{1 + 8E_1^2} - 1 \right) \quad \dots(3.13)$$

From equations (3.11) and (3.12), it is clear that for classical jump $B = 1$, the parameters $k_1 = 1$ and $k_2 = 0$, then equation (3.13) reduces to well-known Belanger equation for classical jump in prismatic channel.

3.5 CALIBRATION OF THE DEVELOPED THEORETICAL EQUATION

The parameters k_1 and k_2 of the equation (3.10) can not be predicted theoretically and hence experimental data are needed to evaluate it. It is necessary to express the parameters k_1 and k_2 as a function of independent known variables like F_1 , B and θ . For the given values of expansion ratio B and channel slope θ , the sequent depth ratio D have been computed from the present experimental study for different values of inflow Froude number F_1 . The observed data are used in equation (3.11) and (3.12) to compute k_1 and k_2 , respectively. The modified Froude number E_1 has been computed from equation (3.10).

Chapter Four
EXPERIMENTAL SETUP

4.1 INTRODUCTION

The experimental study was conducted at the Hydraulics and River Engineering Laboratory of the Department of Water Resources Engineering of Bangladesh University of Engineering and Technology (BUET). The experimental setup as well as the measuring techniques used in the experimental process is discussed in the following articles.

4.2 DESIGN OF EXPANDED SLOPING CHANNEL.

4.2.1 Introduction

The hydraulic jump used for energy dissipation is usually confined partly or entirely to a channel reach that is known as the stilling basin (Chow, 1959). The particular attention of this present study is focused on jumps formed in the sloping stilling basin with a sudden expansion i.e., abrupt expansion of the width of a stilling basin. The most essential part of the present study was the design and fabrication of an expanding stilling basin. Therefore, during the study a considerable period of time was spent in fabricating the expanding sloping stilling basin in the laboratory.

4.2.2 Design

The experiments were performed in the 70-ft long tilting flume in the laboratory. Another flume in the laboratory is 40 ft long and it is comparably easier to operate this flume. But the range of Froude number found in the experiment in this flume is very small. So it was decided to conduct the research in the larger flume. Tilting facility of the flume was used to make it to a sloping channel. It was possible to create only mild slopes in this artificial channel (highest possible slope is 1 in 70). To create a hydraulic jump in the channel it is necessary to install a sluice gate in the channel. A considerable period of time was spent in the design, construction and installation of a new sluice gate in the flume.

4.2.3 Constriction Elements in the Stilling Basin

For maintaining the exact expansion ratio B , several constriction elements were installed in the stilling chamber in the laboratory flume. They were made of well-polished wood. Just downstream of the sluice gate, there were two constriction elements installed along the direction of flow to make a reduced channel in the middle of the chamber. There was no lateral movement of water between the constriction elements and the sidewalls because of watertightness of these elements. Each element of rectangular cross section had a 5-ft (1.52 m) length and 2 ft (0.6098 m) depth, and its width depends on the expansion ratio B . The length of the constriction elements was chosen so because the range of the location of the stabilized classical jump formed on the flume was between 2-ft (0.6096 m) and 9 ft (2.75 m) downstream from the sluice gate.

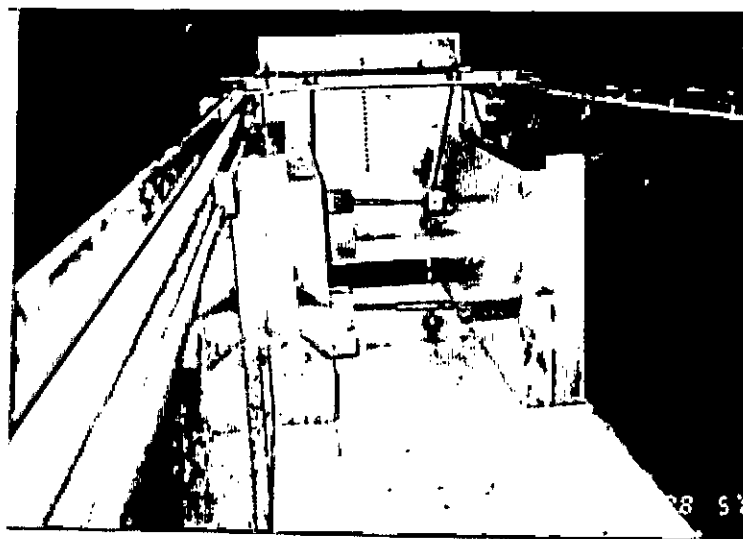


Figure 4.1: Photograph of experimental setup, downstream of sluice gate

4.2.4 Transitions in the Stilling Basin

A channel transition may be defined as a local change in cross-section, which produces a variation of flow from one uniform state to another. The term 'local' is used to signify that the change takes place in a length of channel, which is short compared, to its overall length.

A transition, by reducing the width of the stream without varying the depth, was provided just upstream of the sluice gate to avoid excessive energy losses, and, to eliminate cross-waves and other turbulence. The transition was made of wood having good polish. Thus a gradual transition was created.



Figure 4.2: Photograph of transition elements at upstream of sluice gate

Since the constrictions were placed symmetrically, the width of the each portion of transition depends on the expansion ratio.

The equation of the curvature portion of the transition, which is generally known as Chaturdevi's semi - cubical parabolic transitions, is given below:

$$x = \frac{L \times W_c^{1.5}}{W_c^{1.5} - W_f^{1.5}} \left[1 - \left(\frac{W_f}{W_x} \right)^{1.5} \right] \quad \dots (4.1)$$

Where

x = Distance from the opening of the sluice gate (m)

L = Length of the transition (m), the value is 0.3048 m in this study

W_c = Channel width (m), the value is 0.7620 m in this study

W_f = Width of throat (m), it depends on B

W_x = Width of flume at distance x from throat (m).

Figure 4.1 shows the elements used to create sudden expansion in the channel and Figure 4.2 shows the elements used to make the gradual transition upstream of sluice gate.

4.3 EXPERIMENTAL FACILITIES

The experimental setup involved the use of a laboratory tilting flume having an adjustable sluice gate and an adjustable tailwater gate, water tank, pump, water meter and various constriction elements. A brief description of the apparatus and auxiliary equipment used in the experiments is given in the subsequent articles.

4.3.1 Laboratory Flume

Experiments were performed in a 70 ft (21.34 m) long channel of a uniform rectangular cross section with glass sidewalls and painted steel bed, located in the Hydraulics and River Engineering Laboratory of the Water Resources Engineering

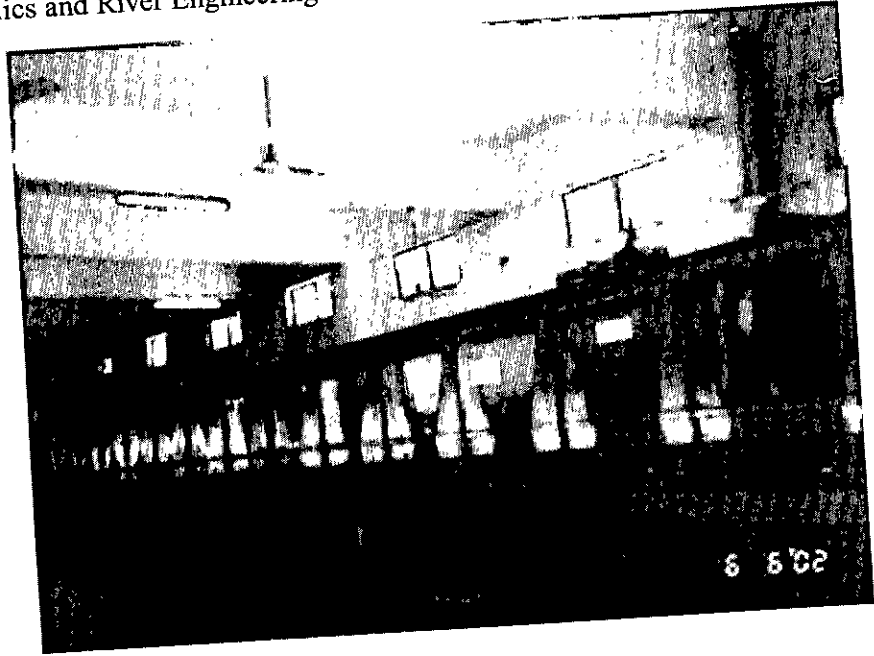


Figure 4.3: Photograph of the 70-ft long Laboratory tilting flume.

Department (Photograph 4.3). The channel width is 2.5-ft (0.7622m) and the sidewall height is approximately 2.5-ft (0.7622 m). It is supported on an elevated steel truss that spans the main supports. The channel slope can be adjusted using a geared lifting mechanism.

The whole flume consists of an upstream reservoir and a stilling chamber with contraction reach. The original channel width was reduced by various constrictions. All constriction elements, which were made of wood, had an inlet of parabolic shape that was located just upstream from the sluice gate. Downstream from the gate, a channel having width = b_1 was the approaching channel to the expansion. Dimension of b_1 was fixed accordingly with the value of expansion ratio, B .

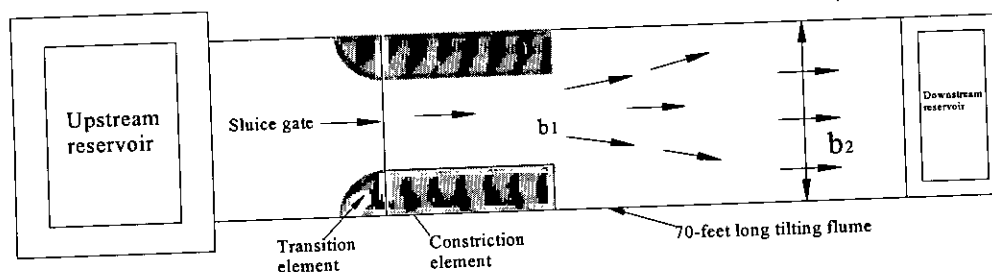


Figure 4.4: experimental setup

The flume has an adjustable sluice gate and an adjustable tailwater gate located, respectively, upstream and downstream of the expansion geometry. The tail water depth was controlled by a vertical gate located at the downstream end of the flume. Water issuing through an opening of the sluice gate, located some 4 m downstream from the reservoir, formed the supercritical stream. During the experiments, the location of the hydraulic jump was controlled by the downstream gate and discharge. The sluice gate and the flow discharge control the quasi-uniform flow upstream of the jump and the tailwater gate acts as a downstream control.

The circulation of the water within the flume is a closed system. From the storage reservoir the water is transported by means of the pipeline to the upstream reservoir. There are two types of pipelines viz. suction and delivery pipeline. Suction pipe sucks the water from the storage reservoir and at the same time passes that water through the pump. The water is delivered to the channel through the delivery pipe and returns to the storage reservoir.

4.3.2 Pump

A centrifugal pump with maximum discharge capacity of 200 l/s draws water from tank through valve and supplies it to the channel. The pump was calibrated so that the water discharge could be set to the desired quantity. The pump used for water circulation can be run for 8 hours at a stretch. No stand by pump is available.

4.3.3 Motor

The capacity of the motor, which drives the pump, is 3 HP. The motor uses the electrical energy by a shaft attached to it to drive the pump.

4.4 MEASURING DEVICES

4.4.1 Water Meter

Two electromagnetic water meters are placed in the delivery pipes. The gate valve just upstream of the meter in the pipeline can control the discharge through the meter. The discharge measurements are made with the help of these water meters.

4.4.2 Miniature Propeller Current Meter

The miniature propeller current meter consists of propellers rotating about a horizontal axis. The propeller is fixed at one end of the shaft while the other end of the shaft is connected with the help of a wire. The revolution of the propeller is displayed in the counter, which is operated by batteries.

The calibration of the present current meter was done by mounting the meter on a carriage that runs on rails along a straight channel and moves the propeller of the

current meter through still water. The speed of the carriage was determined by the time required to travel a known distance. With several runs at various speeds the relation between revolution of the propeller per unit time and water speed was determined. The calibrated results are given below:

1) For $0 < n < 1.31$

$$U = 0.2344n + 0.0313$$

2) For $n \geq 1.31$

$$U = 0.2460n + 0.0161$$

Where n is the revolution per sec displayed in the current meter and U is the velocity of the flowing water in meter per second.

4.4.3 Velocity Meter

For the measurement of velocity, a programmable 2-D electromagnetic liquid velocity meter is used. The name of the meter is "P.-E.M.S.", made in Netherlands, year of manufacture is 1993. Velocity ranges up to 2.5 m/s.

The probe has four-quadrant response that enables direction-independent measurements. By changing the absolute value notations, the velocity vector can be measured. This is, in fact, the inside-out version of the well-known pipe flow meter employing Faraday's Induction Law for measurement of the velocity (U) of a conductive liquid moving through a magnetic field. The magnetic field is induced by a pulsed current through a small coil inside the body of the sensor. Two pairs of diametrically opposed platinum electrodes sense the Faraday-induced voltages produced by the flow past the sensor.

The sensor has been designed in such a way that these voltages are proportional to the sine and cosine of the magnitude of the liquid velocity parallel to the plane of the electrodes. By means of advanced electronics, the low level output signals of the probe are converted into high level output signals from which the magnitude of the velocity and its direction can be derived through the application of common

trigonometry. The induced magnetic field strength is relatively high, although the coil consumes little power. This is achieved by a duty cycle of 25% for the coil. Together with a synchronized detection on system, this will result in minimum interference sensitivity. Synchronization of 50 Hz will make the system insensitive to interference from the power supply.

The device has a display window from where data can be directly read. For continuous data, the device can be attached to a computer and data can be registered very easily. For the present study, 3 data were recorded for a single point and the average of these values is taken as the velocity of that point.

4.4.4 Point Gauge

The water level and the bed level are measured with the help of a point gauge (Figure 4.5). The point gauge is suitable for swiftly flowing liquids without causing appreciable local disturbances. The gauge is mounted on a frame laid across the width of the channel. The whole structure of point gauge could be moved on side rails. The point gauge is accurate within 0.1 mm.

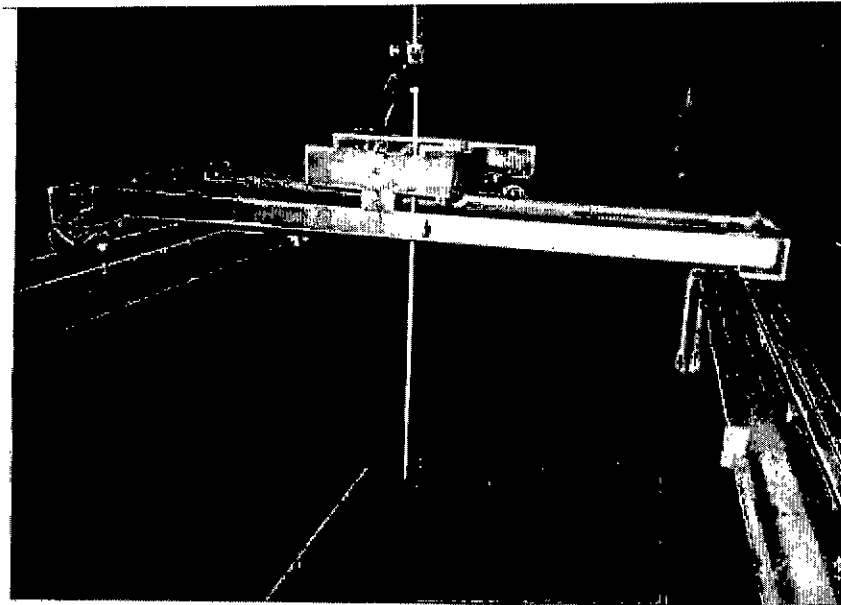


Figure 4.5: Photograph of point gauge

4.5 MEASUREMENTS

4.5.1 Discharge

Discharge, Q in the flowing channel is measured with the help of water meter. The flow-circulating pipe is equipped with two electromagnetic flow meters that enable to measure the discharge through the channel very precisely by digital measuring scale.

4.5.2 Water Surface Elevation

Measurements of water surface elevation were taken both at the upstream and downstream of the jump. Measurements were taken by the point gauge. The gauge reading at the bed was set to zero so when the reading of water surface elevation was taken it gave directly the water depth data. In this way both the initial and sequent depth were taken. At both sections three readings were taken and then the average of these three was used for the analyses.

4.5.3 Velocity

Velocity measurements were taken after jumps had been stabilized; those did not move and became static. Both the probe and the current meter were placed at a constant depth of $0.6h$ from the water level to obtain the average velocity in some of the experiments. By this method some of the readings were taken. Actually the average velocity at the upstream section was required for the analysis mainly to calculate the inflow Froude number. So this average velocity was found by dividing the channel discharge by the cross-sectional area of the upstream section.

Chapter Five

EXPERIMENTAL PROCEDURE

5.1 INTRODUCTION

Whole experimental procedure of the study was divided into two parts: preparation of the flume as per requirement of the experiment and running of experiments. The construction period was more than one month. Running the experiment and collecting the required data require not only a great deal of physical works but also a careful observation. For conducting the experiment the following procedure was followed.

5.2 STEPWISE PRE-EXPERIMENTAL MEASURES

Step 1: The detail drawings of the experimental flume and the accessories were collected.

Step 2: The constriction elements were made and painted to protect from bending and soaking.

Step 3: Three adjustable screws of mild steel rod were made in the machine shop. One was positioned at the approach of the gate on the transition and remaining two on the expanding channel to fix the position of the constriction.

Step 4: For the measurement, the accessories — the point gauge, the current meter, and the electromagnetic probe were placed in a particular position of the flume.

Step 5: Before the experimental run, the sidewall glass was cleaned to make the flume transparent, for ease of data collection through eye observation. Also the bed of the flume was painted to protect it from corrosion due to contact with water.

5.3 STEPWISE EXPERIMENTAL PROCEDURE

Step 1: The first step was the selection of the sluice gate opening. The lowest value of the gate opening was fixed to 5 cm.

Step 2: The second step was the fixation of the discharge. For every gate opening three discharges were taken to get a range of inflow Froude numbers.

Step 3: By adjusting the tailwater gate, location of the hydraulic jump was fixed to the position of abrupt expansion.

Step 4: For the different discharges, the required data for the different jumps with varying Froude numbers were also obtained.

Step 5: The above four steps were performed sequentially at the different sluice gate openings in ascending order.

Step 6: The above five steps were performed for different expansion ratios and different channel slopes.

5.4 EXPERIMENT NUMBERING

In order to carry out the test runs systematically, the experiments are coded. The procedure of experiment numbering is described below.

The experimental numbering is chosen in such a way that all the variables can be recognized. For the experiments, several influences are studied — the expansion ratio B , channel slope, and the inflow Froude number F_1 .

The first term of the experiment code represents the expansion ratio. In the present study, four different expansion ratios were used. The an expansion ratio B of 0.50 is represented by "A", an expansion ratio of 0.60 is represented by "B", an expansion

ratio of 0.70 is represented by "C" and an expansion ratio of 0.80 is represented by "D".

The second number in the code represents the channel slope. Test runs were performed for three slopes. The slope 0.0042 is represented by "1", 0.0089 by "2" and 0.0131 by "3" and "0" represents horizontal channel

The third number in the code represents the gate opening. Data were taken for five gate openings. First reading was taken for gate opening = 5cm. At this time, screw was tightened to 4th hole of the sluice gate. It is represented by "4", similarly fifth reading was taken for gate opening = 15cm. This is represented by "9" as the screw was tightened to 9th hole.

The fourth number in the code represents discharge. For every gate opening, three runs were performed. First run is represented by "A", second run by "B" and third run is represented by "C"

According to this numbering system, the experiment number B27C means that when the sluice gate size is opening = 11 cm, then a stabilized jump is formed in an expanding channel having an expansion ratio of 0.70 and the channel slope = 0.0089. It also indicates the third reading of this particular gate opening with mentioned expansion ratio and channel slope.

5.5 DATA COLLECTION

For collection of data, four different expansion ratios viz. 0.80, 0.70, 0.60 and 0.50 were chosen. For each expansion ratio, there were three channel slopes – 0.0042, 0.0089 and 0.0131 and five gate openings - 5.0 cm, 9.0 cm, 11.0 cm, 13.0 cm and 15.0 cm where water entered into the expansion section. The data on discharges, sequent depths, and inflow Froude numbers are presented in Table 5.1 through 5.14. Various features of the hydraulic jump that was analyzed during the course of the study are shown in figures from 5.1 to 5.6.

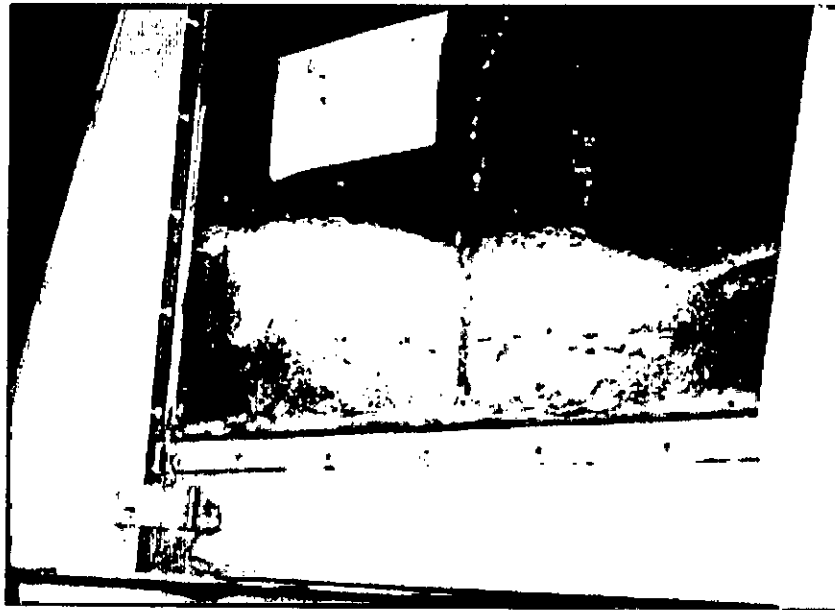


Figure 5.1: Side view of a T – jump ($B = 0.5$, Slope = 0.0131, Gate opening = 13cm)

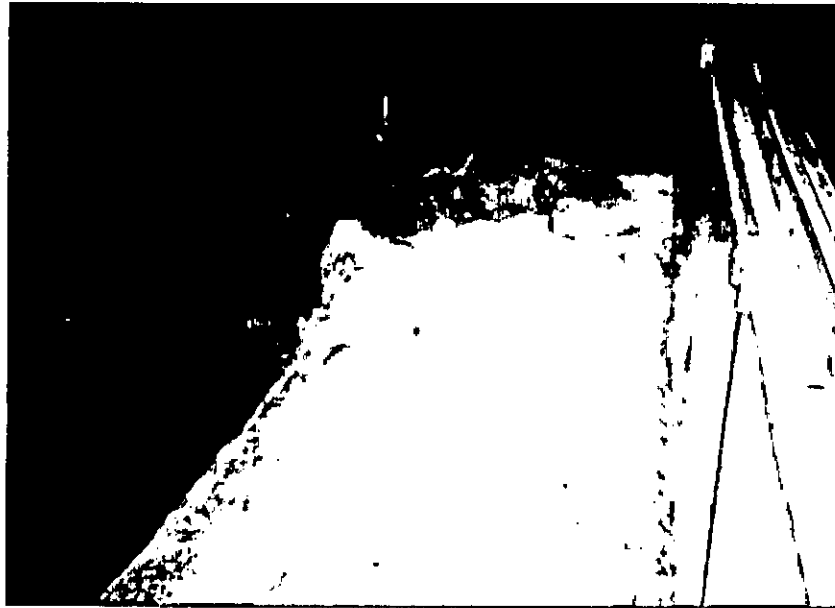


Figure 5.2: hydraulic jump in a horizontal rectangular channel.



Figure 5.3: Close view of turbulence created in jump at the abrupt expansion of a sloping channel.



Figure 5.4: Jump is approaching towards the expansion section due to raising the tail water gate.



Figure 5.5: Asymmetric jump formed at the section of sudden expansion.



Figure 5.6: Initial stage of jump formation in an expanding channel

Table 5.1: Experimental data for B = 0.8, Slope = 0.0042

Run no.	B	Slope	Q (L/s)	h ₁ (m)	h ₂ (m)	D	V (m/s)	F ₁	L _r (m)
A14A	0.8	0.0042	85	0.0615	0.2565	4.17	2.22	2.86	2.14
A14B	0.8	0.0042	94	0.0615	0.2870	4.67	2.46	3.16	3.23
A14C	0.8	0.0042	104	0.0615	0.3027	4.92	2.72	3.50	3.32
A16A	0.8	0.0042	107	0.0662	0.2845	4.30	2.60	3.22	2.87
A16B	0.8	0.0042	114	0.0685	0.3099	4.52	2.67	3.26	3.30
A16C	0.8	0.0042	120	0.0725	0.3251	4.48	2.66	3.15	3.33
A17A	0.8	0.0042	109	0.0771	0.2743	3.56	2.27	2.61	2.47
A17B	0.8	0.0042	119	0.0790	0.2921	3.70	2.42	2.75	2.97
A17C	0.8	0.0042	138	0.0820	0.3302	4.03	2.70	3.02	4.37
A18A	0.8	0.0042	121	0.0881	0.2794	3.17	2.21	2.37	2.47
A18B	0.8	0.0042	153	0.0919	0.3505	3.81	2.68	2.82	3.57
A18C	0.8	0.0042	164	0.0915	0.3683	4.03	2.88	3.04	4.47
A19A	0.8	0.0042	156	0.1003	0.3353	3.34	2.50	2.52	2.67
A19B	0.8	0.0042	172	0.1000	0.3567	3.57	2.76	2.79	3.54
A19C	0.8	0.0042	186	0.0995	0.3937	3.96	3.00	3.04	4.87

Table 5.2: Experimental data for B = 0.8, Slope = 0.0089

Run no.	B	Slope	Q (L/s)	h ₁ (m)	h ₂ (m)	D	V (m/s)	F ₁	L _r (m)
A29A	0.8	0.0089	180	0.1025	0.4216	4.11	2.82	2.81	4.47
A29B	0.8	0.0089	139	0.0989	0.3556	3.60	2.26	2.29	2.97
A29C	0.8	0.0089	150	0.1000	0.3745	3.75	2.41	2.43	3.50
A28A	0.8	0.0089	116	0.0862	0.3048	3.54	2.16	2.35	1.47
A28B	0.8	0.0089	147	0.0871	0.3556	4.08	2.71	2.93	2.47
A28C	0.8	0.0089	175	0.0885	0.4216	4.76	3.18	3.41	4.47
A27A	0.8	0.0089	147	0.0795	0.3886	4.89	2.97	3.36	3.47
A27B	0.8	0.0089	119	0.0783	0.3353	4.28	2.44	2.79	2.07
A27C	0.8	0.0089	84	0.0719	0.2540	3.53	1.88	2.24	0.47
A26A	0.8	0.0089	127	0.0650	0.3683	5.67	3.14	3.93	2.97
A26B	0.8	0.0089	103	0.0635	0.3175	5.00	2.61	3.30	2.47
A26C	0.8	0.0089	74	0.0610	0.2438	4.00	1.95	2.52	3.67
A24A	0.8	0.0089	68	0.0394	0.2692	6.83	2.77	4.46	3.93
A24B	0.8	0.0089	52	0.0335	0.2311	6.90	2.49	4.35	3.43
A24C	0.8	0.0089	46	0.0326	0.2256	6.92	2.27	4.01	3.02

Table 5.3: Experimental data for B = 0.8, Slope = 0.0131

Run no.	B	Slope	Q (L/s)	H ₁ (m)	h ₂ (m)	D	V (m/s)	F ₁	L _r (m)
A34A	0.8	0.0131	73.0	0.0435	0.2600	5.98	2.70	4.13	2.47
A34B	0.8	0.0131	52.5	0.0415	0.1900	4.58	2.03	3.19	1.27
A34C	0.8	0.0131	62.0	0.0420	0.2200	5.24	2.37	3.70	1.87
A36A	0.8	0.0131	119.5	0.0675	0.3683	5.46	2.84	3.50	3.97
A36B	0.8	0.0131	105.0	0.0655	0.3429	5.24	2.58	3.21	3.47
A36C	0.8	0.0131	84.0	0.0605	0.2550	4.21	2.23	2.90	1.47
A37A	0.8	0.0131	151.0	0.0825	0.4115	4.99	2.94	3.27	5.47
A37B	0.8	0.0131	123.5	0.0785	0.3632	4.63	2.53	2.88	3.47
A37C	0.8	0.0131	91.5	0.0725	0.3175	4.38	2.03	2.40	0.97
A38A	0.8	0.0131	174.0	0.0925	0.4445	4.81	3.02	3.17	6.27
A38B	0.8	0.0131	137.0	0.0945	0.3683	3.90	2.33	2.42	3.47
A38C	0.8	0.0131	99.5	0.0835	0.3175	3.80	1.91	2.12	0.97
A39A	0.8	0.0131	162.0	0.0995	0.3886	3.91	2.62	2.65	3.47
A39B	0.8	0.0131	190.5	0.1065	0.4445	4.17	2.87	2.81	6.27
A39C	0.8	0.0131	178	0.1021	0.4102	4.02	2.80	2.80	4.67

Table 5.4: Experimental data for B = 0.7, Slope = 0.0131

Run no.	B	Slope	Q (L/s)	H ₁ (m)	h ₂ (m)	D	V (m/s)	F ₁	L _r (m)
B39A	0.7	0.0131	155	0.1032	0.3937	3.81	2.75	2.73	5.47
B39B	0.7	0.0131	172	0.1045	0.4369	4.18	3.01	2.98	5.97
B39C	0.7	0.0131	161	0.1033	0.4106	3.97	2.85	2.84	5.62
B38A	0.7	0.0131	135	0.0905	0.3861	4.27	2.73	2.90	4.97
B38B	0.7	0.0131	154	0.0915	0.4140	4.52	3.08	3.25	5.97
B38C	0.7	0.0131	100	0.0860	0.2700	3.14	2.13	2.32	1.67
B37A	0.7	0.0131	130	0.0803	0.3861	4.81	2.96	3.34	5.47
B37B	0.7	0.0131	96.5	0.0755	0.3251	4.31	2.34	2.72	2.97
B37C	0.7	0.0131	80	0.0740	0.2972	4.02	1.98	2.32	1.57
B36A	0.7	0.0131	113.5	0.0660	0.3708	5.62	3.15	3.91	5.47
B36B	0.7	0.0131	90	0.0635	0.3404	5.36	2.60	3.29	2.97
B36C	0.7	0.0131	60	0.0585	0.1850	3.16	1.88	2.48	0.97
B34A	0.7	0.0131	75	0.0410	0.2997	7.31	3.35	5.28	3.97
B34B	0.7	0.0131	44	0.0375	0.1600	4.27	2.15	3.54	2.07
B34C	0.7	0.0131	55	0.0392	0.2100	5.36	2.57	4.14	2.57

Table 5.5: Experimental data for B = 0.7, Slope = 0.0089

Run no.	B	Slope	Q (L/s)	h ₁ (m)	h ₂ (m)	D	V (m/s)	F ₁	L _r (m)
B24A	0.7	0.0089	70.5	0.0400	0.2692	6.73	3.23	5.15	4.47
B24B	0.7	0.0089	44	0.0390	0.1450	3.72	2.07	3.34	1.67
B24C	0.7	0.0089	62	0.0390	0.2234	5.73	2.91	4.71	2.54
B26A	0.7	0.0089	111	0.0655	0.3378	5.16	3.10	3.87	5.47
B26B	0.7	0.0089	78	0.0625	0.2743	4.39	2.29	2.92	2.17
B26C	0.7	0.0089	136.5	0.0785	0.3810	4.85	3.18	3.63	5.47
B27A	0.7	0.0089	108	0.0780	0.3000	3.85	2.54	2.90	2.47
B27B	0.7	0.0089	86	0.0745	0.2420	3.25	2.11	2.47	1.77
B27C	0.7	0.0089	152	0.0909	0.3886	4.28	3.06	3.24	5.97
B28A	0.7	0.0089	131	0.0857	0.3556	4.15	2.80	3.05	4.47
B28B	0.7	0.0089	101	0.0835	0.2600	3.11	2.21	2.45	2.17
B28C	0.7	0.0089	120	0.0842	0.3000	3.56	2.61	2.87	3.21
B29A	0.7	0.0089	172	0.1025	0.4064	3.96	3.07	3.06	5.87
B29B	0.7	0.0089	139	0.1011	0.3607	3.57	2.52	2.53	3.47
B29C	0.7	0.0089	153	0.1000	0.3800	3.80	2.80	2.83	4.05

Table 5.6: Experimental data for B = 0.7, Slope = 0.0042

Run no.	B	Slope	Q (L/s)	h ₁ (m)	h ₂ (m)	D	V (m/s)	F ₁	L _r (m)
B19A	0.7	0.0042	172	0.1032	0.3912	3.79	3.05	3.03	2.97
B19B	0.7	0.0042	126	0.0970	0.3175	3.27	2.38	2.44	5.97
B19C	0.7	0.0042	145	0.1014	0.3547	3.50	2.62	2.63	4.21
B18A	0.7	0.0042	153	0.0935	0.3683	3.94	3.00	3.13	5.77
B18B	0.7	0.0042	119	0.0870	0.3000	3.45	2.50	2.71	3.37
B18C	0.7	0.0042	102	0.0847	0.2550	3.01	2.21	2.42	2.37
B17A	0.7	0.0042	136	0.0785	0.3759	4.79	3.17	3.62	5.47
B17B	0.7	0.0042	108	0.0775	0.2972	3.83	2.55	2.93	2.47
B17C	0.7	0.0042	90	0.0755	0.2413	3.20	2.18	2.54	1.77
B16A	0.7	0.0042	115	0.0675	0.3353	4.97	3.12	3.83	5.27
B16B	0.7	0.0042	80	0.0625	0.2718	4.35	2.34	2.99	2.17
B16C	0.7	0.0042	98	0.0642	0.3018	4.70	2.80	3.52	3.65
B14A	0.7	0.0042	75	0.0415	0.2667	6.43	3.31	5.19	4.47
B14B	0.7	0.0042	46	0.0385	0.1623	4.22	2.19	3.56	1.67
B14C	0.7	0.0042	60	0.0402	0.2234	5.56	2.73	4.35	3.54

Table 5.7: Experimental data for B = 0.7, Slope = 0.0000

Run no.	B	Slope	Q (L/s)	h ₁ (m)	h ₂ (m)	D	V (m/s)	F ₁	L _r (m)
B04A	0.7	0.0000	42	0.0485	0.1300	2.68	1.59	2.30	1.47
B04B	0.7	0.0000	67	0.0555	0.2100	3.78	2.21	3.00	2.27
B06A	0.7	0.0000	94	0.0720	0.2500	3.47	2.39	2.84	4.27
B06B	0.7	0.0000	77	0.0695	0.2250	3.24	2.03	2.46	2.47
B06C	0.7	0.0000	60	0.0605	0.1700	2.81	1.82	2.36	1.47
B07A	0.7	0.0000	127	0.0915	0.3000	3.28	2.54	2.68	4.47
B07B	0.7	0.0000	101	0.0885	0.2500	2.82	2.09	2.24	2.97
B08A	0.7	0.0000	85	0.0825	0.2100	2.55	1.89	2.10	2.47
B08B	0.7	0.0000	153	0.0935	0.3683	3.94	3.00	3.13	5.77
B09A	0.7	0.0000	119	0.0870	0.3000	3.45	2.50	2.71	3.37
B09B	0.7	0.0000	102	0.0847	0.2550	3.01	2.21	2.42	2.37

Table 5.8: Experimental data for B = 0.6, Slope = 0.0042

Run no.	B	Slope	Q (L/s)	h ₁ (m)	h ₂ (m)	D	V (m/s)	F ₁	L _r (m)
C19A	0.6	0.0042	150	0.1125	0.4140	3.68	2.84	2.70	5.97
C19B	0.6	0.0042	102	0.0955	0.2570	2.69	2.27	2.35	3.37
C19C	0.6	0.0042	132	0.1052	0.3105	2.95	2.67	2.63	4.42
C18A	0.6	0.0042	135	0.0965	0.3988	4.13	2.98	3.06	5.67
C18B	0.6	0.0042	114	0.0855	0.3759	4.40	2.84	3.10	3.67
C18C	0.6	0.0042	90	0.0875	0.2743	3.14	2.19	2.36	2.47
C17A	0.6	0.0042	112	0.0745	0.3454	4.64	3.20	3.74	5.17
C17B	0.6	0.0042	85	0.0750	0.2731	3.64	2.41	2.81	2.67
C17C	0.6	0.0042	70	0.0755	0.1905	2.52	1.97	2.29	1.67
C16A	0.6	0.0042	84	0.0695	0.2286	3.29	2.57	3.12	3.47
C16B	0.6	0.0042	90	0.0630	0.3404	5.40	3.04	3.87	4.27
C16C	0.6	0.0042	56	0.0535	0.1829	3.42	2.23	3.07	1.27
C14A	0.6	0.0042	62	0.0475	0.2311	4.87	2.78	4.07	2.47
C14B	0.6	0.0042	45	0.0455	0.1803	3.96	2.10	3.15	1.27
C14C	0.6	0.0042	52	0.0462	0.2102	4.55	2.40	3.56	2.05

Table 5.9: Experimental data for B = 0.6, Slope = 0.0131

Run no.	B	Slope	Q (L/s)	h ₁ (m)	h ₂ (m)	D	V (m/s)	F ₁	L _r (m)
C39A	0.6	0.0131	148.5	0.1125	0.4166	3.70	2.81	2.67	5.97
C39B	0.6	0.0131	105.0	0.0975	0.2600	2.67	2.29	2.34	3.37
C39C	0.6	0.0131	121.0	0.1060	0.3100	2.92	2.43	2.38	4.38
C38A	0.6	0.0131	135.0	0.0975	0.4013	4.12	2.95	3.01	5.67
C38B	0.6	0.0131	114.0	0.0855	0.3759	4.40	2.84	3.10	3.67
C38C	0.6	0.0131	89.5	0.0875	0.2750	3.14	2.18	2.35	2.47
C37A	0.6	0.0131	111.5	0.0745	0.3480	4.67	3.19	3.73	5.17
C37B	0.6	0.0131	82.0	0.0750	0.2750	3.67	2.33	2.71	2.67
C37C	0.6	0.0131	69.0	0.0755	0.1900	2.52	1.94	2.26	1.67
C36A	0.6	0.0131	84.5	0.0695	0.2300	3.31	2.59	3.13	3.47
C36B	0.6	0.0131	92.0	0.0630	0.3429	5.44	3.11	3.95	4.27
C36C	0.6	0.0131	55.0	0.0535	0.1850	3.46	2.19	3.02	1.27
C34A	0.6	0.0131	61.0	0.0475	0.2300	4.84	2.73	4.00	2.47
C34B	0.6	0.0131	42.0	0.0457	0.1800	3.94	1.96	2.92	1.27
C34C	0.6	0.0131	51.0	0.0462	0.2100	4.55	2.35	3.49	2.08

Table 5.10: Experimental data for B = 0.6, Slope = 0.0089

Run no.	B	Slope	Q (L/s)	h ₁ (m)	h ₂ (m)	D	V (m/s)	F ₁	L _r (m)
C24A	0.6	0.0089	62	0.0455	0.1950	4.29	2.90	4.34	2.47
C24B	0.6	0.0089	37.5	0.0430	0.1750	4.07	1.86	2.86	1.57
C24C	0.6	0.0089	51	0.0442	0.1825	4.13	2.46	3.73	2.05
C26A	0.6	0.0089	83	0.0685	0.2000	2.92	2.58	3.15	2.47
C26B	0.6	0.0089	90.5	0.0785	0.2450	3.12	2.45	2.80	3.27
C26C	0.6	0.0089	109.5	0.0860	0.3404	3.96	2.71	2.95	4.97
C27A	0.6	0.0089	92	0.0625	0.3404	5.45	3.13	4.00	5.17
C27B	0.6	0.0089	85	0.0695	0.2286	3.29	2.60	3.15	2.67
C27C	0.6	0.0089	55	0.0525	0.1819	3.46	2.23	3.11	1.67
C28A	0.6	0.0089	90	0.0855	0.2718	3.18	2.24	2.45	2.47
C28B	0.6	0.0089	115	0.0925	0.3759	4.06	2.65	2.78	3.67
C28C	0.6	0.0089	140	0.0975	0.4013	4.12	3.06	3.12	5.67
C29A	0.6	0.0089	110	0.0945	0.2591	2.74	2.48	2.57	3.37
C29B	0.6	0.0089	150	0.1115	0.4115	3.69	2.86	2.74	5.97
C29C	0.6	0.0089	132	0.1054	0.3546	3.36	2.67	2.62	4.32

Table 5.11: Experimental data for B = 0.5, Slope = 0.0042

Run no.	B	Slope	Q (L/s)	h ₁ (m)	h ₂ (m)	D	V (m/s)	F ₁	L _r (m)
D14A	0.5	0.0042	55	0.0585	0.195	3.33	2.39	3.15	2.47
D14B	0.5	0.0042	38	0.0495	0.17	3.43	1.95	2.80	1.77
D14C	0.5	0.0042	64	0.0640	0.21	3.28	2.54	3.21	2.87
D16A	0.5	0.0042	90	0.0965	0.28	2.90	2.37	2.43	4.17
D16B	0.5	0.0042	65	0.0735	0.21	2.86	2.25	2.65	2.47
D16C	0.5	0.0042	53	0.0645	0.17	2.64	2.09	2.62	1.67
D17A	0.5	0.0042	110	0.1125	0.28	2.49	2.48	2.36	4.97
D17B	0.5	0.0042	70	0.0875	0.22	2.51	2.03	2.19	2.47
D17C	0.5	0.0042	95	0.1025	0.27	2.63	2.35	2.35	2.87
D18A	0.5	0.0042	115	0.1175	0.3	2.55	2.49	2.32	5.47
D18B	0.5	0.0042	75	0.0925	0.21	2.27	2.06	2.16	2.17
D18C	0.5	0.0042	90	0.0975	0.255	2.62	2.34	2.40	3.37
D19A	0.5	0.0042	125	0.1175	0.33	2.81	2.70	2.52	5.97
D19B	0.5	0.0042	100	0.1125	0.28	2.49	2.26	2.15	2.37
D19C	0.5	0.0042	112	0.1154	0.3	2.60	2.47	2.32	3.54

Table 5.12: Experimental data for B = 0.5, Slope = 0.0089

Run no.	B	Slope	Q (L/s)	h ₁ (m)	h ₂ (m)	D	V (m/s)	F ₁	L _r (m)
D24A	0.5	0.0089	55	0.0585	0.195	3.33	2.39	3.15	2.47
D24B	0.5	0.0089	35	0.0475	0.17	3.58	1.87	2.74	1.67
D24C	0.5	0.0089	43	0.0520	0.18	3.46	2.10	2.94	2.21
D26A	0.5	0.0089	88	0.0945	0.29	3.07	2.37	2.46	4.27
D26B	0.5	0.0089	63	0.0735	0.22	2.99	2.18	2.56	2.47
D26C	0.5	0.0089	52	0.0645	0.18	2.79	2.05	2.57	1.57
D27A	0.5	0.0089	113	0.1135	0.3302	2.91	2.53	2.40	5.67
D27B	0.5	0.0089	75	0.0975	0.23	2.36	1.95	2.00	2.07
D27C	0.5	0.0089	94	0.1014	0.29	2.86	2.35	2.36	3.87
D28A	0.5	0.0089	90	0.1025	0.265	2.59	2.23	2.22	3.47
D28B	0.5	0.0089	138	0.1175	0.33	2.81	2.98	2.78	5.27
D28C	0.5	0.0089	114	0.1104	0.31	2.81	2.62	2.52	4.15
D29A	0.5	0.0089	128	0.1075	0.3	2.79	3.02	2.95	3.47
D29B	0.5	0.0089	110	0.0995	0.26	2.61	2.81	2.84	2.67
D29C	0.5	0.0089	100	0.1020	0.24	2.35	2.49	2.49	2.60

Table 5.13: Experimental data for B = 0.5, Slope = 0.0131

Run no.	B	Slope	Q (L/s)	h ₁ (m)	h ₂ (m)	D	V (m/s)	F ₁	L _r (m)
D34A	0.5	0.0131	59	0.0525	0.23	4.38	2.85	3.98	2.27
D34B	0.5	0.0131	36	0.0465	0.18	3.87	1.97	2.91	1.77
D34C	0.5	0.0131	45	0.0493	0.2	4.06	2.32	3.34	2.08
D36A	0.5	0.0131	90	0.0845	0.28	3.31	2.71	2.97	3.67
D36B	0.5	0.0131	66	0.0665	0.245	3.68	2.52	3.12	2.47
D36C	0.5	0.0131	55	0.0670	0.2	2.99	2.09	2.57	1.97
D37A	0.5	0.0131	112	0.1070	0.3683	3.44	2.66	2.60	4.97
D37B	0.5	0.0131	88	0.0950	0.29	3.05	2.35	2.44	2.47
D37C	0.5	0.0131	102	0.1050	0.3245	3.09	2.47	2.43	3.21
D38A	0.5	0.0131	71	0.0925	0.25	2.70	1.95	2.05	1.47
D38B	0.5	0.0131	128	0.1175	0.35	2.98	2.77	2.58	5.47
D38C	0.5	0.0131	100	0.1050	0.31	2.95	2.42	2.38	3.36
D39A	0.5	0.0131	140	0.1125	0.31	2.76	2.71	2.58	3.67
D39B	0.5	0.0131	105	0.1025	0.29	2.83	2.60	2.59	2.47
D39C	0.5	0.0131	112	0.1056	0.3	2.84	2.69	2.65	3.06

Table 5.14: Experimental data for B = 0.5, Slope = 0.0000

Run no.	B	Slope	Q (L/s)	h ₁ (m)	h ₂ (m)	D	V (m/s)	F ₁	L _r (m)
D04A	0.5	0.0000	64	0.0720	0.205	2.85	2.26	2.69	1.97
D04B	0.5	0.0000	38	0.0515	0.16	3.11	1.87	2.64	0.97
D06A	0.5	0.0000	83	0.0770	0.26	3.38	2.74	3.15	3.27
D06B	0.5	0.0000	58	0.0670	0.18	2.69	2.20	2.71	1.47
D06C	0.5	0.0000	69	0.0675	0.18	2.67	2.60	3.19	2.47
D07A	0.5	0.0000	111	0.1058	0.3	2.84	2.66	2.62	4.47
D07B	0.5	0.0000	89	0.0985	0.26	2.64	2.30	2.33	2.97
D08A	0.5	0.0000	69	0.0932	0.22	2.36	1.88	1.97	0.97
D08B	0.5	0.0000	125	0.1175	0.3	2.55	2.70	2.52	5.87
D09A	0.5	0.0000	115	0.1155	0.27	2.34	2.53	2.38	3.67
D09B	0.5	0.0000	100	0.0995	0.25	2.51	2.55	2.58	2.57

Chapter Six

RESULTS AND DISCUSSIONS

6.1 INTRODUCTION

This chapter deals with the analysis and discussion of various results that were obtained from the laboratory experiments and subsequent analyses from the experimental data. As stated earlier, the experiments were conducted in the Hydraulics and River Engineering Laboratory of Department of Water Resources Engineering, BUET. Experimental investigations were conducted under different flow conditions; for Froude number ranging from 1.19 to 5.28. Four different expansion ratios ($B = 0.50, 0.60, 0.70$ and 0.80); three slopes of the channel ($0.0042, 0.0089$ and 0.0131) and four different gate openings (5.0 cm, 9.0 cm, 11.0 cm, 13.0 cm and 15.0 cm) were used. The discharges were varied accordingly with different slopes and gate openings to get the required range of inflow Froude number. Initial depth, sequent depth, discharge, average velocity and jump length were measured for the analyses. Results of different analyses are described in subsequent articles in this chapter.

6.2 ANALYSIS OF INFLOW FROUDE NUMBER WITH DISCHARGE FOR DIFFERENT HYDRAULIC CONDITIONS

For each gate opening, four discharges were used to maintain the upstream depth below the critical depth of the channel flow. Figure 6.1 shows the relationship between the inflow Froude number and the discharge for different gate openings and for different channel slopes when the value of the expansion ratio is 0.50 . Similarly, the Figure 6.2, 6.3 and 6.4 represent the same relationships for the expansion ratio of $0.60, 0.70$ and 0.80 , respectively. From these figures, it is seen that the inflow Froude number increases with the increase in the value of discharge. Again the Froude number increases with decreasing the sluice gate opening and channel width b_1 .

6.3 VARIATION OF SEQUENT DEPTH RATIO WITH INFLOW FROUDE NUMBER

Main objective of this research work was to find a mathematical model to determine the sequent depth ratio, D from some associated known variables like Inflow Froude number, expansion ratio and channel slope.

From the entire test runs, sequent depth ratio and Inflow Froude number are obtained for different hydraulic conditions i.e., for different combination of expansion ratio and channel slope. Graphs of sequent depth ratio (D) versus Inflow Froude number (F_1) were plotted for different expansion ratio and channel slopes. Best-fit curve of all the plotting show a linear variation with a well agreement with the Belenger's format prediction model. Graphs are shown in Figure 6.5 to Figure 6.8. The graphs show an increasing trend of the value of sequent depth ratio with the inflow Froude number.

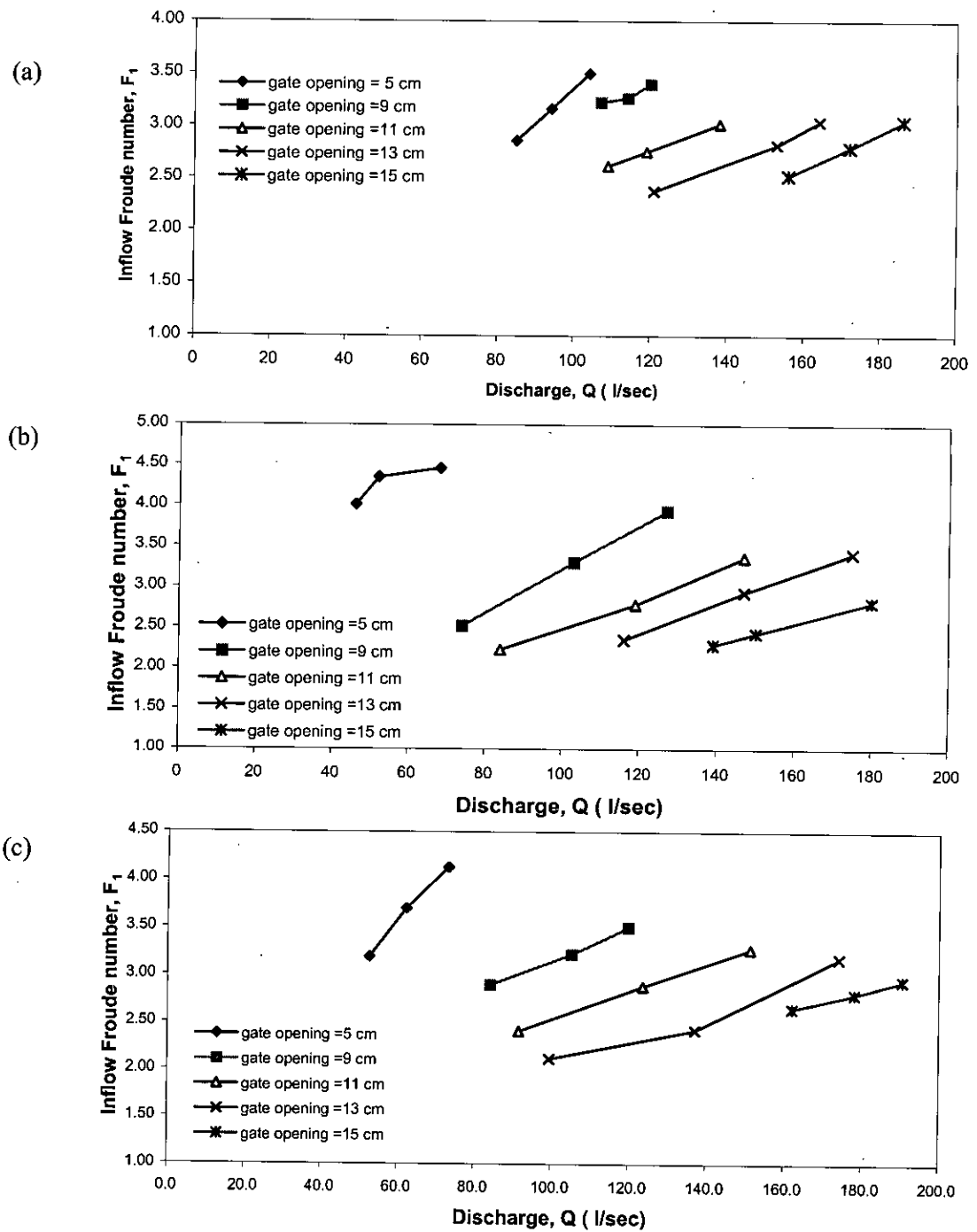
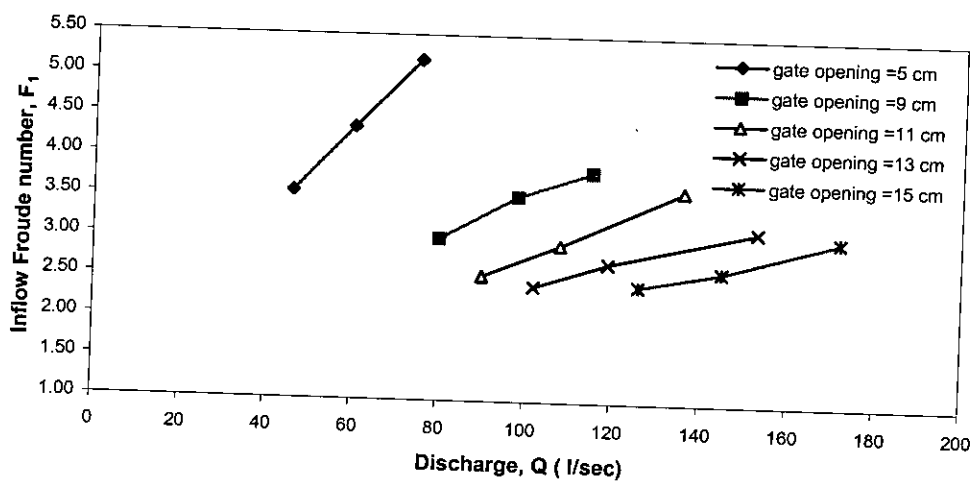
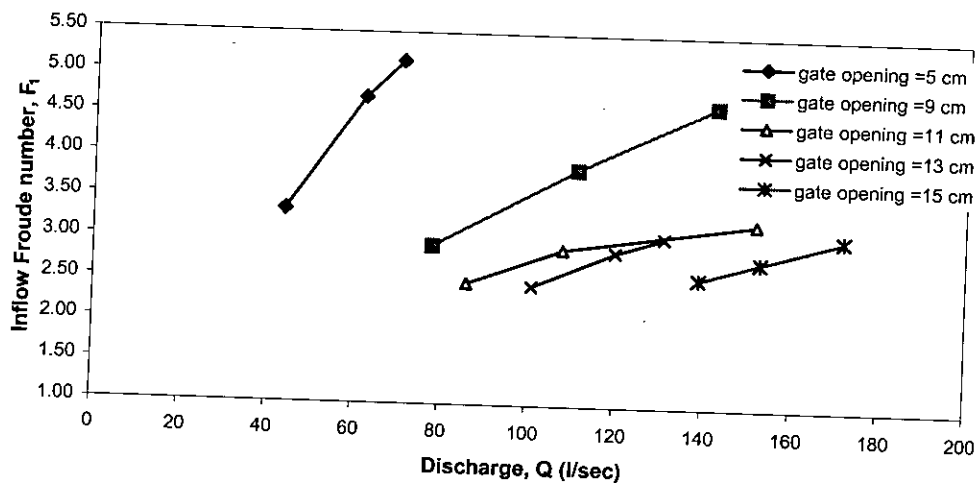


Figure 6.1: Inflow Froude number Vs Discharge for various channel slope and gate openings with expansion ratio $B = 0.80$; (a) Slope = 0.0042, (b) Slope = 0.0089, (c) Slope = 0.0131

(a)



(b)



(c)

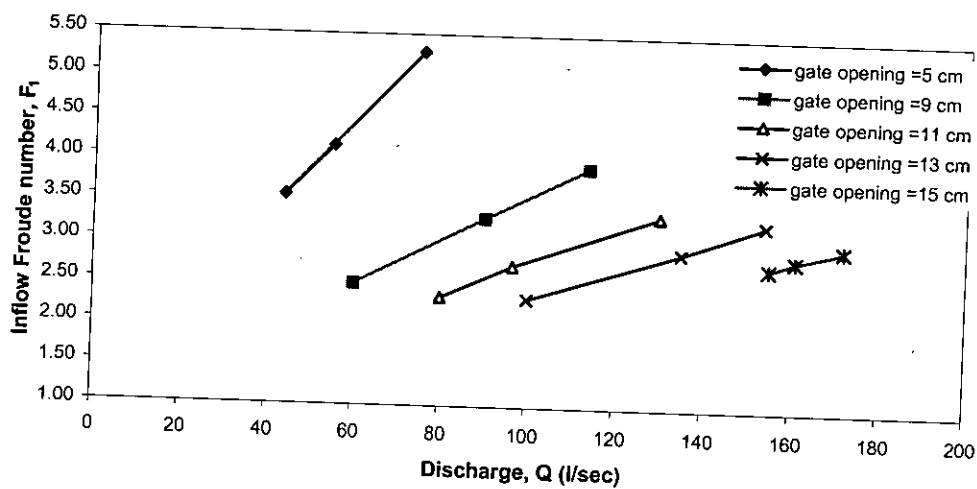


Figure 6.2: Inflow Froude number Vs Discharge for various gate opening and channel slopes with expansion ratio, $B = 0.7$; (a) Slope = 0.0042, (b) Slope = 0.0089, (c) Slope = 0.0131

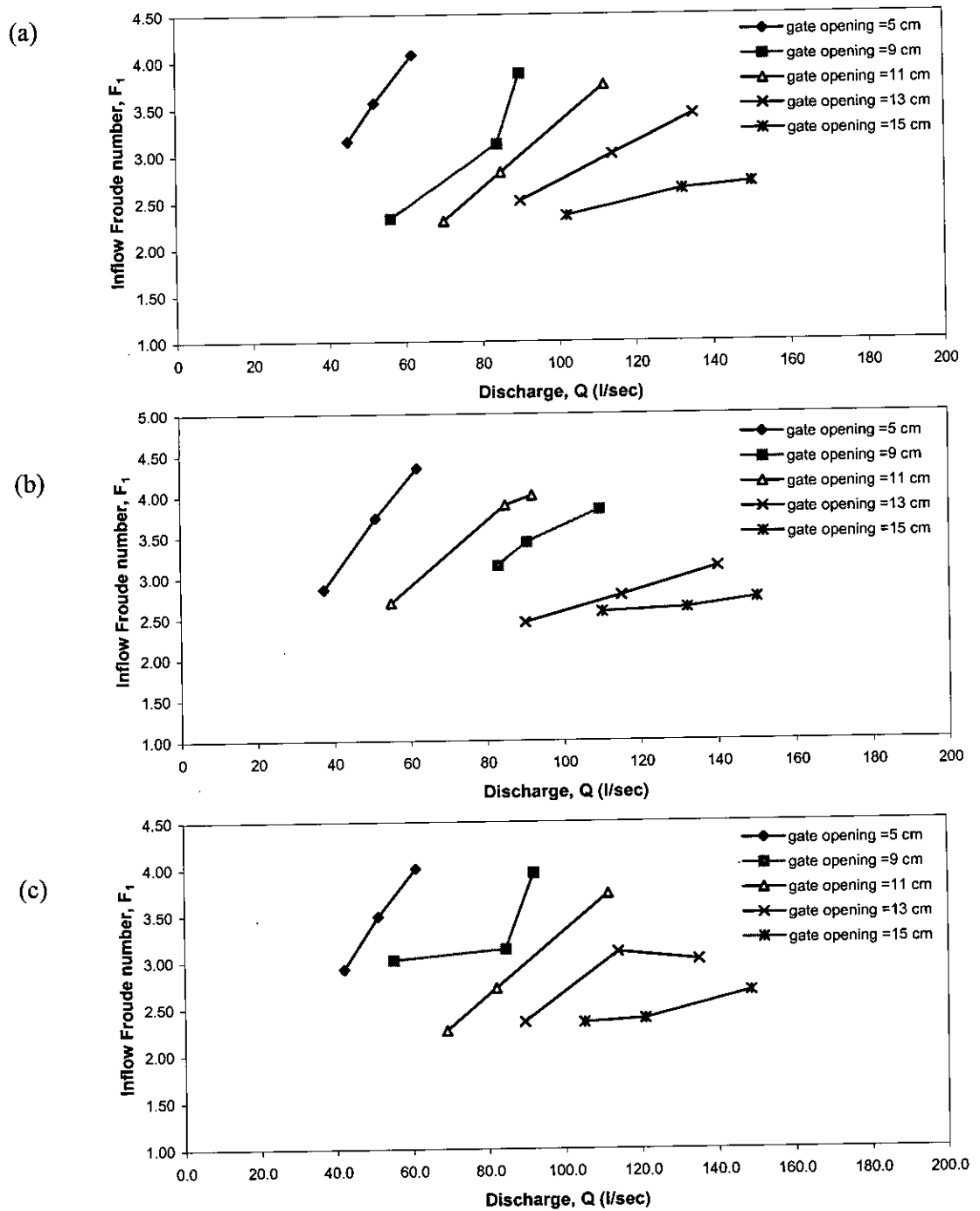


Figure 6.3: Inflow Froude number Vs Discharge for various gate opening and channel slopes with expansion ratio, $B = 0.6$; (a) Slope = 0.0042, (b) Slope = 0.0089, (c) Slope = 0.0131

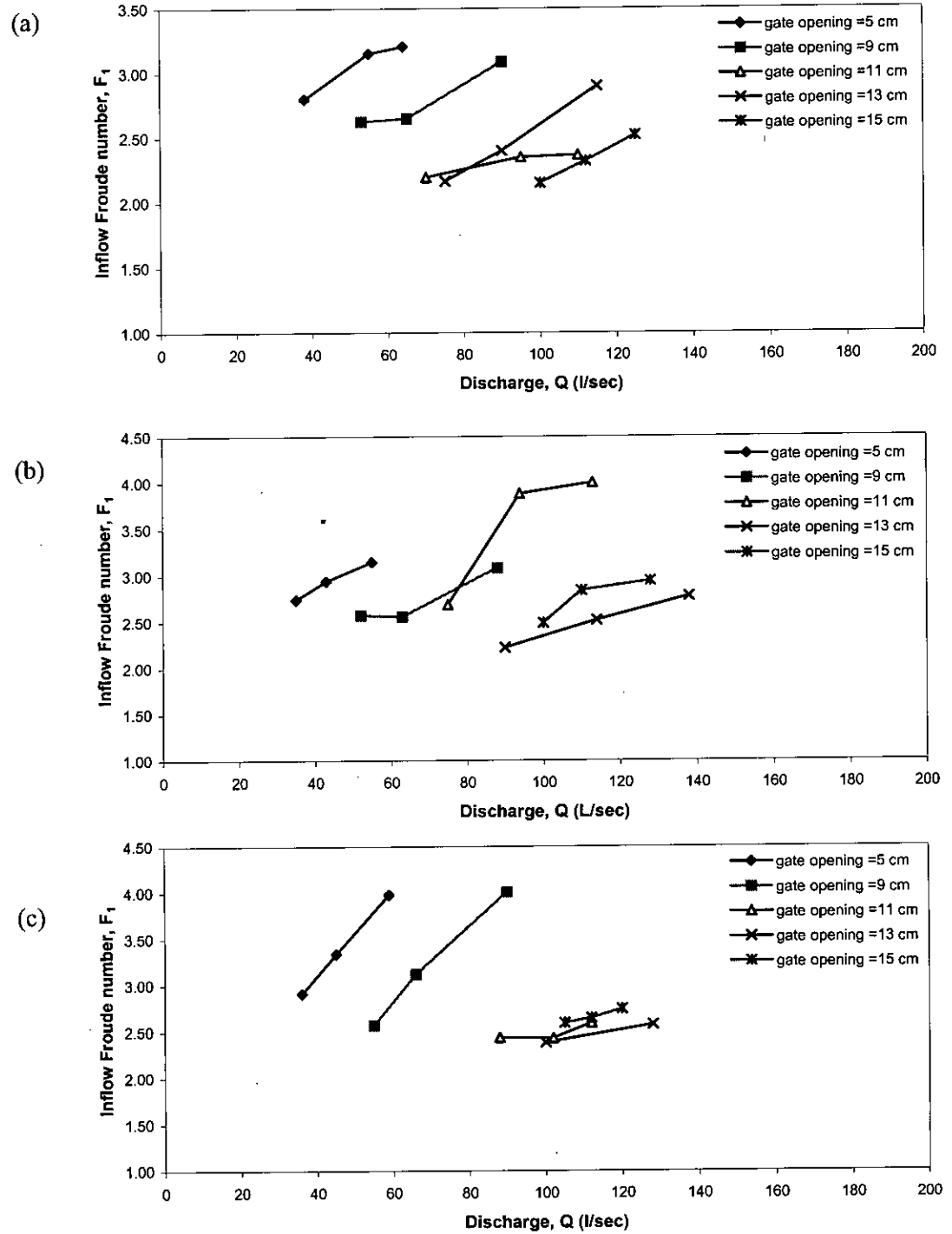


Figure 6.4: Inflow Froude number Vs Discharge for various gate opening and channel slopes with expansion ratio, $B = 0.5$; (a) Slope = 0.0042, (b) Slope = 0.0089, (c) Slope = 0.0131

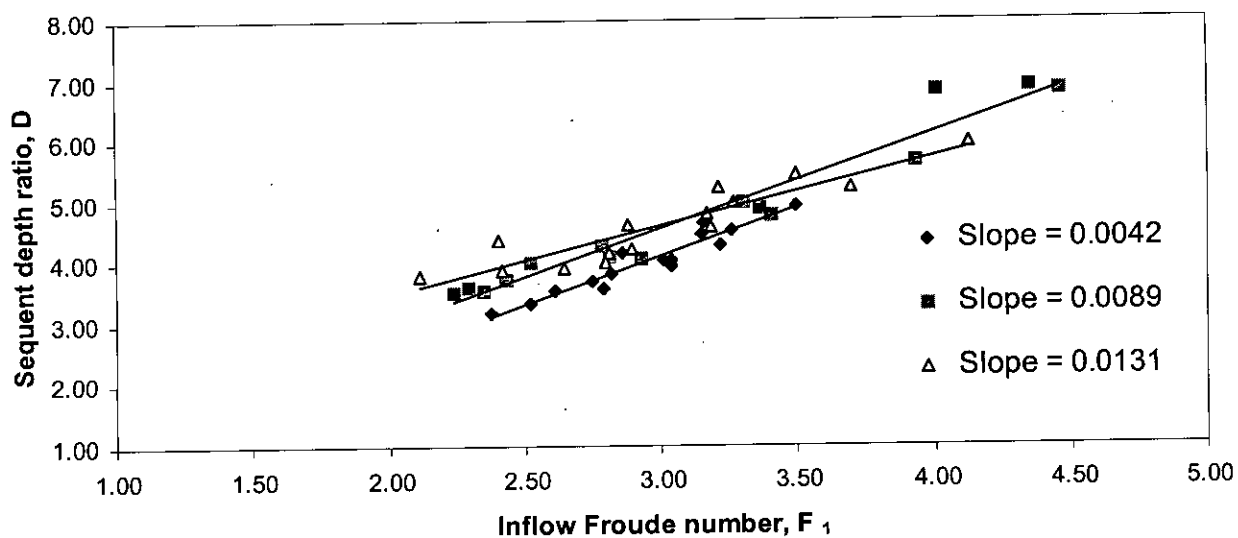


Figure 6.5: D Vs F_1 for different channel slopes with expansion ratio, $B = 0.80$.

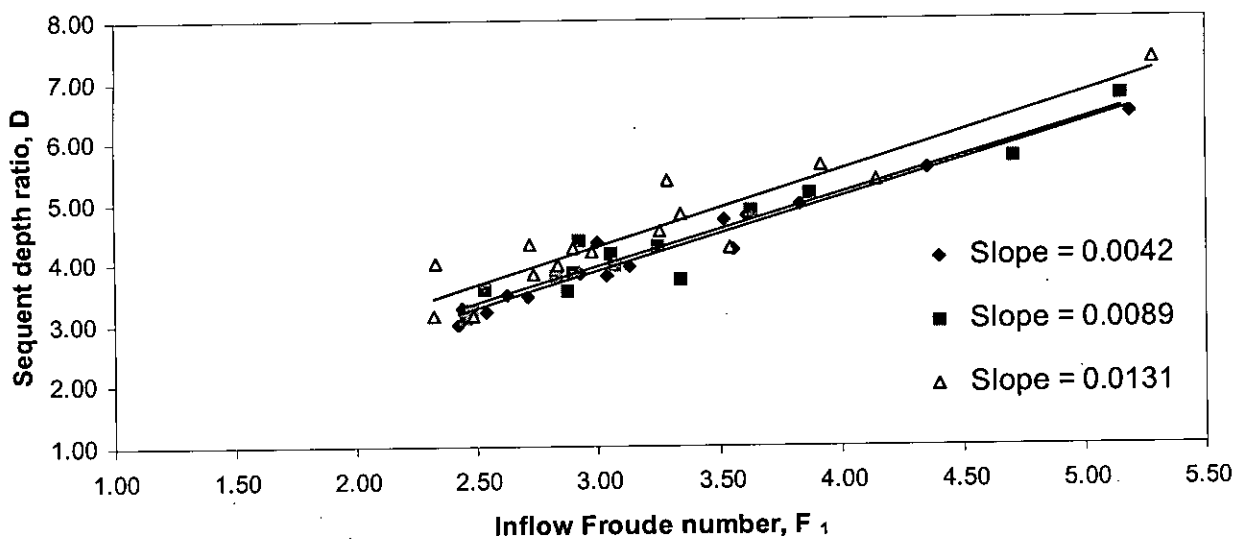


Figure 6.6: D Vs F_1 for different channel slopes with expansion ratio, $B = 0.70$.

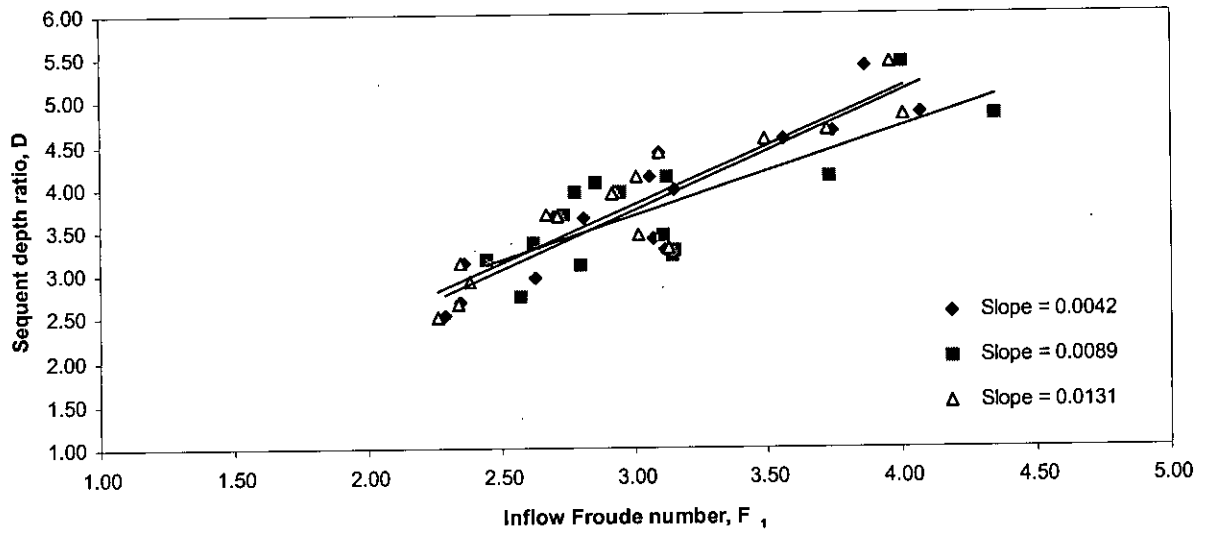


Figure 6.7: D Vs F_1 graph for different channel slopes with expansion ratio, $B = 0.60$.

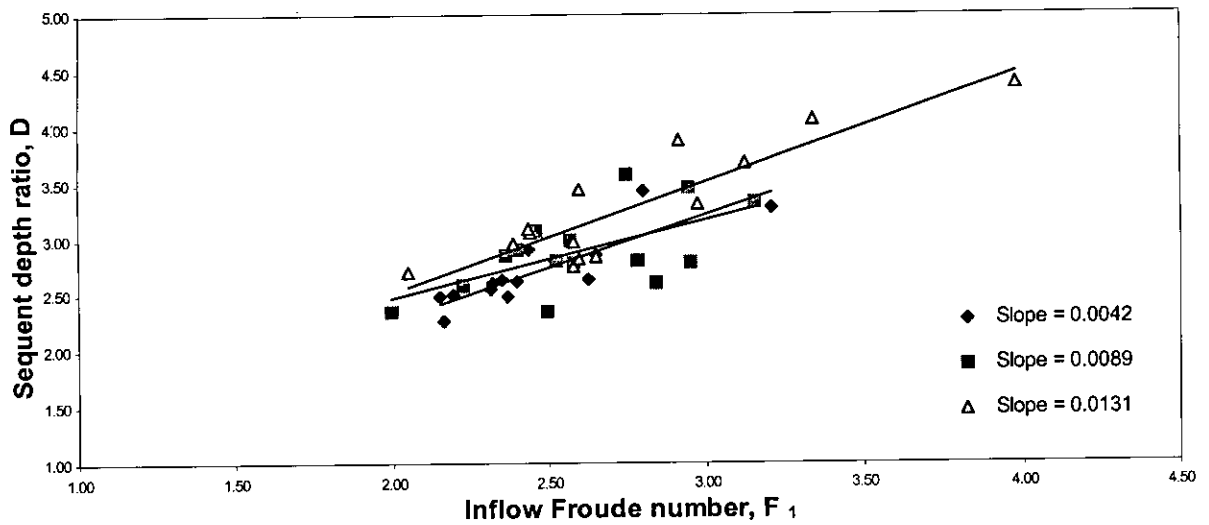


Figure 6.8: D Vs F_1 graph for different channel slopes with expansion ratio, $B = 0.50$.

6.4 VARIATION OF THE PARAMETERS k_1 AND k_2 AT DIFFERENT HYDRAULIC CONDITIONS

As stated earlier, proposed prediction model follows the Belanger's format that involves the determination of modified Froude number, E_1 (Equation 3.13). It requires two parameters k_1 and k_2 . Values of these parameters are determined from the experimental data and then it is tried to develop an equation for each parameter relating with associated known variables. These are described in subsequent articles:

6.4.1 Variation of parameter k_1 with inflow Froude number, F_1

Theoretically the parameter k_1 is dependent on expansion ratio B and sequent depth ratio D . the value of k_1 is calculated as follows:

$$k_1 = \frac{(1-D)}{B(B-D)} \quad \dots (3.11)$$

The parameter k_1 is calculated from the set of experimental data and plotted against Inflow Froude number F_1 for different hydraulic conditions. The graphs are shown in Figure 6.9. It is evident from the figures that the parameter value decreases with increase in value of expansion ratio. The channel slope value has very minor influence on the value of the parameter.

6.4.2 Modification of the prediction equation of k_1

D is a dependent variable, so k_1 cannot be predicted directly from equation 3.11. So it is tried to develop a mathematical equation to calculate the factor k_1 from known independent variables like F_1 and B . Best-fit equation of the curves (shown in Figure 6.9) representing k_1 Vs F_1 shows a logarithmic nature. For example when expansion ratio, $B = 0.8$ and channel slope = 0.0089, then the regression equation is as follows ($R^2 = 0.974$):

$$k_1 = 0.0759 \ln F_1 + 1.0972 \quad \dots (6.1)$$

This equation is modified to incorporate the effect of expansion ratio, B . Again it was also taken into consideration that when $B = 1$, i.e., for the case of a horizontal channel, value of k_1 must be equal to one. From all of these considerations the proposed equation to calculate k_1 is as follows:

$$k_1 = 1 - 0.37 \ln B(1.23 + \ln F_1) \quad \dots (6.2)$$

6.4.3 Comparison between observed and predicted values of k_1

After the mathematical formulation, the next step was to compare the predicted values of k_1 with the observed ones. For this purpose k_1 Vs F_1 graphs are plotted for predicted and observed values in the same graph paper for different combination of expansion ratio and channel slope.

Figures from 6.10 to 6.13 show the comparison between the observed and predicted values of the factor k_1 with the inflow Froude number. It is revealed from the figures that the proposed equation to calculate the parameter k_1 predicts the value very closely to the observed values. Statistically the percentage of deviation of the observed value from the predicted value varies from -0.53% to $+4.86\%$ that can be taken as very satisfactory. More importantly, the deviation of the predicted value from the observed one is very less in case of lower range of Inflow Froude number and slightly increases with higher range of Froude numbers.

6.4.4 prediction equation for parameter k_2

Value of the parameter k_2 can not be calculated directly from equation 3.12, because it needs data like K . so an indirect procedure is followed here. First, the modified Froude number, E_1 was calculated by the method of back calculation from equation:

$$D = \frac{1}{2} \left(\sqrt{1 + 8E_1^2} - 1 \right) \quad \dots (3.13)$$

Now, Inflow Froude number F_1 , modification factor k_1 , channel slope and the modified Froude number, E_1 are known. So the value of k_2 is calculated using the following equation:

$$E_1^2 = \frac{F_1^2}{k_1(1 - k_2) \cos \theta} \quad \dots (3.10)$$

When this parameter is plotted against the Inflow Froude number, it does not show a general trend for individual case, i.e., for a particular combination of expansion ratio and channel slope. It was kept in mind that objective of this research was to incorporate the effects of channel expansion and channel slope. Effect of channel expansion is incorporated in the factor k_1 . So it was tried to incorporate the effect of channel slope in the factor k_2 . From all the experimental data a trend line equation

has been developed relating the channel slope and Inflow Froude number. The equation is as follows:

$$k_2 = 0.52(0.1 + 0.35F_1 - 0.055F_1^2)\sin\theta(\theta)^{-1} \quad \dots \quad (6.2)$$

6.4.5 comparison between predicted and observed values of k_2

For a particular case, i.e., for a certain combination of channel slope and expansion ratio, the prediction equation shows mentionable variation with the observed data that is shown in figure 6.14. This may be happened due to the fact that the effect of expansion ratio is not incorporated in this equation. But this proposed equation is taken as satisfactory because when the parameters k_1 and k_2 are used together to modify the inflow Froude number, then the results match with the observed data very closely (shown in figures from 6.15 to 6.22).

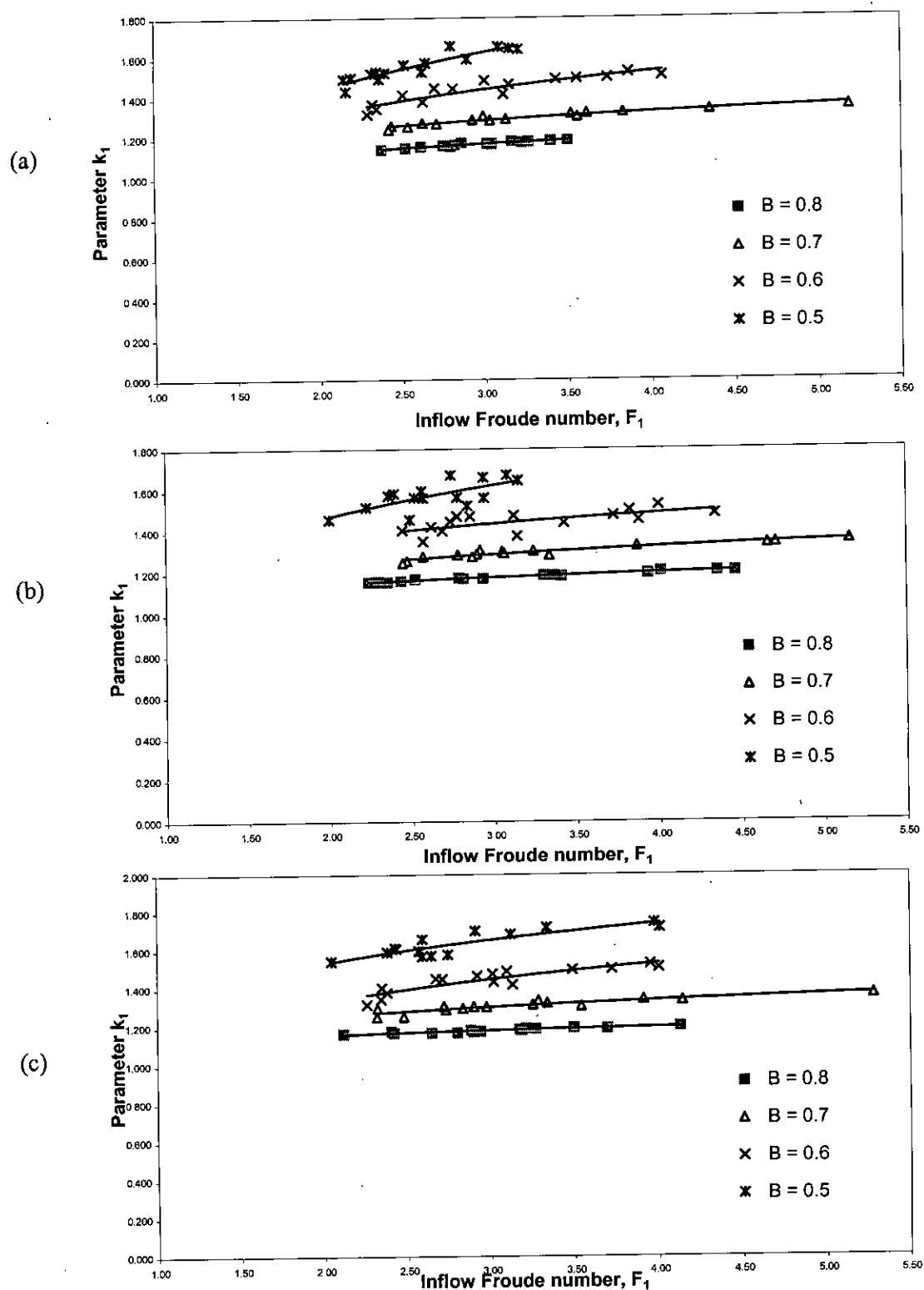


Figure 6.9: Variation of parameter k_1 with F_1 for different expansion ratios; (a) Slope = 0.0042, (b) Slope = 0.0089, (c) Slope = 0.0131

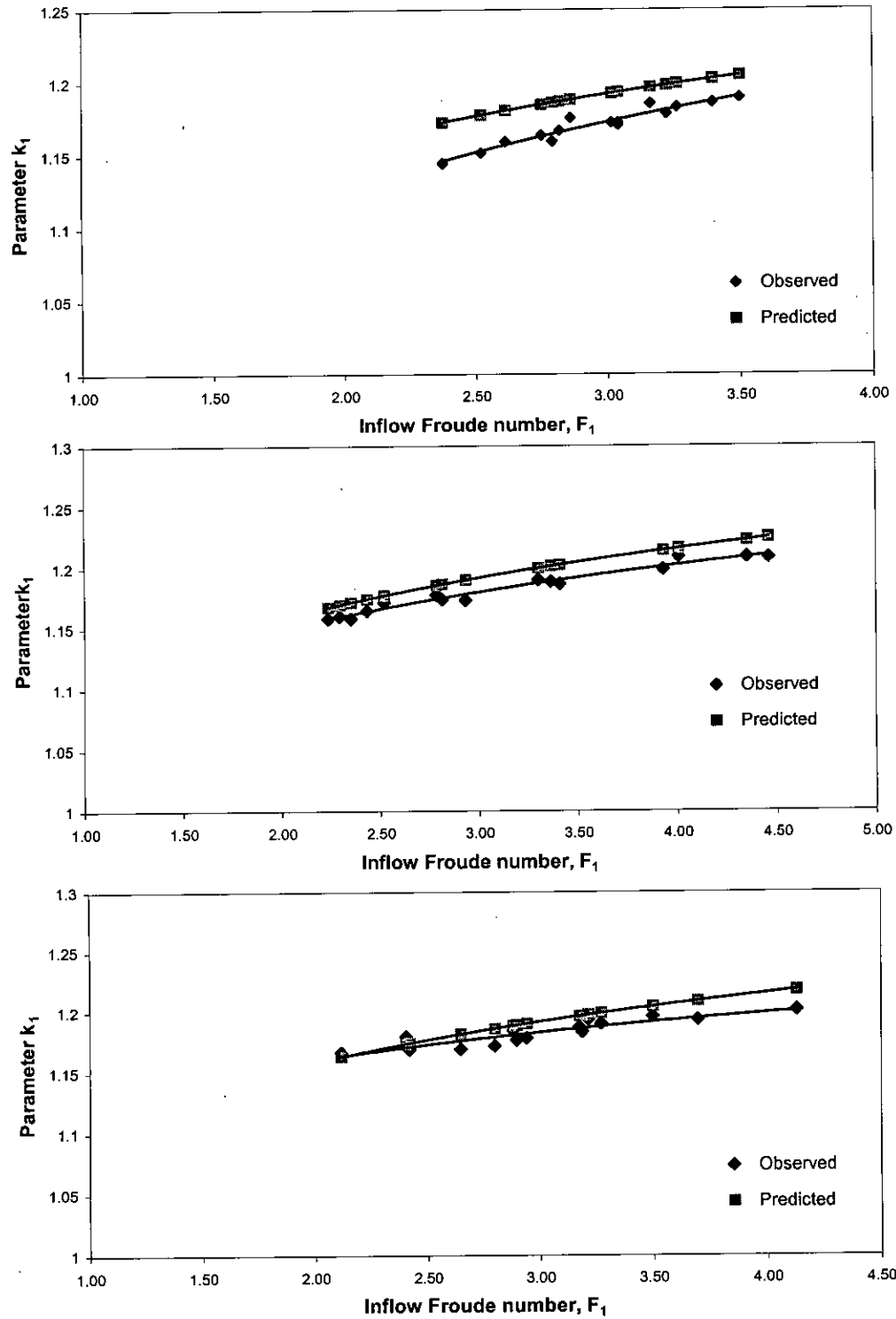


Figure 6.10: k_1 Vs Inflow Froude number, F_1 with expansion ratio, $B = 0.8$; (a) Slope = 0.0042, (b) Slope = 0.0089, (c) Slope = 0.0131

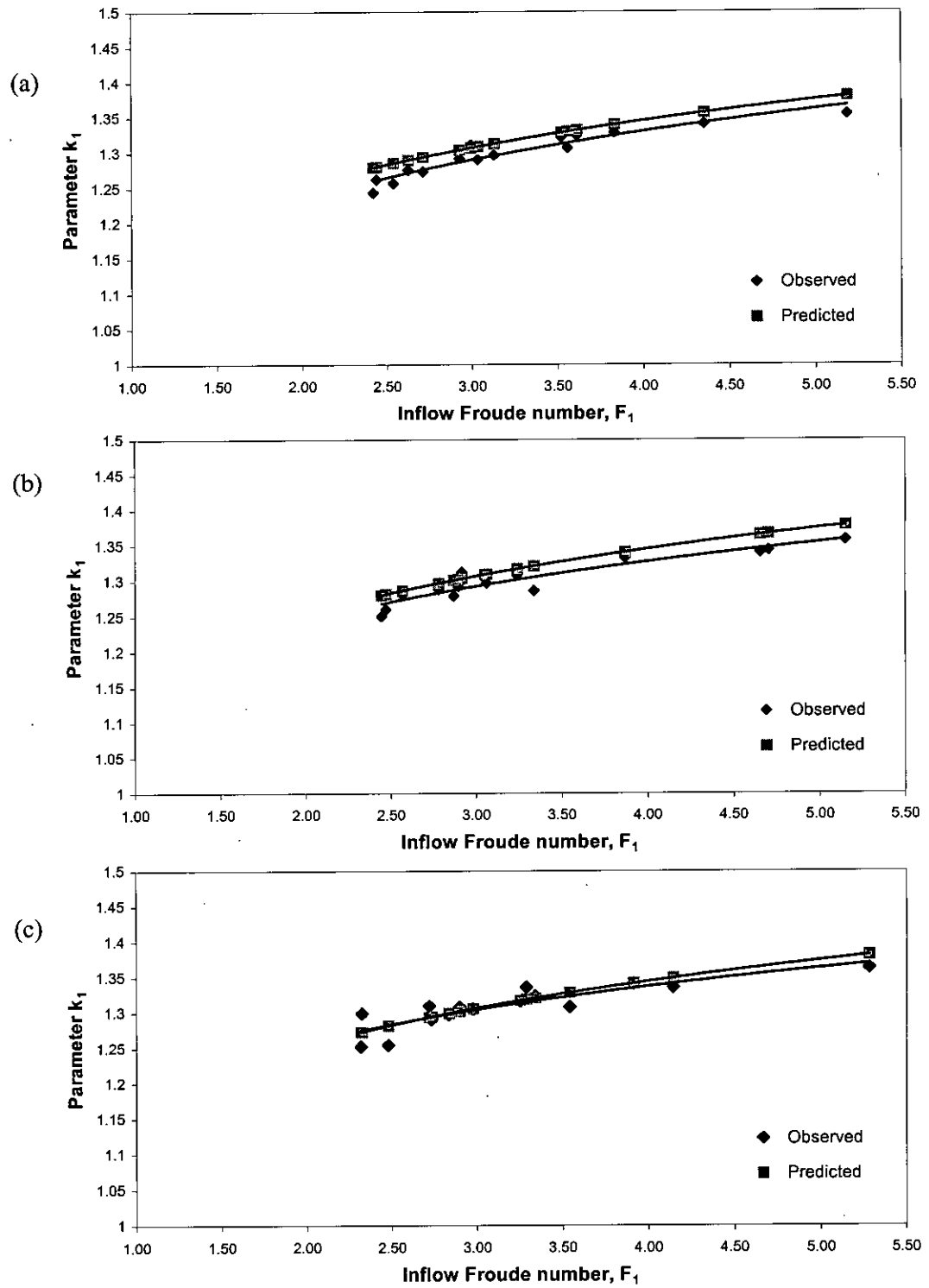


Figure 6.11: k_1 Vs Inflow Froude number, F_1 with expansion ratio, $B = 0.7$; (a) Slope = 0.0042, (b) Slope = 0.0089, (c) Slope = 0.0131

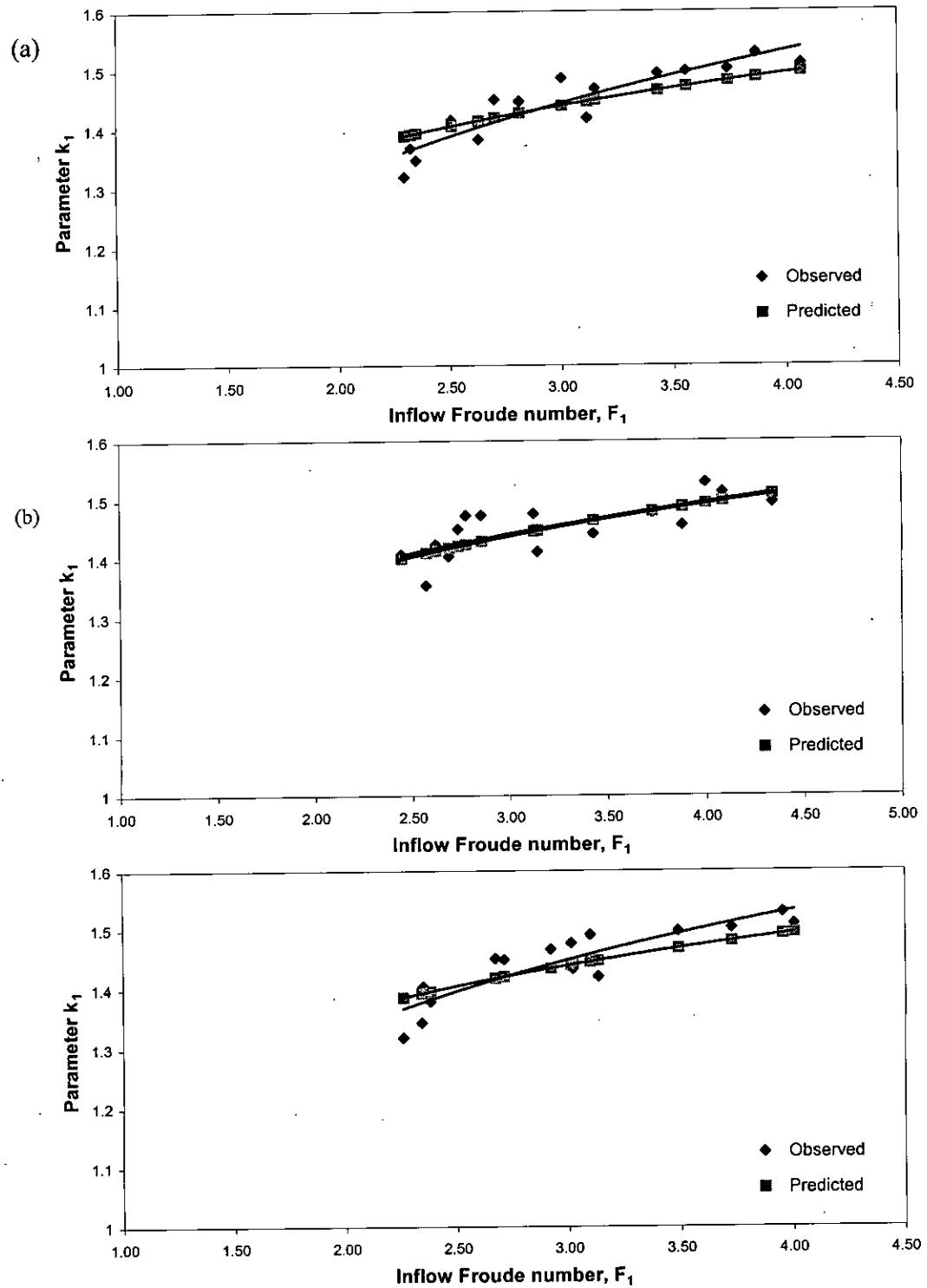


Figure 6.12: k_1 Vs Inflow Froude number, F_1 with expansion ratio, $B = 0.6$; (a) Slope = 0.0042, (b) Slope = 0.0089, (c) Slope = 0.0131.

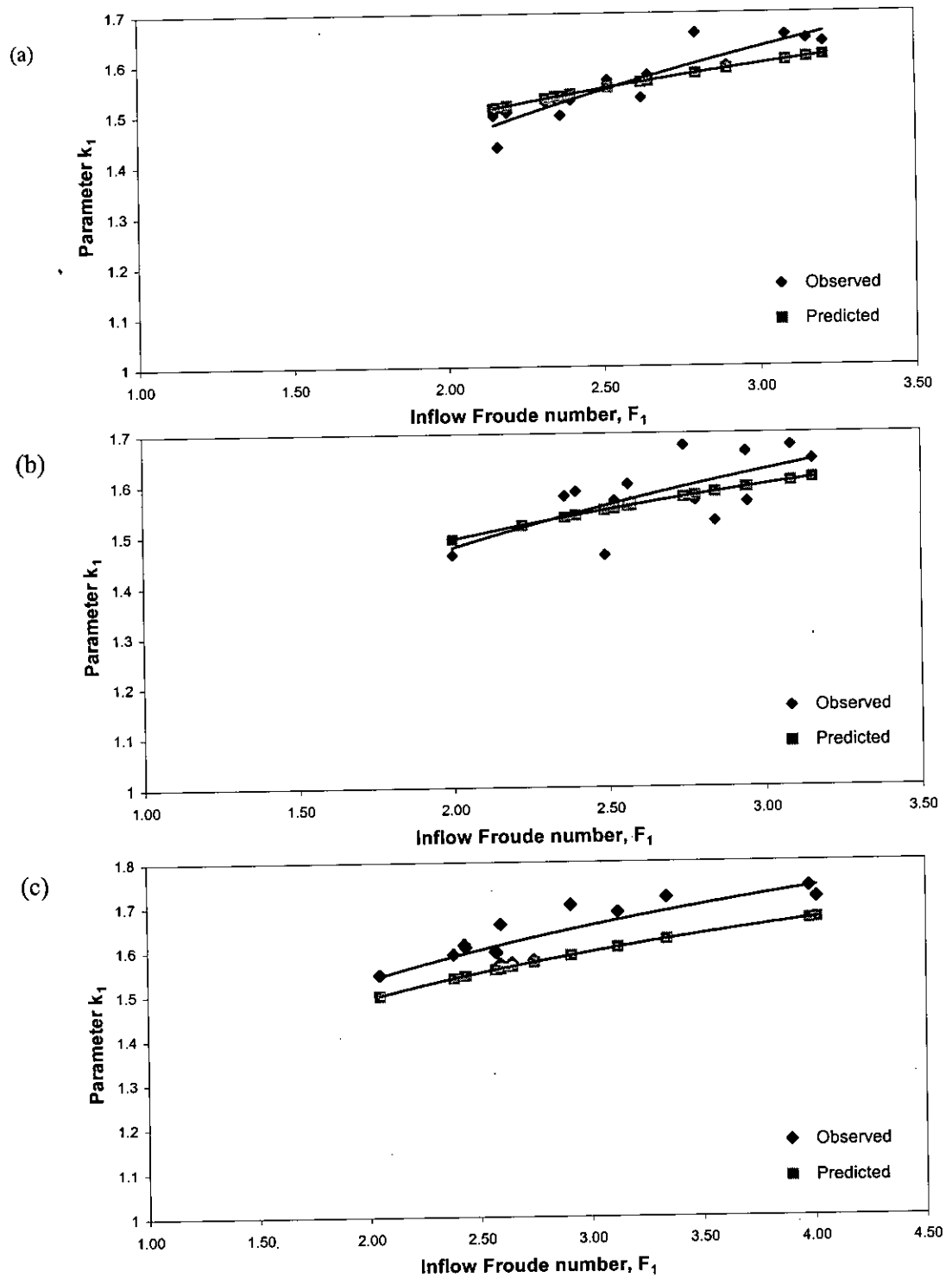


Figure 6.13: k_1 Vs Inflow Froude number, F_1 with expansion ratio, $B = 0.5$; (a) Slope = 0.0042, (b) Slope = 0.0089, (c) Slope = 0.0131

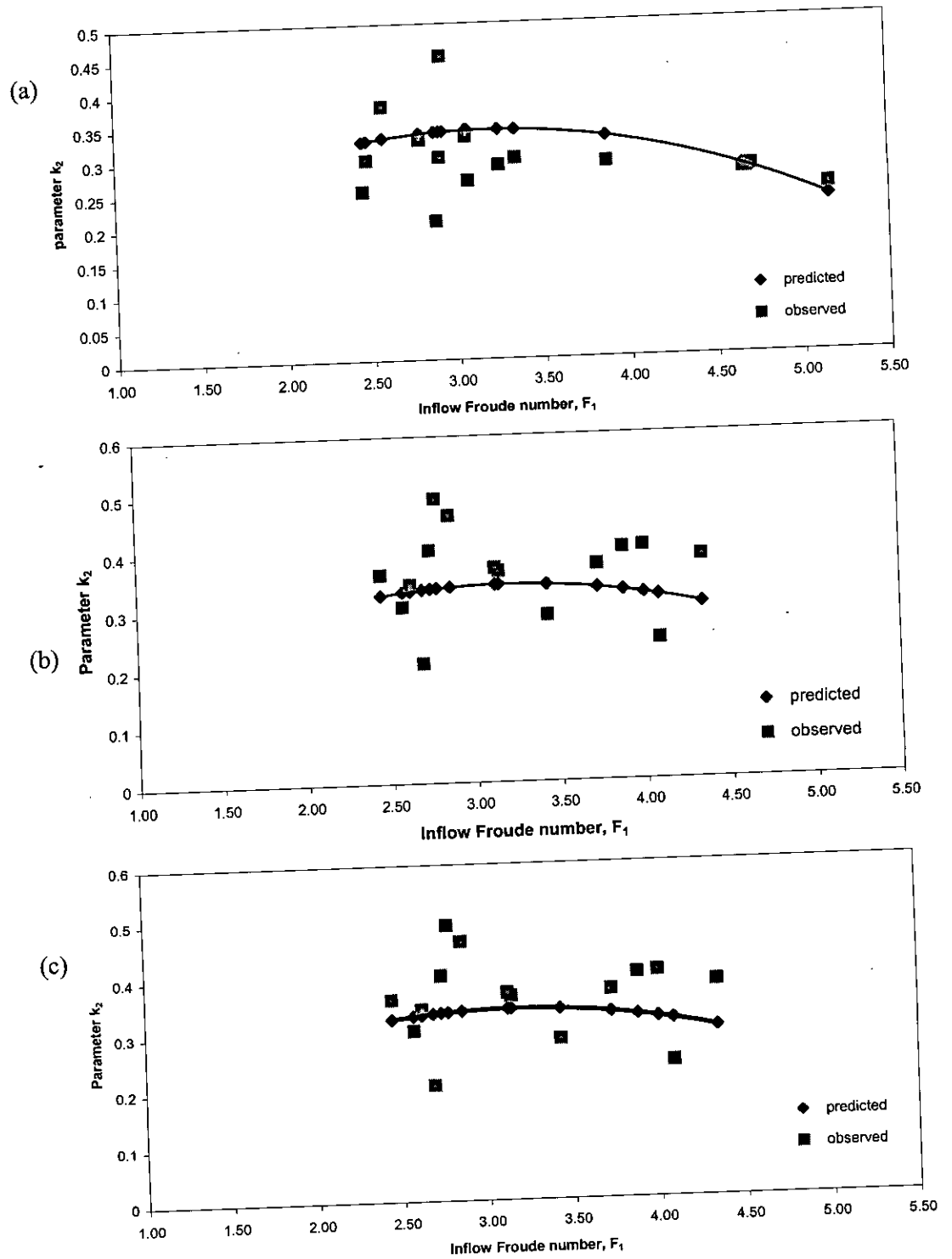


Figure 6.14: k_2 Vs Inflow Froude number, F_1 with expansion ratio, $B = 0.5$; (a) Slope = 0.0042, (b) Slope = 0.0089, (c) Slope = 0.0131.

6.5 CALIBRATION OF THE PREDICTION MODEL

Prediction equation (Equation 3.13) developed in the course of this study is compared with the observed data from the series of experiments. Some plotting have been done to compare the predicted results with observed data. Sequent depth ratio versus Inflow Froude number graphs for different expansion ratio and channel slopes are plotted with the prediction equation and with the experimental data. These plotting are shown in Figure 6.15-6.18. From the graphs it is seen that the proposed equation predicts the value of sequent depth ratio very close to the value of observed ones. For expansion ratio $B = 0.8$ and $B = 0.7$, this relation holds true for the entire range of Froude numbers. Again for expansion ratio $B = 0.6$ and $B = 0.5$, observed and predicted values match closely for the lower range of Froude number but differ slightly for higher range of Froude number.

Moreover, Predicted sequent depth ratio (D) values are plotted against the observed ones. These are shown in from Figure 6.19 to Figure 6.22. Again the performance of the prediction equation is shown in table 6.1. From the graphs and tables it performance of the prediction equation can be taken as quite satisfactory. From the graphs it is revealed that for expansion ratio, $B = 0.8$, predicted D slightly differs from the observed D . for slope = 0.0042, the equation slightly overestimates the sequent depth ratio but for channel slope = 0.0089, predicted values are lower than corresponding observed values. For other expansion ratios, predicted value of D matches with the observed values in a satisfactory manner. For these cases plotted points lie above and bellow the line of perfect agreement in acceptable manner. In the case of $B = 0.8$, effect of expansion is less than other cases. This may be the cause of slight mismatch of result with the experimental data. For all expansion ratios with different channel slopes, percentage deviation varies from the actual data varies from -12.76% to $+12.98\%$.

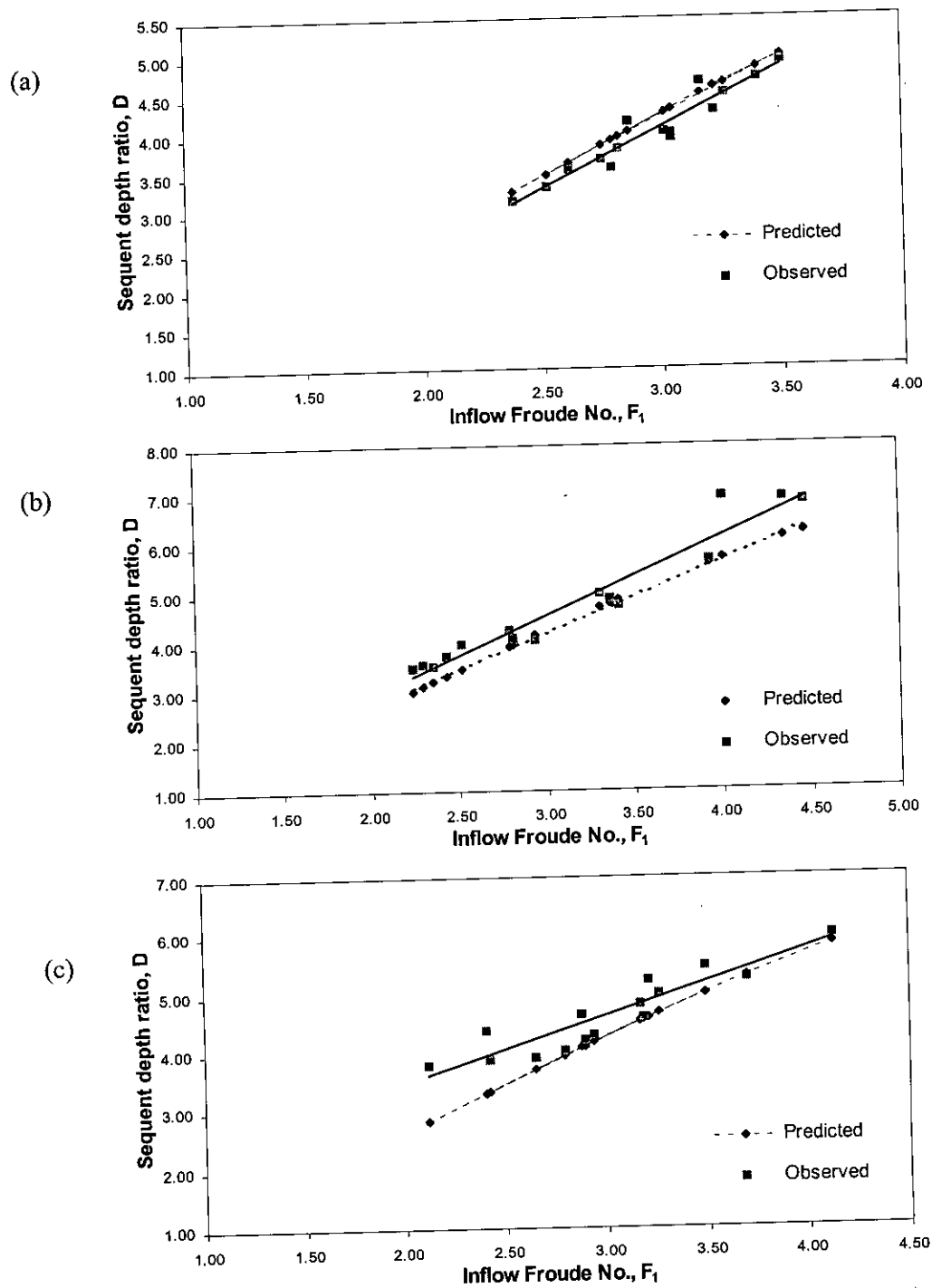


Figure 6.15: D Vs F_1 with expansion ratio, $B = 0.8$; (a) Slope = 0.0042, (b) Slope = 0.0089, (c) Slope = 0.0131

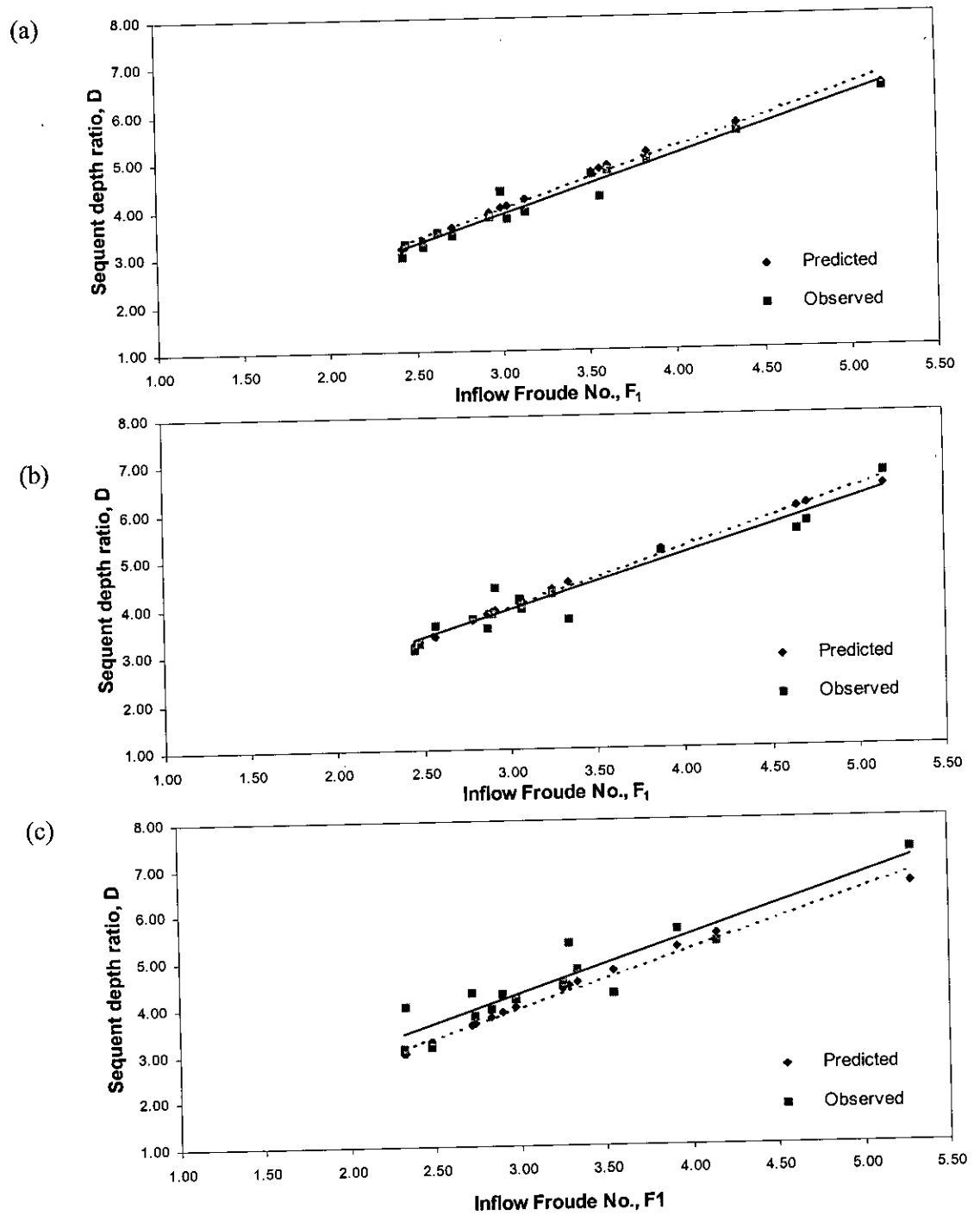


Figure 6.16: D Vs F_1 with expansion ratio, $B = 0.7$; (a) Slope = 0.0042, (b) Slope = 0.0089, (c) Slope = 0.0131

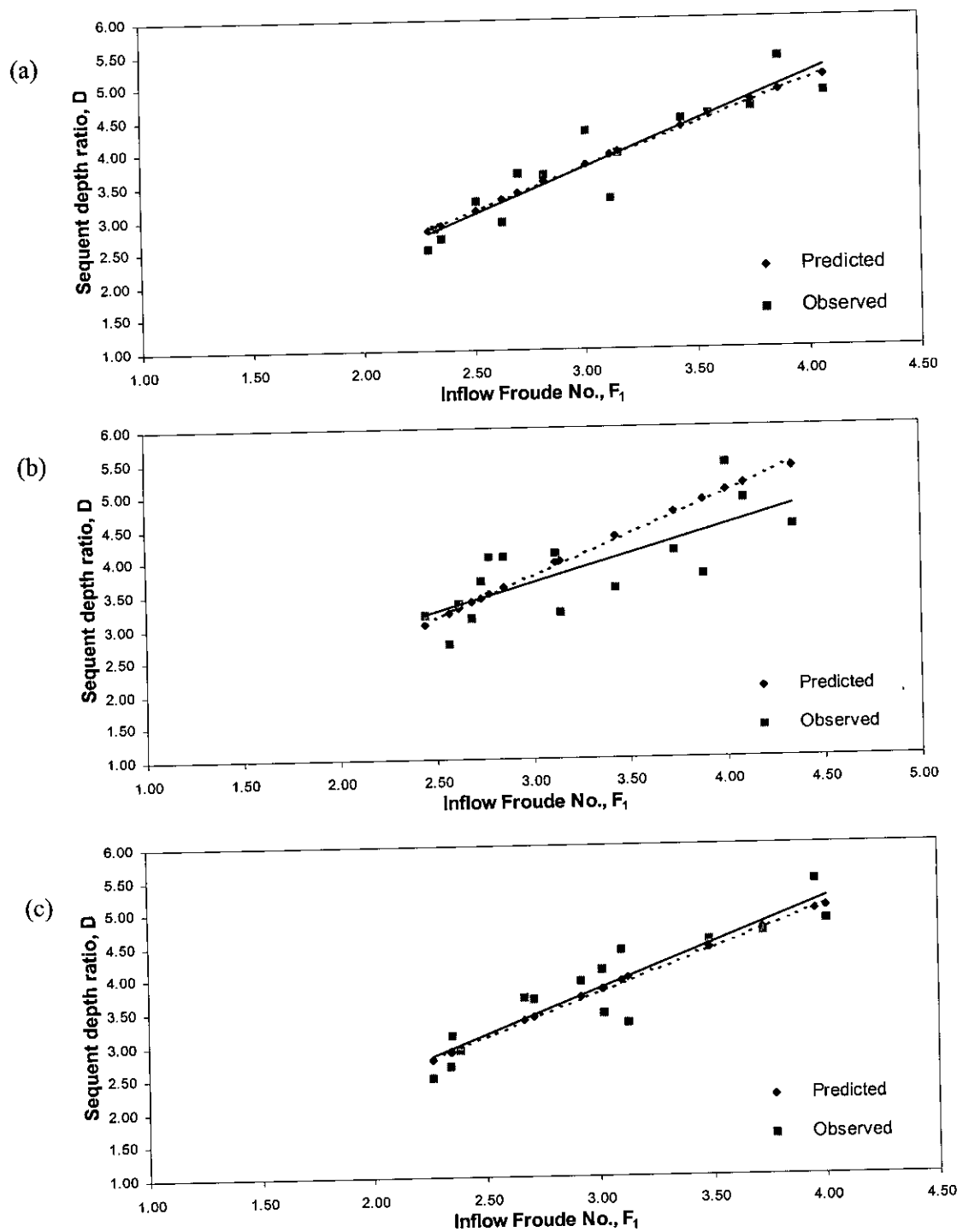


Figure 6.17: D Vs F_1 with expansion ratio, $B = 0.6$; (a) Slope = 0.0042, (b) Slope = 0.0089, (c) Slope = 0.0131.

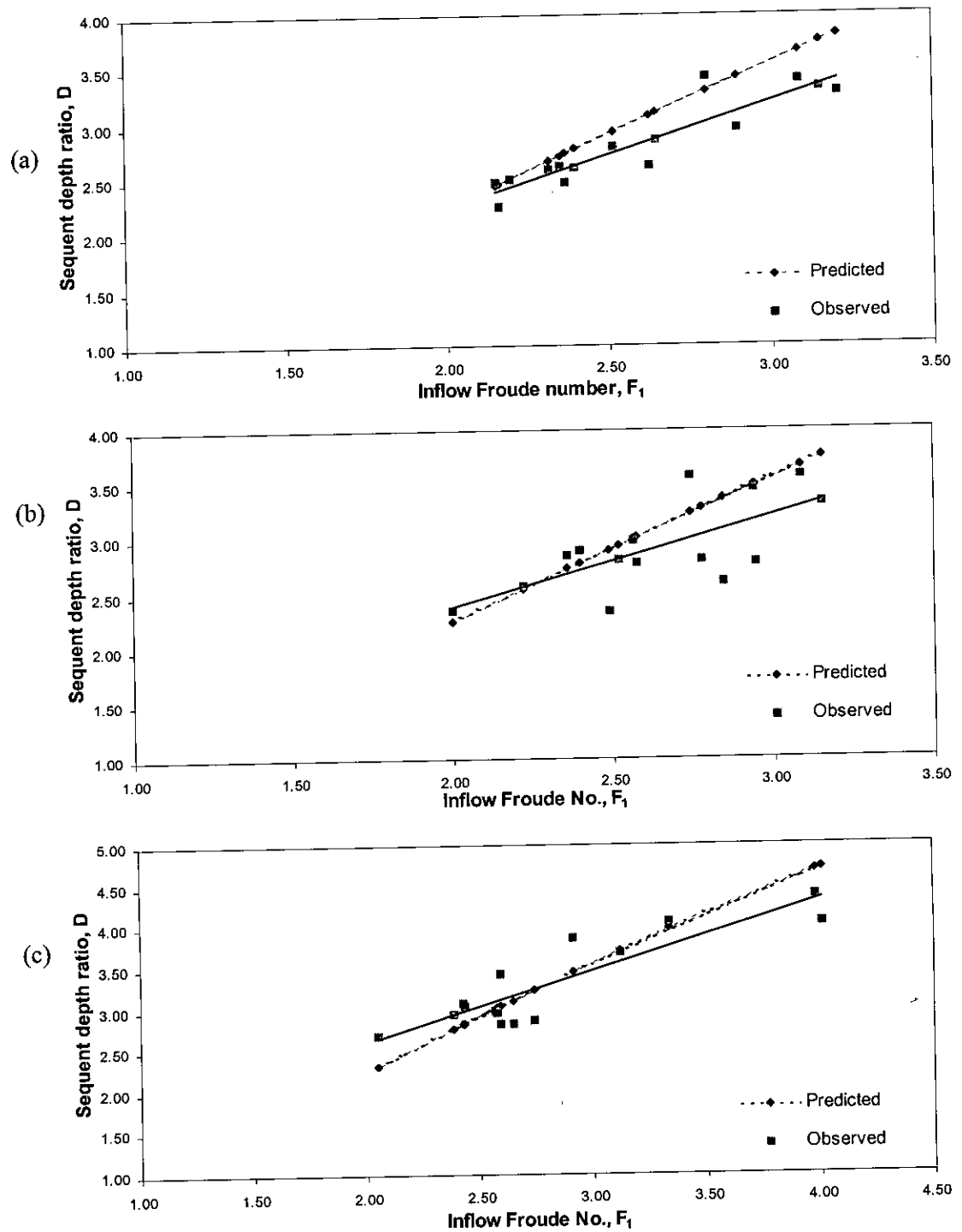


Figure 6.18: D Vs F_1 with expansion ratio, $B = 0.5$ (a) Slope = 0.0042, (b) Slope = 0.0089, (c) Slope = 0.0131

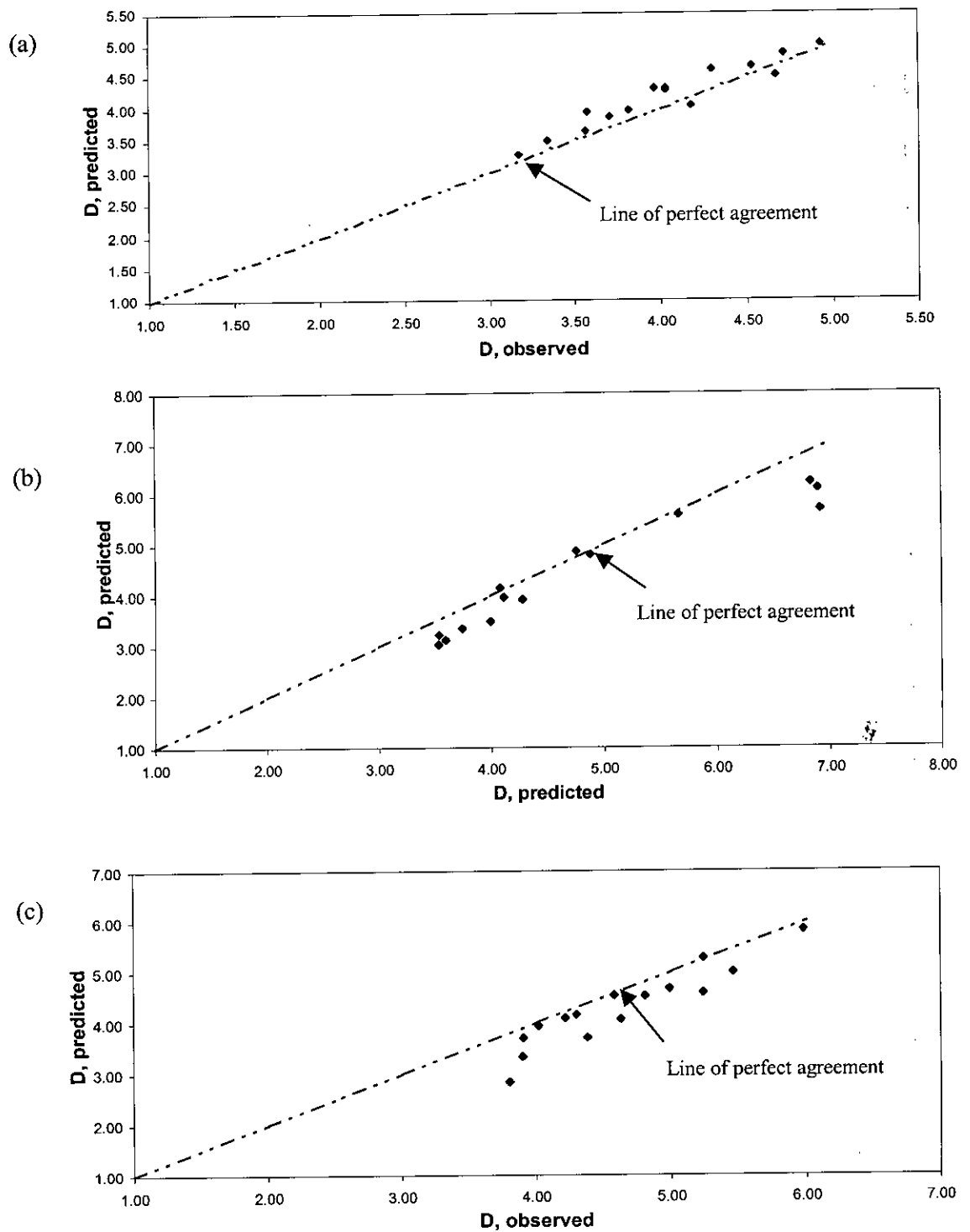


Figure 6.19: Comparison between predicted D and observed D with expansion ratio, $B = 0.8$; (a) Slope = 0.0042, (b) Slope = 0.0089, (c) Slope = 0.0131

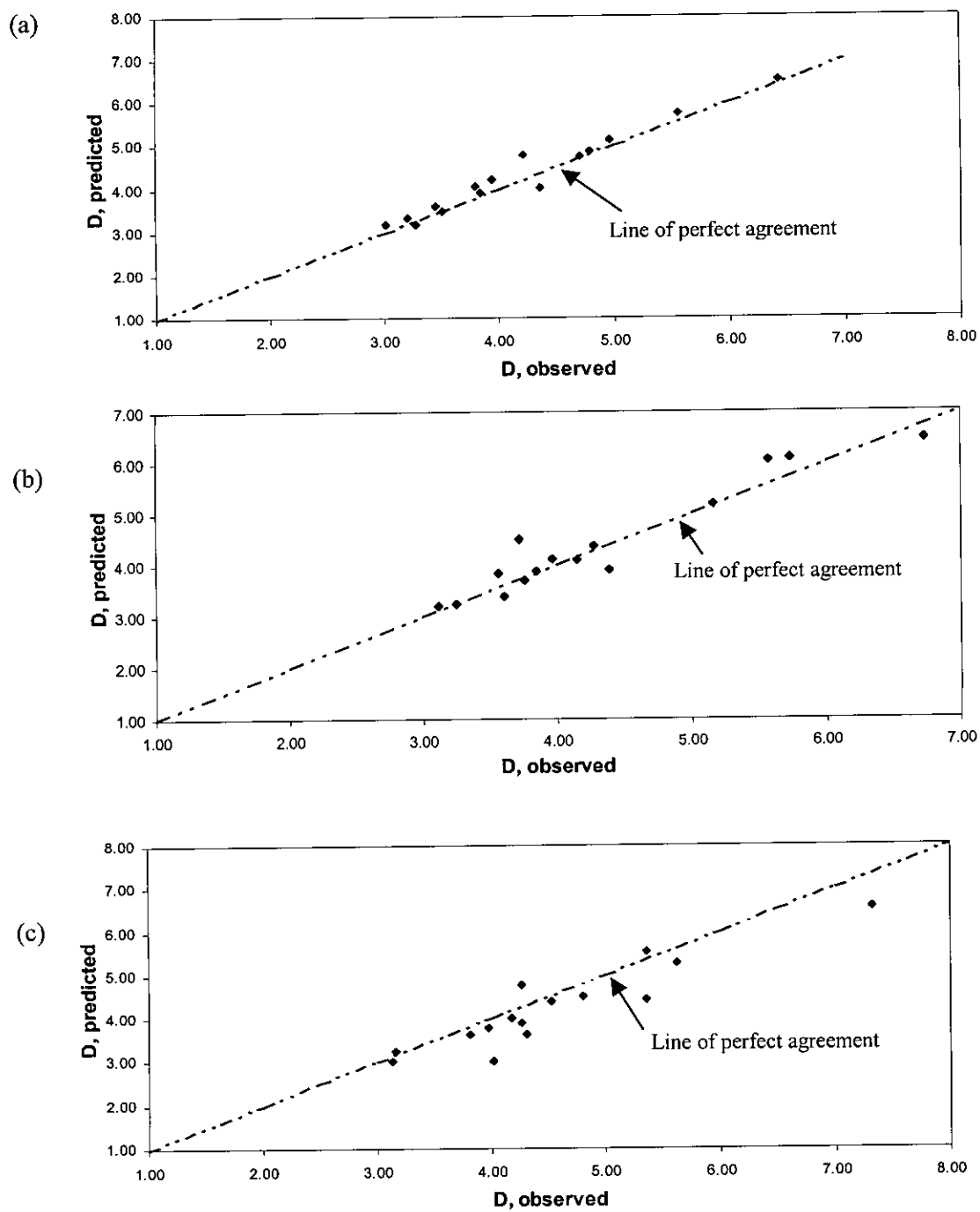


Figure 6.20: Comparison between predicted D and D observed D with expansion ratio, $B = 0.7$; (a) Slope = 0.0042, (b) Slope = 0.0089, (c) Slope = 0.0131

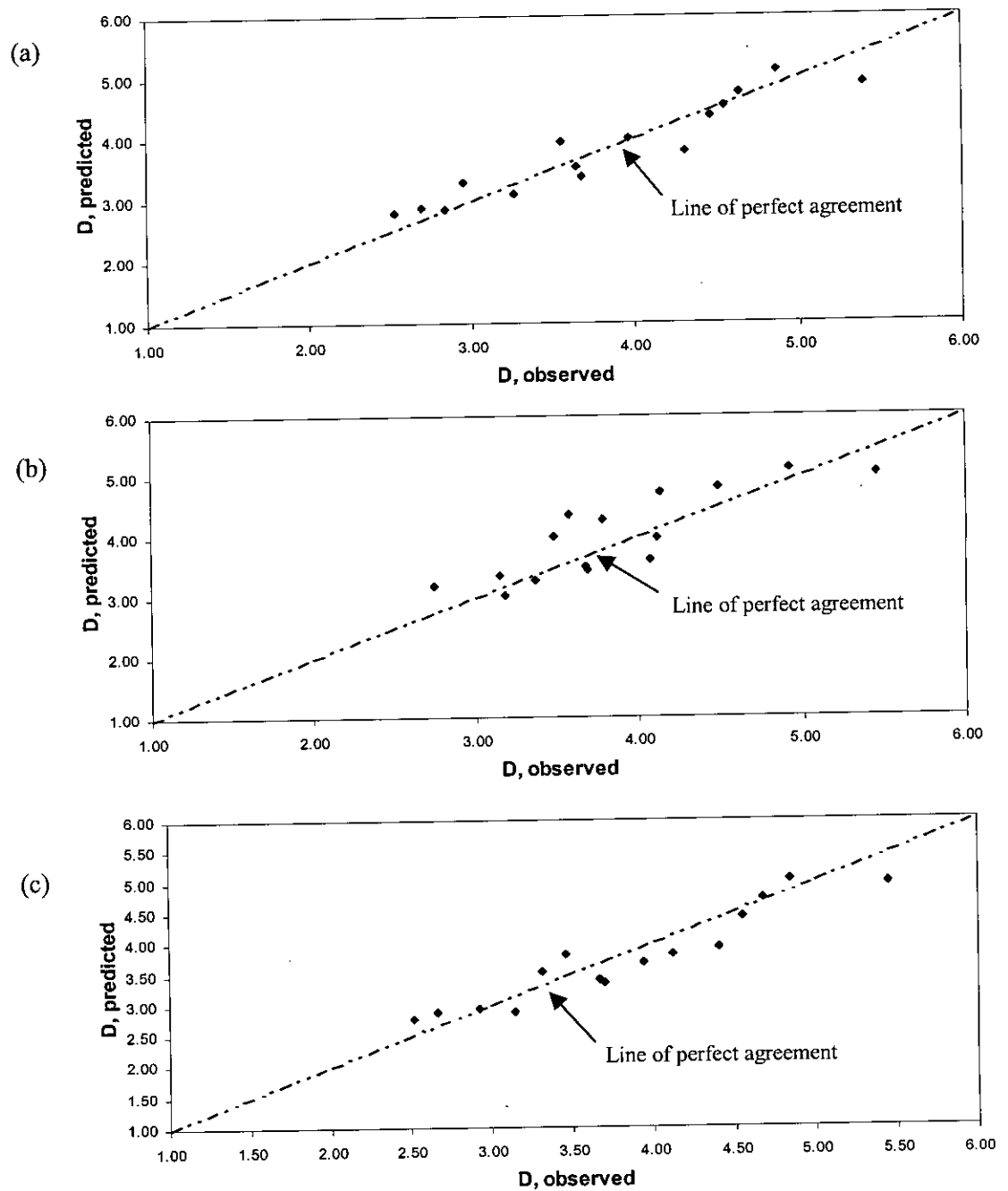


Figure 6.21: Comparison between predicted D and observed D with expansion ratio, $B = 0.6$; (a) Slope = 0.0042, (b) Slope = 0.0089, (c) Slope = 0.031

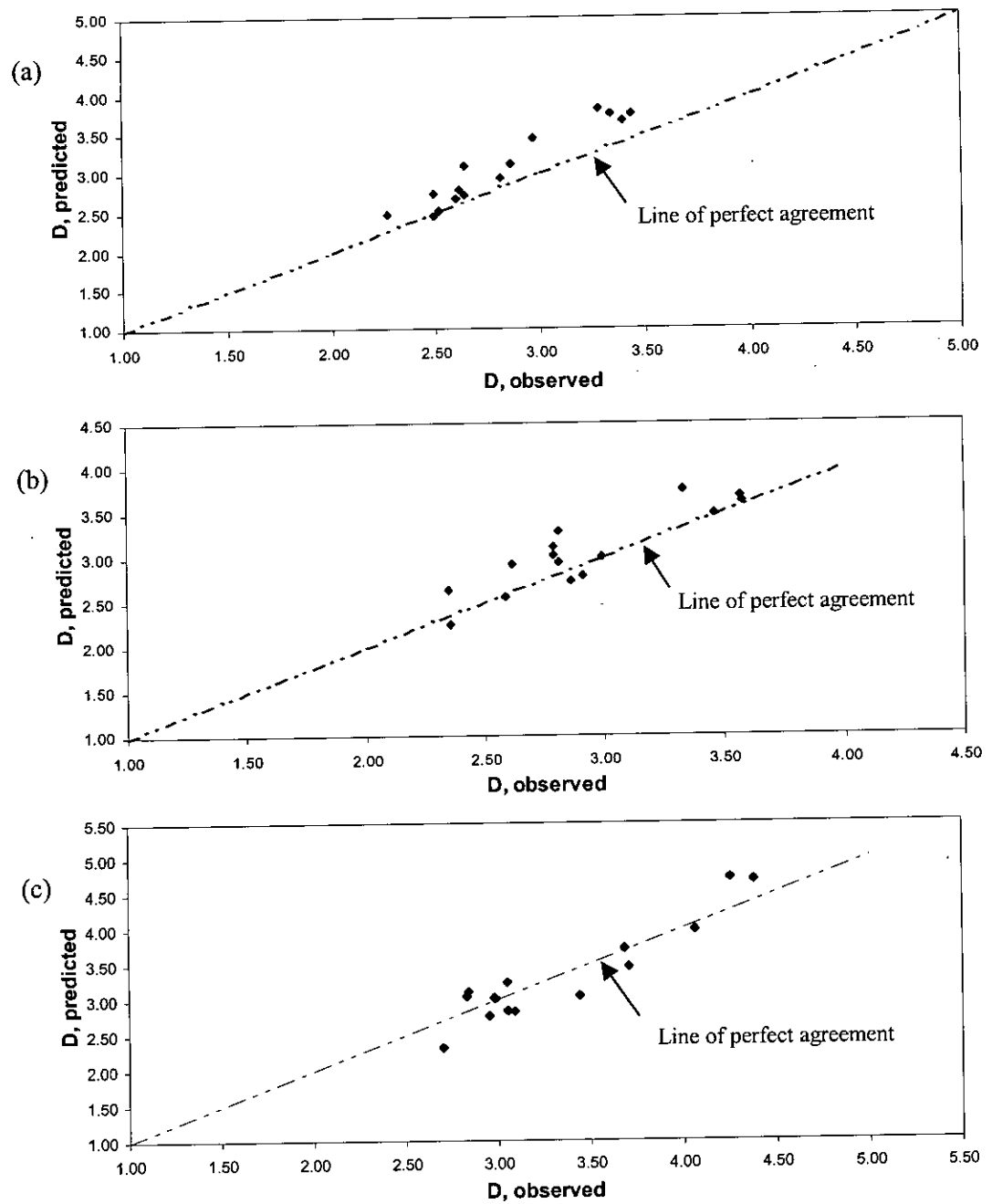


Figure 6.22: Comparison between predicted D and observed D with expansion ratio, $B = 0.5$; (a) Slope = 0.0042, (b) Slope = 0.0089, (c) Slope = 0.0131

Table 6.1: Statistical result of the performance of the prediction equation

B = 0.8, Channel slope = 0.0042

D (obs.)	D (calib.)	% deviation
4.17	4.04	3.25
4.67	4.51	3.54
4.92	5.00	-1.60
4.30	4.60	-6.56
4.52	4.66	-2.87
4.71	4.86	-2.96
3.56	3.65	-2.46
3.70	3.87	-4.38
4.03	4.28	-5.98
3.17	3.26	-2.81
3.81	3.97	-4.03
4.03	4.32	-6.85
3.34	3.50	-4.46
3.57	3.93	-9.28
3.96	4.32	-8.45

B = 0.8, Channel slope = 0.0089

D (obs.)	D (calib.)	% deviation
4.11	3.97	3.64
3.60	3.45	4.19
3.75	3.52	6.53
3.54	3.24	9.12
4.08	4.16	-1.79
4.76	4.88	-2.27
4.89	4.81	1.66
4.28	3.93	9.08
3.53	3.69	-4.32
5.67	5.59	1.34
5.00	4.72	5.99
4.00	3.82	4.64
6.83	6.22	9.81
6.90	6.32	9.19
6.92	6.30	9.89

B = 0.8, Channel slope = 0.0131

D(obs.)	D (calib.)	% deviation
5.98	5.84	2.39
5.24	5.28	-0.75
4.58	4.54	0.76
5.46	5.00	9.15
5.24	4.87	7.39
4.21	4.10	2.85
4.99	4.67	6.84
4.63	4.23	9.42
4.02	3.71	8.36
4.81	4.52	6.21
3.62	3.34	8.47
2.80	2.84	-1.52
4.30	4.17	3.19
4.02	3.95	1.82
3.91	3.71	5.40

B = 0.7, Channel slope = 0.0131

D(obs.)	D (calib.)	% deviation
3.81	3.64	4.94
3.97	3.79	5.00
4.18	3.99	4.71
4.52	4.38	3.20
4.27	3.88	9.97
3.14	3.01	4.33
4.81	4.50	6.73
3.85	3.61	6.51
3.26	3.02	8.04
5.62	5.24	7.16
4.90	4.43	10.52
3.16	3.25	-2.81
7.21	6.56	9.90
5.12	4.78	7.20
5.36	5.51	-2.78

B = 0.7, Channel slope = 0.0089

D(obs.)	D (calib.)	% deviation
6.73	6.46	4.13
5.73	6.09	-5.90
4.02	4.50	-10.75
5.57	6.04	-7.80
5.16	5.19	-0.66
4.21	3.91	7.73
4.28	4.37	-2.17
3.85	3.88	-0.83
3.25	3.24	0.14
4.15	4.10	1.16
3.56	3.84	-7.19
3.11	3.21	-2.86
3.96	4.12	-3.73
3.76	3.71	1.36
3.61	3.39	6.38

B = 0.7, Channel slope = 0.0042

D(obs.)	D (calib.)	% deviation
3.79	4.07	-6.95
3.50	3.47	0.69
3.27	3.19	2.55
3.94	4.21	-6.43
3.45	3.60	-4.27
3.01	3.16	-4.81
4.79	4.87	-1.68
3.83	3.92	-2.16
3.20	3.34	-4.31
4.97	5.15	-3.48
4.70	4.75	-1.01
4.35	4.02	8.27
6.43	6.49	-0.98
5.56	5.74	-3.14
4.32	4.80	-9.98

B = 0.6, Channel slope = 0.0042

D (obs.)	D (calib.)	% deviation
3.68	3.39	8.70
2.95	3.28	-10.14
2.69	2.89	-6.82
4.46	4.36	2.40
4.18	3.80	10.03
3.26	3.11	4.74
4.64	4.73	-2.00
3.64	3.54	2.87
2.52	2.81	-10.19
5.40	4.87	10.83
3.55	3.95	-10.09
2.84	2.85	-0.60
4.87	5.10	-4.51
4.55	4.51	0.84
3.96	4.00	-0.79

B = 0.6, Channel slope = 0.0089

D (obs.)	D (calib.)	% deviation
3.70	3.35	10.59
2.92	2.94	-0.43
2.67	2.88	-7.47
4.12	3.81	7.96
4.40	3.93	11.97
3.14	2.89	8.73
4.67	4.71	-0.88
3.67	3.40	7.78
2.52	2.76	-8.91
5.44	4.97	9.50
3.31	3.54	-6.52
3.46	3.82	-9.53
4.84	5.03	-3.66
4.55	4.43	2.64
3.94	3.69	6.78

B = 0.6, Channel slope = 0.0131

D(obs.)	D (calib.)	% deviation
4.49	4.81	-6.65
4.13	4.72	-12.45
4.07	3.60	12.99
3.48	3.99	-12.76
3.92	4.35	-9.97
4.92	5.12	-3.85
5.45	5.02	8.43
3.78	4.28	-11.72
3.15	3.37	-6.62
3.18	3.03	4.99
3.68	3.49	5.39
4.12	3.96	3.91
3.69	3.44	7.39
3.36	3.27	2.75
2.94	3.21	-8.31

B = 0.5, Channel slope = 0.0042

D(obs.)	D (calib.)	% deviation
3.38	3.82	-11.44
3.33	3.75	-11.16
3.43	3.75	-8.42
3.40	3.67	-7.42
2.86	3.11	-8.15
2.84	3.08	-7.87
2.49	2.74	-9.19
2.63	2.72	-3.12
2.51	2.51	0.03
3.12	3.43	-9.14
2.62	2.78	-6.09
2.27	2.47	-8.15
2.81	2.94	-4.56
2.60	2.68	-2.93
2.49	2.45	1.39

B = 0.5, Channel slope = 0.0089

D(obs.)	D (calib.)	% deviation
3.33	3.75	-11.16
3.46	3.49	-0.80
3.58	3.62	-1.13
3.57	3.67	-2.65
2.99	3.00	-0.38
2.79	3.02	-7.53
2.91	2.78	4.50
2.86	2.74	4.51
2.36	2.25	4.73
2.59	2.55	1.20
2.81	2.95	-4.73
2.91	3.28	-11.37
2.79	3.11	-10.27
2.61	2.92	-10.51
2.35	2.63	-10.53

B = 0.5, Channel slope = 0.0131

D(obs.)	D (calib.)	% deviation
4.38	4.68	-6.36
4.06	3.98	2.12
3.71	3.45	7.33
4.25	4.71	-9.72
3.68	3.71	-0.80
2.99	3.02	-0.99
3.32	3.05	9.02
3.09	2.83	9.21
3.05	2.84	7.57
2.98	3.02	-1.43
2.95	2.77	6.71
2.60	2.32	12.17
3.05	3.24	-5.89
2.84	3.11	-8.74
2.83	3.04	-7.08

6.6 APPLICABILITY OF THE PROPOSED EQUATION

6.6.1 Introduction

The new model is proposed for abruptly expanding and sloping channel. These two effects are considered by two factors, k_1 and k_2 . The equation may work for either the sloping channel or the horizontal channel with sudden expansion. Analyses with these two situations are presented in subsequent articles here

6.6.2 Horizontal channel with sudden expansion

For the horizontal channel, $k_2 = 0$ and for this type of abruptly expanding channel the Inflow Froude number will be modified by the parameter k_1 only. Then the equation will be as follows:

$$E_1^2 = \frac{F_1^2}{k_1}$$

Where k_1 is the only function of expansion ratio B and Froude number F_1 . Graph 6.23 shows the relationship between the Sequent depth ratio and Inflow Froude number for a horizontal abruptly expanding channel for different values of expansion ratio, B (0.8, 0.7, 0.6 and 0.5). The figure shows that the value of D decreases with the decrease in the value of expansion ratio, B . again this model is compared with the actual data for expansion ratio, $B = 0.7$ which is shown in figure 6.25. In this case it is revealed that the prediction equation slightly overestimates the sequent depth ratio (average percentage deviation of the observed data from the predicted values = +5.84%). This equation is also compared with the equation of Matin et.al. (1998). These two equations show almost similar result.

6.6.3 Sloping rectangular channel

In the case of a sloping rectangular channel with no abrupt expansion, modified Froude number will be corrected by the factor k_2 only, in that case the equation will be like this:

$$E_1^2 = \frac{F_1^2}{(1 - k_2) \cos \theta}$$

Where the factor k_2 is a function of channel slope and Froude number. Figure 6.24 shows the graphs of D Vs F_1 for different channel slopes (0.087, 0.175, 0.262 and 0.349). These results are compared with that for a jump in a horizontal channel, for a classical jump. This is evident from the figure that value of D increases with the increase in the value of channel slope. But from this figure it is clear that for a mild slope = 0.087, value of sequent depth ratio increases very sharply compared to the corresponding value in case of a classical jump. Whereas in case of other slopes the difference in predicted values are not very significant. This means, the prediction model does not predict the value of sequent depth ratio in case of sloping rectangular channel in a satisfactory manner. Actually the range of slope taken in the study is quite low. Very flat slopes are taken here. So the effect of slope is not well described by the prediction equations.

Again the proposed equation is compared with the actual data for channel slope = 0.0131 which is shown in figure 6.26. This figure shows closeness of the predicted value with the observed value (Average percentage deviation = +6.31%).

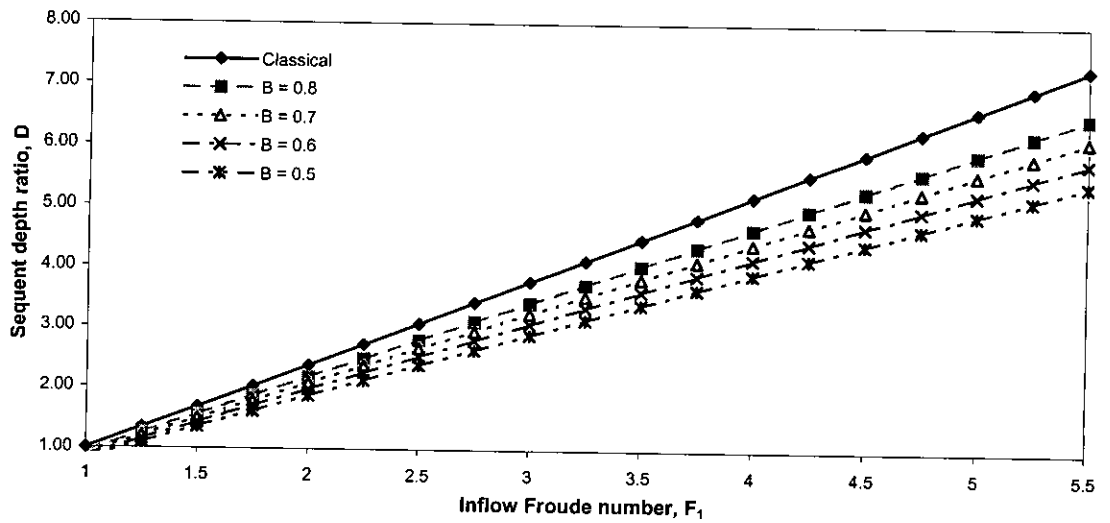


Figure 6.23: Sequent depth ratio Vs Inflow Froude number for different expansion ratios

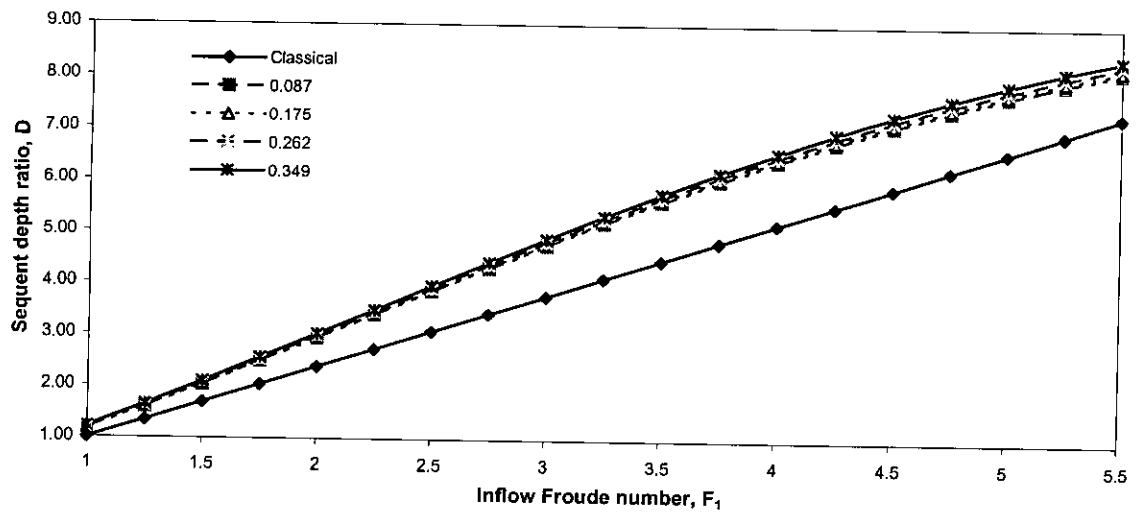


Figure 6.24: Sequent depth ratio Vs Inflow Froude number for different channel slopes

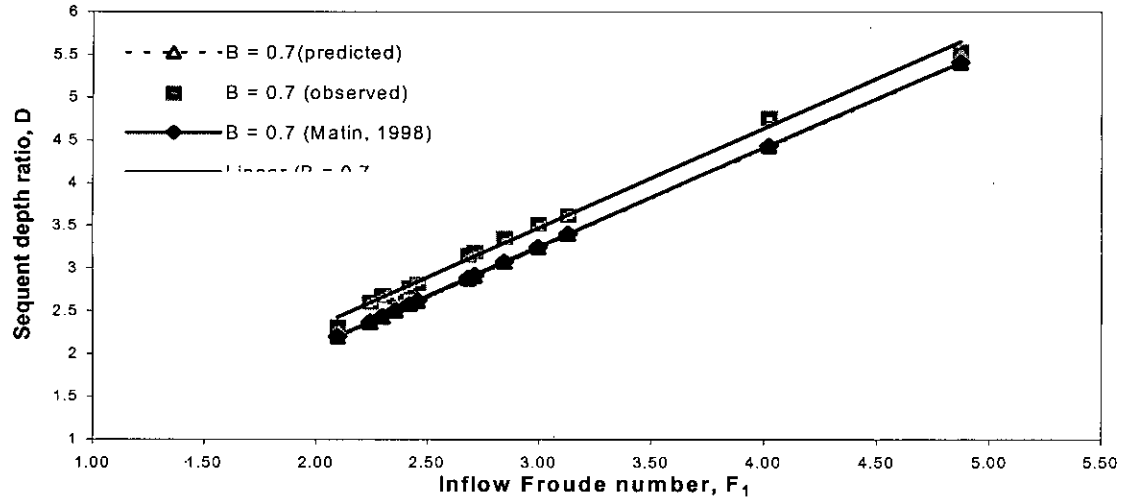


Figure 6.25: Sequent depth ratio Vs Inflow Froude number with observed and predicted data for a horizontal abruptly expanding channel.

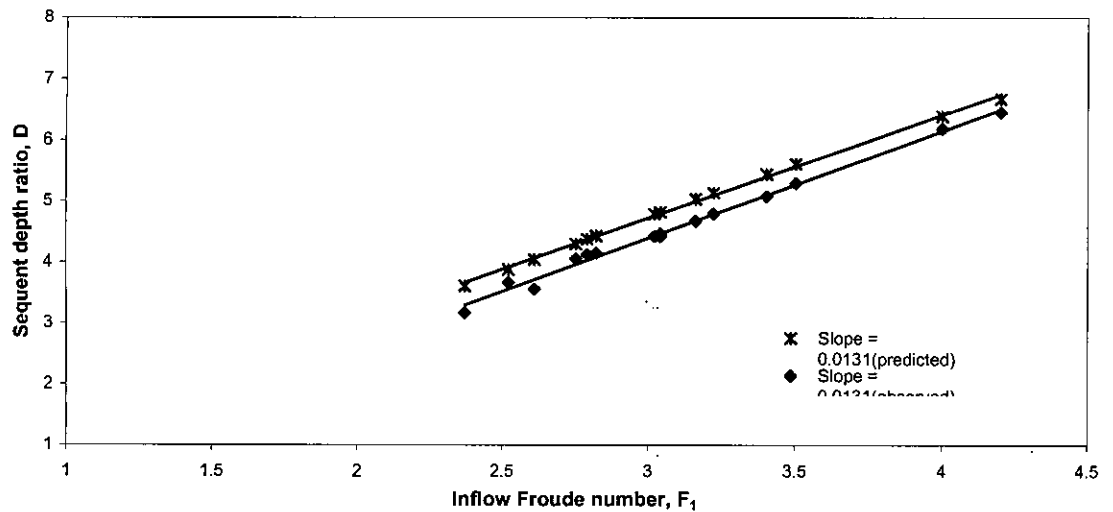


Figure 6.26: Sequent depth ratio Inflow Froude number with observed and predicted data for a rectangular sloping channel.

Chapter Seven

CONCLUSIONS AND RECOMMENDATIONS

7.1 INTRODUCTION

The hydraulic jump in abrupt symmetrical expansions of a sloping rectangular channel have been studied under a wide range of experimental conditions, such as various combinations of expansion ratio and channel slope, which has conducted in the Hydraulics and River Engineering Laboratory of WRE Dept., BUET. The conclusions so far obtained from the study and recommendations for further study are given in the subsequent articles.

7.2 CONCLUSIONS

Following conclusions can be drawn, albeit tentatively, from the research carried out in this work:

1. The theoretical equation (3.13) developed for predicting the sequent depth ratio of a free hydraulic jump permits simple and easy application in the design of expanding and sloping stilling basin, because it avoids the graphical procedure. From the known variables like expansion ratio, channel slope and Inflow Froude number the modified Froude number can be calculated.
2. The main difficulty arose in expanding channels is the tendency for asymmetric flow associated with large dead water zones and poor spreading of the inflow jet, which has been shown in chapter five (figure 5.5).
3. In the case of hydraulic jump in expanded sloping channel less tail water depth is needed than for a classical jump. The sequent depth of a jump decreases with decreasing the channel width, i.e., the expansion ratio of the channel. Again due to the effect of channel slope the sequent depth increases compared to classical jump.

4. Use of the prediction equation (equation 3.13) needs two parameters k_1 and k_2 to modify the inflow Froude number. Theoretically the value of parameter k_1 depends on the expansion ratio and the sequent depth ratio. After the analysis from the experimental data the modified equation (equation 6.1) is developed, where the factor depends on known variables like B and F_1 .
5. The parameter k_2 depends on the inflow Froude number, F_1 and the channel slope, θ . Analysis shows that expansion ratio, B has very little effect upon this value. After the analysis from all the experimental data a modified equation (equation 6.2) is developed to compute the parameter k_2 . The equation shows a clear disagreement with the experimental data. But when k_1 and k_2 values are used combined to modify the inflow Froude number, this shows a reasonable accuracy of the prediction model. So the equation is taken as satisfactory. The equation needs two independent variables like inflow Froude number F_1 and channel slope θ .
6. The results of the present study indicate that the hydraulic jump in the abruptly expanding sloping channel results in lesser downstream depth. So this type of hydraulic jump can be used as an energy dissipator in low tail water condition.

7.3 RECOMMENDATIONS

Based on the present research, the following recommendations are made for further study:

1. The sequent depth ratio of the abruptly expanding sloping channel was investigated here. Energy loss in the same condition should also be investigated.
2. The highest value of F_1 found in this experiment is 5.28, which covers the range of steady jump. The whole study may be conducted for higher range of

discharges so that higher range of Froude number can be achieved which covers the range of strong jump.

3. Velocity distribution and pressure distribution at upstream and downstream of the jump can be observed.
4. The main difficulty of the present study was the value of channel slope achieved. Here very mild slope was considered (three slopes were 0.0042, 0.0089 and 0.0131). From this range of channel slope a definite decision cannot be made. So the experiments should be conducted for higher range of channel slope.
5. The results of the experiment should be simulated with a mathematical computer model.

REFERENCES

Agarwal, V.C. (2001), "Graphical solution to the problem of sequent depth and energy loss in spatial hydraulic jump", Proc. ICE, Water and Maritime Engineering, Vol. 148, No.1, pp. 1-3.

Alhamid, A.A. and M. Negm, A.A (1996), "Depth ratio of hydraulic jump in rectangular stilling basins", Journal of Hydraulic Research, Vol. 34, No. 5.

Ali, H.S. (1991), " Effects of Roughened-Bed Stilling Basin on Length of Rectangular Hydraulic Jump", Journal of Hydraulic Engineering, Vol. 117, No. 1, pp. 83-93.

Bakhmeteff, B.A. and Matzke, A.E. (1946), "The hydraulic jump in terms of dynamic similarity", Tans. Am. Soc. Civil Engrs. 101, 630-680.

Bradeley, J.N. and Peterka, A.J. (1957), "Hydraulic design of stilling basins: Stilling basin with sloping apron (Basin V)", J. Hydraulics Div., Am. Soc. Civil Engineers. 83, HY5, 1-32

Bremen, R. and Hager, W.H. (1993), "T-Jump in Abruptly Expanding Channel", Journal of Hydraulic Research, Vol. 31, No.1, pp. 61-73.

Chow, V.T. (1959), Open Channel Hydraulics, McGraw-Hill, New York.

Hager, W. H. (1989), "B- jump in sloping channel", Journal of Hydraulic Research, Vol. 27, No. 1, pp. 539-558.

Hager, W.H. (1985), "Hydraulic Jumps in Nonprismatic Rectangular Channels", Journal of Hydraulic Research, Vol. 23, No.1, pp 21-35.

Hager, W.H. (1992), "Energy Dissipators & Hydraulic Jumps", Kluwer Academic Publication, Dordrecht, The Netherlands, pp. 151-173.

Hasan, M.R. (2001), "A study on the sequent depth ratio of hydraulic jump in abruptly expanding channel", M. Engg. thesis, Dept. of WRE, BUET

Henderson, F. M. (1966). Open Channel Flow. MacMillan Co., New York, N.Y.

Herbrand, K. (1973), "The Spatial Hydraulic Jump", Journal of Hydraulic Research, Vol. 11(3), pp. 205-218.

Husain, D., Alhamid, A.A. and Negm, Abdel-Azim M. (1995), "Length and depth of hydraulic jump in sloping channels". Journal of Hydraulic Research, Vol. 33, No. 3, pp. 305-316.

Kindsvater, C.E. (1944), "The Hydraulic jump in sloping channels", Trans. Am. Soc. Civil Engineers 109, 1107-1154.

Magalhaes, L.E. (1981), "Lateral diffusion of a sluice jet discharged along a wall", V Canadian Hydrotechnical Conf., Fredericton, NB, pp. 951-965.

Magalhaes, L.E. and Minton, P. (1975), "Design implications of hydraulic jumps at sudden enlargements, Proc. Inst. Civil Engineers (London), Part 2, Vol. 59, pp. 168-174.

Matin, M.A., A. Alhamid & A.M. Negm (1998), "Prediction of Sequent Depth Ratio of Hydraulic Jump in Abruptly Expanding Channels", Advances in Hydro-science and Engineering, Vol. III, (ICHE-98), published in CD-ROM file, /// EL/ Document/ Exp.channels.4.paperhtml, Cottbus/ Berlin, Germany, 1998.

Matin, M.A., Negm, A.M., El-Saiad, A.A. and Alhamid, A.A. (1997), "Prediction of Sequent Depth Ratio of Free Hydraulic Jump in Abruptly Enlarged Channels", Egyptian Journal for Engineering Sciences & Technology, Vol. 2, No.1, pp. 31-36.

McCorquodale, J.A. (1986), "Hydraulic Jumps and Internal Flows", Encyclopedia of Fluid Mechanics, Gulf Publishing Company, Houston, Texas, Vol. 2, pp. 122-173.

Nettleton, P.C. and McCorquodale, J.A. (1989), "Radial flow stilling basins with baffle blocks", Canadian J. Civil Engineering, Vol. 16, No. 4, pp. 489-497.

Ohtsu, I. And Yasuda, Y. (1991), "Hydraulic jump in sloping channels", Journal of Hydraulic Engineering, ASCE, Vol. 117, No. 7, pp. 905 - 921.

Peterka, A.J. (1958), "Hydraulic design of stilling basins and energy dissipators", Engineering Monograph 25 Dept. Interior, US Bureau of Reclamation, Denver, Co.

Rajaratnam, N. (1967), "Hydraulic jumps." Advances in Hydrosience, V.T. Chow, ed., Vol. 4, Academic Press, New York, N. Y. , pp. 197-280.

Rajaratnam, N. and Subramanya, K. (1968), "Hydraulic Jumps Below Abrupt Symmetrical Expansions", Proc. ASCE, Journal of Hydraulics Division, Vol. 94, HY3, pp. 481-503.

Ranga Raju, K.G. (1993), Flow Through Open Channels, Tata McGraw-Hill Pub. Co. Ltd., New Delhi, 2nd ed.

Unny, T. E. (1961), "The Spatial Hydraulic Jump", IX IAHR Congress, Belgrade, pp. 32-42.

Whittington, R.B. and Ali, K.H.M. (1969), "Convergent Hydraulic Jumps", Proceedings of Institute of Civil Engineers, Vol. 43, pp. 157-173.

